

MONITORING AND CONTROL IN FRICTION STIR WELDING

By

PAUL A. FLEMING

Dissertation

Submitted to the Faculty of the

Graduate School of Vanderbilt University

In partial fulfillment of the requirements

for the degree of

DOCTOR OF PHILOSOPHY

In

Electrical Engineering

May, 2009

Nashville, Tennessee

Approved:

Professor George Cook

Professor D. M. Wilkes

Professor Alvin Strauss

Professor David DeLapp

Professor Jim Davidson

To Katherine, Mom, Dad, Adam and all those who made this possible.

ACKNOWLEDGEMENTS

Financial support for this work was provided by a fellowship from the American Welding Society. Additional funding was provided by Los Alamos National Laboratories and the NASA Tennessee Space Grant Consortium.

I am very grateful to my adviser Dr. D. M. Wilkes for his help and support throughout my time at Vanderbilt. I would also like to thank Dr. George Cook for bringing me into the welding automation lab and for his support and encouragement. Thanks also to Dr. David DeLapp and Dr. Alvin Strauss for so many suggestions, tips and answers. Thank you Dr. Davidson for serving on my committee.

I would also like to thank Bob Patchin and John Fellenstein for their time and knowledge very generously shared. Thank you to Lewis Saettel for being so friendly and helpful. Thank you to Flo Wahidi, who always kept an eye out for me and my fellow graduate students. Thanks to Gary Shearer for his help setting up the welder for automatic control. Thanks to Dr. Kate Lansford for her many hours helping me cross-section weld samples. Thanks to Robin Midgett for helping me with mechanical testing of weld samples. Thanks to Dr. Daniel Hartman for his suggestions and guidance. Thank you to Dr. Wayne Thomas for his time and very helpful correspondence.

Thanks to my fellow students in the Vanderbilt Welding Lab and Center for Intelligent Systems, I have enjoyed working with all of you and wish you the best of luck for the future. A huge thanks to all of my friends and family, for their essential support. And finally to my wife Katherine: merci beaucoup et je t'aime! J'ai fini, maintenant c'est ton tour!

TABLE OF CONTENTS

| | |
|---|-----|
| ACKNOWLEDGEMENTS | iii |
| LIST OF FIGURES | vii |
| I. INTRODUCTION | 2 |
| Overview of dissertation | 4 |
| II. DOCUMENTATION OF EQUIPMENT UPGRADE | 6 |
| Initial configuration | 6 |
| Modifications | 7 |
| III. BACKGROUND LITERATURE REVIEW: FSW - FLAWS, MONITORING AND CONTROL | 11 |
| Friction Stir Welding | 11 |
| Faults in Friction Stir Welding | 14 |
| Flaw Detection in Friction Stir Welding | 23 |
| Control of Friction Stir Welding | 49 |
| IV. BACKGROUND LITERATURE REVIEW: DETECTION AND CLASSIFICATION TECHNIQUES | 55 |
| Principal Components | 55 |
| Linear Discriminant Analysis | 58 |
| Support Vector Machines | 60 |
| K-means clustering | 63 |
| Neural Networks | 65 |
| V. PAPER 1A: IN-PROCESS GAP DETECTION IN FRICTION STIR WELDING (SENSOR REVIEW) | 68 |
| Abstract | 68 |
| Introduction | 69 |
| Experiment Setup | 71 |
| Results | 73 |
| Conclusions and Future Work | 78 |
| VI. PAPER 1B: AUTOMATIC FAULT DETECTION IN FRICTION STIR WELDING (MS&T 2007) | 80 |
| Abstract | 80 |

| | | |
|-------|---|-----|
| | Introduction | 80 |
| | Gap Detection and Ranking | 82 |
| | Results | 84 |
| | Conclusion | 86 |
| VII. | PAPER 2: MISALIGNMENT DETECTION AND ENABLING OF SEAM TRACKING FOR FRICTION STIR WELDING | 87 |
| | Abstract | 87 |
| | Introduction | 88 |
| | Force as a process feedback mechanism | 91 |
| | Experimental setup | 92 |
| | Results | 97 |
| | Discussion | 99 |
| | Conclusions and future work | 101 |
| VIII. | PAPER 3: AUTOMATIC SEAM-TRACKING OF FRICTION STIR WELDED T-JOINTS USING WEAVING | 102 |
| | Abstract | 102 |
| | Introduction | 102 |
| | Experimental Results | 106 |
| | Discussion | 110 |
| | Conclusion | 113 |
| IX. | PAPER 4: SEAM-TRACKING FOR FRICTION STIR WELDED LAP JOINTS | 114 |
| | Introduction | 114 |
| | WeaveTrack System | 117 |
| | Experimental Setup | 119 |
| | Results | 119 |
| | Discussion | 124 |
| | Conclusion | 126 |
| X. | SYSTEM MODELING WITH MATLAB AND SIMULINK | 128 |
| | Introduction | 128 |
| | Simulink model | 128 |
| | Verification of model | 130 |
| | Analysis with model | 130 |
| | Conclusion | 133 |
| XI. | AUTOMATIC TOOL WEAR DETECTION | 134 |
| | Introduction | 134 |
| | Experimental setup | 134 |

| | | |
|-------|---|-----|
| | Analysis | 136 |
| | Discussion and conclusion | 136 |
| XII. | HYDROGEN GENERATION IN SUBMERGED FRICTION STIR WELDING OF ALUMINUM | 139 |
| | Abstract | 139 |
| | Introduction | 140 |
| | Experiment | 142 |
| | Discussion | 145 |
| | Conclusions and future work | 145 |
| | Acknowledgments | 145 |
| XIII. | DISCUSSION OF RESULTS | 147 |
| | Overview | 147 |
| | Gap Detection | 147 |
| | Misalignment detection | 148 |
| | Seam-tracking | 148 |
| XIV. | RECOMMENDATIONS FOR FUTURE WORK | 150 |
| | Gap Fault and Misalignment Detection | 150 |
| | Seam Tracking | 152 |
| | Other future recommendations | 156 |
| XV. | CONCLUSIONS | 161 |
| | REFERENCES | 162 |

LIST OF FIGURES

| | | |
|-----|--|----|
| 1. | Schematic Drawing of FSW from [Mishra and Ma, 2005] | 2 |
| 2. | Picture of initial welding system at VUWAL | 6 |
| 3. | Screenshot of control software | 8 |
| 4. | Block diagram of computer board | 8 |
| 5. | Schematic of complete system after upgrade | 10 |
| 6. | Key Benefits of FSW [Mishra and Ma, 2005] | 11 |
| 7. | Friction stir weld regions [Threadgill, 2007] | 13 |
| 8. | FSW Configurations from left to right: lap, t-joint and butt | 13 |
| 9. | A void flaw from [Threadgill, 2007] | 15 |
| 10. | A weld line flaw from [Threadgill, 2007] | 15 |
| 11. | A joint line remnant from [Leonard and Lockyer, 2003] | 15 |
| 12. | FSW flaws and their causes from [Leonard and Lockyer, 2003] | 17 |
| 13. | Effects of weld problems on ultimate strength of butt joints in FSW [Barnes et al., 2006] | 18 |
| 14. | Cross sections of FSW butt joints with different flaw types present [Barnes et al., 2006] | 19 |
| 15. | A bend test indicates a root flaw is present in a weld made in 6082-T6 aluminum [Dickerson and Przydatek, 2003] | 20 |
| 16. | Range of optimum conditions for increasing plunge depths from [Kim et al., 2005] | 21 |
| 17. | “Simulation results for pin rotational speed=5s-1, workpiece translational speed=1mm/s, with top tool shoulder active and no pin thread: (a) streamlines on the mid-plane (z=0), (b) temperature distribution, (c) strength distribution and (d) distribution of internal porosity.” [He et al., 2007] | 22 |

| | | |
|-----|---|----|
| 18. | Flaw types from [Kim et al., 2005] | 23 |
| 19. | Tensile test coupons of type (a) transverse and (b) longitudinal [Khaled, 2005] | 24 |
| 20. | Fatigue test coupons [Khaled, 2005] | 26 |
| 21. | Lap joint strength and fatigue coupons [Khaled, 2005] | 27 |
| 22. | Ultrasonic testing of material [Center,] | 28 |
| 23. | “Ultrasonic beam path for the detection of voids (shown on left) and the detection of the root flaw or the lack of penetration (shown on right) [Vugrin et al., 2004] | 29 |
| 24. | An ultrasonic scan of an FS weld from [Vugrin et al., 2004] | 29 |
| 25. | An ultrasonic scan of an FS weld from [Vugrin et al., 2004] | 30 |
| 26. | Material for Ultrasonic testing [Bird, 2003] | 31 |
| 27. | Ultrasonic testing of material [Bird, 2003] | 32 |
| 28. | Ultrasonic image of FS weld [Bird, 2003] | 33 |
| 29. | Comparisons of welds with different amounts of oxide [Bird, 2003] . | 33 |
| 30. | A typical AE setup [Huang et al., 1998] | 35 |
| 31. | Setup for Acoustic Emissions detection in [Chen et al., 2003b] . . . | 36 |
| 32. | Wavelet transform of the AE signals from weld with gaps inserted [Chen et al., 2003b] | 37 |
| 33. | Table comparing welding parameters and fundamental frequencies [Muthukumaran et al., 2006] | 38 |
| 34. | “Effect of tool rotational speed and rake angle on fundamental frequency” [Muthukumaran et al., 2006] | 39 |
| 35. | Regular contours from a good weld [Sinha et al., 2006] | 40 |
| 36. | A weld run with lack of penetration [Sinha et al., 2006] | 41 |
| 37. | Contours from weld with lack of penetration [Sinha et al., 2006] . . | 41 |
| 38. | Flaw detection classification [Boldsai Khan et al., 2006a] | 43 |
| 39. | Tensile strength classification [Boldsai Khan et al., 2006a] | 43 |

| | | |
|-----|--|----|
| 40. | An FSW monitoring system [Hattingh et al., 2004] | 44 |
| 41. | FSW “force footprints” obtained for two different tool geometries [Hattingh et al., 2004] | 45 |
| 42. | FSW “force footprints” shown changing with the weld parameters [Hattingh et al., 2004] | 46 |
| 43. | The LOSTIR device [Beamish et al., 2006] | 47 |
| 44. | Influence of weld parameters on down-force [Beamish et al., 2006] . | 48 |
| 45. | FSW control architecture from [Kruger et al., 2004] | 50 |
| 46. | Computer screen for welding control and monitoring used in the paper [Loftus et al., 1999] | 51 |
| 47. | Load control loop from [Kinton and Thusty, 2000] | 53 |
| 48. | Travel load and travel speed from [Stotler and Trapp, 2007] | 54 |
| 49. | An input vector | 56 |
| 50. | After applying PCA | 57 |
| 51. | Hyperplanes [Abe, 2005] | 61 |
| 52. | K-means clustering from [Wikipedia, 2007] | 64 |
| 53. | A basic feed-forward neural network [Jain et al., 1996] | 65 |
| 54. | Outline of friction stir welding [Cook et al., 2004] | 69 |
| 55. | Control Loop in FSW | 71 |
| 56. | Samples clamped in position | 72 |
| 57. | Inserted Gap of 0.0008” | 73 |
| 58. | Surface of weld with 0.0050” gap | 74 |
| 59. | Axial forces | 74 |
| 60. | Principal Component Projections | 77 |
| 61. | Linear Discriminant Analysis | 79 |

| | | |
|-----|---|-----|
| 62. | Friction Stir Welding Basic Diagram [Cook et al., 2004] | 81 |
| 63. | Friction Stir Lap Welding Setup | 82 |
| 64. | Accuracy Results of SVM given varying bin counts | 85 |
| 65. | Accuracy of SVM with 200 Bins | 85 |
| 66. | The essential schematic diagram of FSW from [Mishra and Ma, 2005] | 88 |
| 67. | Lap FSW (left) and T-joint FSW (right) | 89 |
| 68. | T-Joint clamping methods illustrated, from left to right: full clamps with no fillet, with fillet and “open-air” | 90 |
| 69. | The fundamentals of a force sample using a Kistler dynamometer during FSW | 92 |
| 70. | Schematic diagram of T-joint welding configuration used in this paper | 93 |
| 71. | Comparing axial forces and offset | 94 |
| 72. | Comparing torque and offset | 95 |
| 73. | Comparing planar forces and offset | 95 |
| 74. | Offset predictions of GRNN | 97 |
| 75. | Predicted and actual offsets over time | 98 |
| 76. | Predicted and actual offsets over time | 100 |
| 77. | Illustration of weaving | 106 |
| 78. | Diagram of T-joint fixturing used in research | 107 |
| 79. | Tracking a straight weld-seam with weaving | 108 |
| 80. | Tracking a linearly changing weld-seam with weaving | 109 |
| 81. | Comparing cross-sections of weaved and non-weaved welds | 111 |
| 82. | Left: Tensile test fixturing Right: Tensile test results | 112 |
| 83. | Lap Welding Diagram | 118 |
| 84. | WeaveTrack Algorithm | 118 |

| | | |
|------|---|-----|
| 85. | Step response | 120 |
| 86. | Comparing Tracked and Non-Tracked Welds Given Changing Center Position | 121 |
| 87. | Tracking A Changing Center Position | 122 |
| 88. | Tensile Results | 123 |
| 89. | S-Bend Results | 124 |
| 90. | Step Test | 129 |
| 91. | Simulink model of VUWAL FSW welder | 129 |
| 92. | Comparing predicted and actual forces | 130 |
| 93. | Comparing predicted and actual forces | 131 |
| 94. | Simulated input motor reference velocity and resulting stage velocity | 132 |
| 95. | Attenuation vs. frequency for several amplitude inputs | 133 |
| 96. | Bead on plate welding with mild steel tool | 135 |
| 97. | Shadowgraph of worn tool (left) and un-used tool (right) | 135 |
| 98. | Average planar forces | 136 |
| 99. | Average axial forces | 137 |
| 100. | Average torque | 137 |
| 101. | Frequency based analysis | 138 |
| 102. | The essential schematic diagram of FSW[Mishra and Ma, 2005] . . | 140 |
| 103. | Submerged FSW setup | 142 |
| 104. | Block diagram of experimental setup | 143 |
| 105. | Fuel cell voltage in experiment 1: dashed lines indicate start and stop of welds. | 144 |
| 106. | Resistor voltage in experiment 2 | 144 |

| | | |
|------|---|-----|
| 107. | Categories of work-piece based enhancement | 157 |
| 108. | Examples of workpiece based enhancements in T-joints | 158 |
| 109. | Examples of workpiece based enhancements in butt-joints | 158 |
| 110. | Categories of machine/fixturing based enhancement | 159 |
| 111. | Examples of machine/fixturing based enhancements in T-joints . . . | 159 |
| 112. | Examples of machine/fixturing based enhancements in T-joints . . . | 160 |
| 113. | Examples of machine/fixturing based enhancements in butt-joints . . | 160 |

Part I
Introduction and Literature
Review

CHAPTER I

INTRODUCTION

Friction stir welding (FSW) is a relatively new (1991) solid-state welding technique. In FSW, a rotating tool traverses along the joint seam of the material to be joined and accomplishes welding via mechanical stirring. It was first patented in Great Britain by Wayne Thomas et al from the Welding Institute in 1991 [Thomas et al., 1991a]. The United States Patent is dated 1995 [Thomas et al., 1995].

The essential operation can be explained clearly with reference to figure 1.

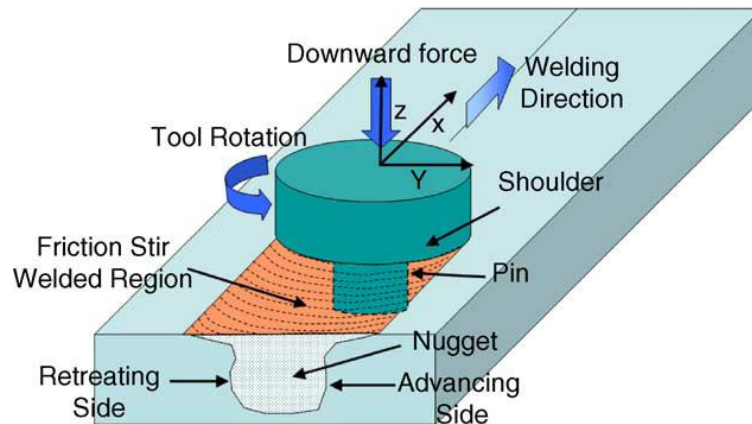


Figure 1: Schematic Drawing of FSW from [Mishra and Ma, 2005]

The FSW tool rotates about its axis and the probe (or pin) plunges into the material. The shoulder of the tool applies force to the top of the material. Heat is generated through the downward force on the shoulder which softens the material along the joint line. The tool then traverses along the weld line, and the rotating tool probe drags the plasticized material to the back of the probe. This causes the solid-state joining of the material [Khaled, 2005]. FSW has been demonstrated to be applicable to a number of joint types, including butt (demonstrated in figure 1), lap-, and T-joints.

The focus of this research has been in the monitoring and control of FSW. Specifically, research was performed and published in the areas of gap-detection, and in the area of misalignment detection and automatic seam-tracking (with patent-pending). Additional research examined related techniques for monitoring tool wear. As will be discussed in the following papers, these technologies, particularly seam-tracking, will allow improved robustness to variations in terms of both the fixturing and position of the material, as well as the FSW tool.

These improvements will broaden the applicability of FSW by enabling an automated welding robot to accommodate variations in fixturing. Additionally, the seam-tracking technologies enable rough, or perhaps no, path-planning. This ability of a welding robot to automatically follow the weld-seam has proven very valuable in more established welding technologies, such as arc welding.

An example application of the technologies developed in this research is in the welding of blind T-joints. Chapters VIII and IX discuss alignment monitoring and tracking for this joint-type. One way to stiffen a long sheet of aluminum is to weld stiffeners (bars of material) to the underside of the sheet. The stiffeners can be bent prior to welding in S-curves to provide rigidity in two directions in some applications. In the current state of FSW T-joints, where centering of the tool in the vertical member is important throughout the weld, the exact shape and position of the stiffeners is critical because they are unobservable through the horizontal sheet through which welding is accomplished. A precise path plan is also required and finally it is critical to monitor both plant and fixture to ensure that there are no changes in the plant or fixturing over time. By including the seam-tracking technology reported in this dissertation, the welding robot need only be started approximately and can then follow the weld-seam automatically. This relaxes the demand for precision in the process. This example demonstrates how seam-tracking can open new possibilities for FSW, by making it more robust and adaptive.

Additionally, the technologies provide quality control for existing FSW technologies. Because proper fixturing and alignment are important for ensuring quality welds, the technologies described in this paper provide means for in-process detection of both gaps in fixturing and misalignment.

Because of the importance of seam-tracking in other welding technologies, it is expected that seam-tracking for FSW represents an important step-forward for FSW and will be found to be a beneficial inclusion in many industrial processes. Importantly, as will be discussed in depth in the related publication chapters, the cost of inclusion is minimal. This is first because the signals used in all methods of this paper are force and torque, which are intrinsic to the welding process, and are very commonly monitored in FSW. It is unlikely that any robotic FSW system would not have force and torque monitoring capabilities. Secondly, the seam-tracking system can be set-up in such a way as to incorporate other important force-based FSW control and monitoring techniques, such as load control. This is an important result, as it would not do to have to sacrifice axial load control to gain seam-tracking.

The findings indicate that the monitoring and control techniques documented in this dissertation are likely to have a positive impact in the industrial application of FSW.

Overview of dissertation

This dissertation presents research through published and submitted journal papers, with supplemental additional material from conference papers and unpublished research. The dissertation is broken down in to four parts.

Part I reviews work completed in upgrading the machinery and background literature. Chapter II reviews the work done upgrading the system from manual operation to computer control. In chapters III and IV, the background literature for the research is presented. Chapter III reviews the literature of FSW, with specific focuses

on flaws and faults in FSW, and publications on automatic monitoring and control of FSW. Chapter IV reviews the literature of modern mathematical techniques for detection and classification. These techniques are employed in several of the published papers included in the dissertation.

Part II presents published or submitted journal papers (except for chapter VI which is a conference paper included because it provides further information from the research submitted in the journal article in chapter V). Chapters V and VI present research in automatic gap detection. The article in chapter VII, demonstrates automatic mis-alignment detection for T-joint FSW. Finally, chapters VIII and IX demonstrate seam-tracking for FSW in T- and lap-joints, respectively.

In Part III, research which was not published but is relevant to the dissertation is presented. Chapter X documents research done modeling the welding system at the Vanderbilt University Welding and Automation Lab (VUWAL) and its applications for future research. Chapter XI shows research presented at Aeromat 2007 which demonstrates a technique, similar to those above, for monitoring and identifying tool wear in FSW. Chapter XII gives research which demonstrates the release of Hydrogen in submerged FSW (which is FSW performed underwater).

Part IV presents discussion, conclusions and recommendations for future work. Chapter XIII is a discussion of research presented and its implications for FSW. Chapter XIV suggests future directions for this research. Finally, chapter XV provides conclusions.

CHAPTER II

DOCUMENTATION OF EQUIPMENT UPGRADE

Initial configuration

In order to complete this research, it was necessary to upgrade the existing FSW equipment in the Vanderbilt University Welding and Automation Laboratory (VUWAL). The original setup was based on a converted milling machine which provided the overall platform. The milling machine was modified to hold an FSW tool, which was driven by a 7HP motor through a belt. Additionally, a Kistler dynamometer was placed in the system to record forces experienced by the tool. Finally, a second motor was added to drive the horizontal stage at speeds greater than those provided by the milling machine. Both of these motors were originally controlled manually through separate motor drives. A picture of this initial system is shown in figure 2.

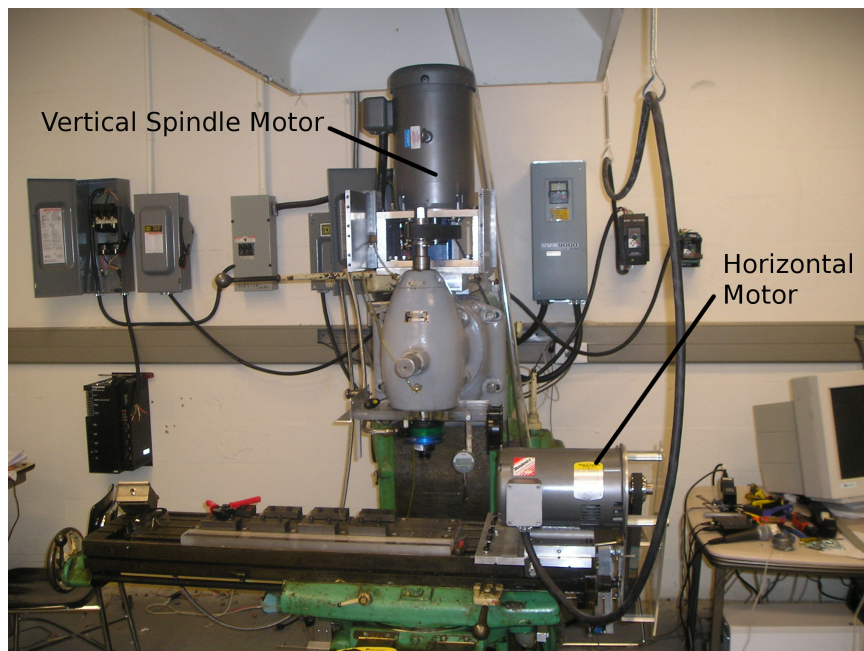


Figure 2: Picture of initial welding system at VUWAL

Modifications

In order to conduct research and build systems for monitoring and control, the system was adapted into a computer-controlled welding set-up. A networked group of computers now control all motors and monitor all feedback signals. This system provides safety, both for graduate student operators and to the system itself. Importantly, it also enables feedback control, which is currently employed in the research described, as well as other research conducted in the lab. Finally, the system automates the recording of data and running of weld cycles for ease and consistency of experimentation.

The following sections quickly outline work done improving the system.

Computers and computer programs

Two computers were set-up to control the FSW process, by both reading the system sensors, and controlling the motors. Additionally, software programs were written, both for manually monitoring and controlling the software, and for running automated operations, such as tracking. The main screen for software control is shown in figure 3.

In addition to the computers, a computer board was set up for the continuous reading of analog and digital sensors. This board continuously polled the sensors and then transmitted the data back to the computers via an ethernet connection. A block diagram of this board is shown in figure 4.

Sensors

Sensors were added to the system for monitoring purposes. A complete list of the added sensors follows.

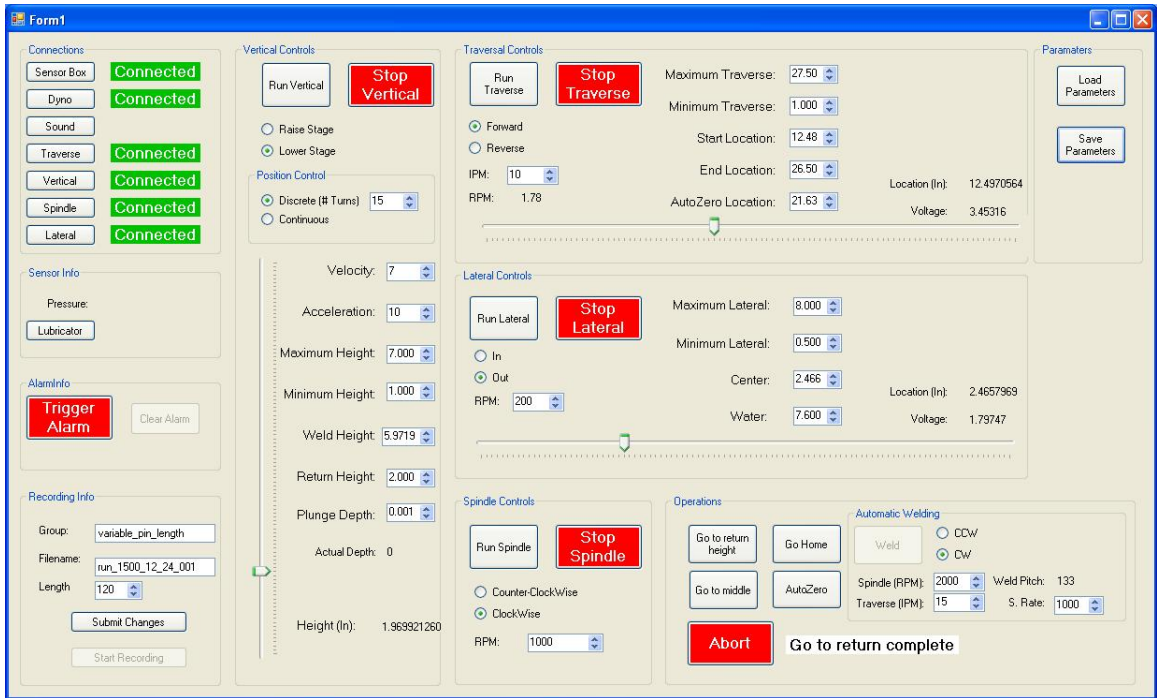


Figure 3: Screenshot of control software

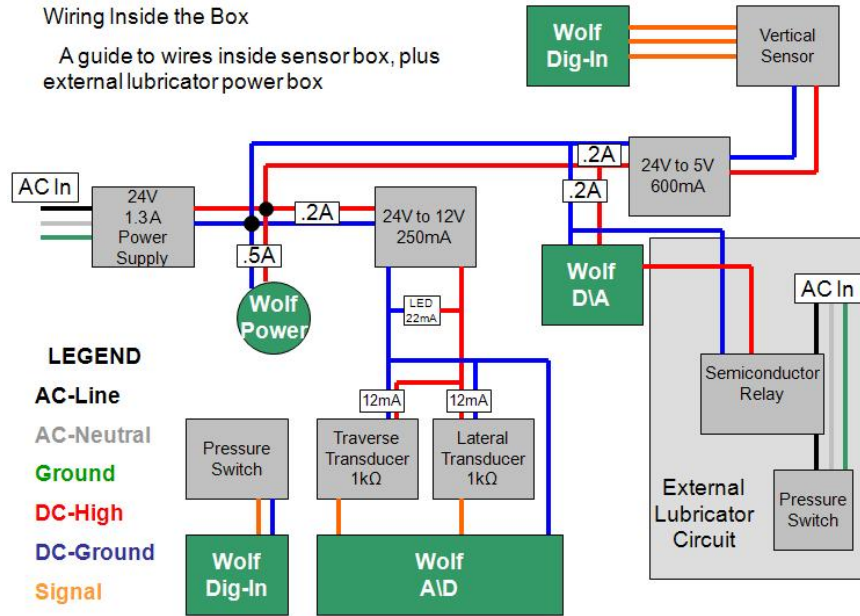


Figure 4: Block diagram of computer board

String Potentiometers Monitor stage position in both traverse and lateral directions.

Magnetic linear position encoder Monitors the vertical position of the stage

Rotary encoder on tool spindle Monitors rotary position of tool during welding to enable the relating of tool position with collected force

Rotary encoder on lateral motor Monitors position of lateral motion, providing information on lateral motor speed and position prior to non-linear effects of stage gearing such as backlash for higher precision control.

Safety switch Ensures safety door is closed prior to welding

Pressure switch Ensures lubricator pressure is on prior to welding

Emergency button Allows emergency stop by user not seated at operating computer

Motors

Two additional motors were included to drive the stage laterally and vertically. Additionally, the motor drives for all four motors are controlled directly by the computer network.

Total system

A schematic diagram of the complete system is shown on in figure 5.

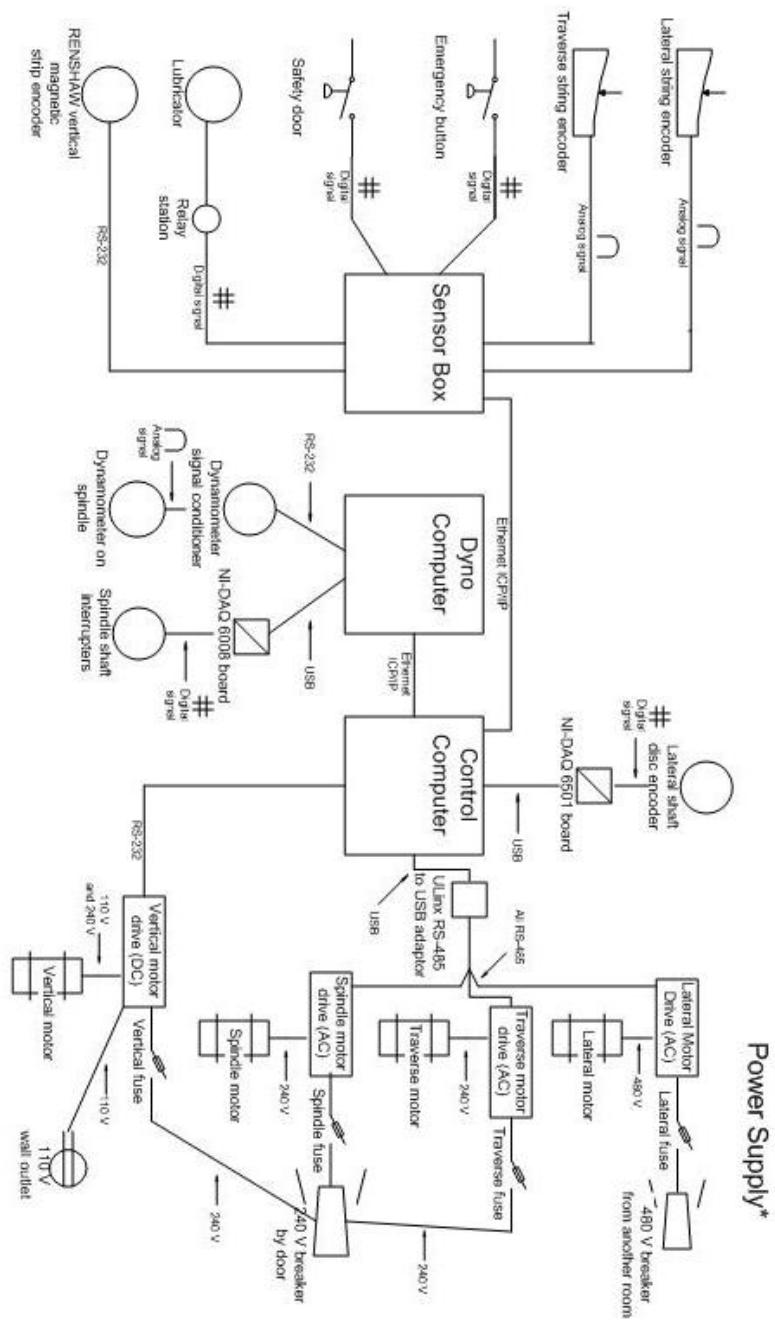


Figure 5: Schematic of complete system after upgrade

CHAPTER III

BACKGROUND LITERATURE REVIEW: FSW - FLAWS, MONITORING AND CONTROL

Friction Stir Welding

Friction Stir Welding Overview

As was discussed in the introduction, FSW is a solid-state welding process in which the material is joined via mechanical stirring.

Advantages of Friction Stir Welding

Friction Stir Welding has a number of advantages over other joining methods. One of the most commonly cited is that the solid-state process causes the material to undergo plastic deformation resulting in the “generation of fine and equiaxed recrystallized grains”; this fine micro structure produces good mechanical properties [Mishra and Ma, 2005]. Additionally, FSW uses no filler material, and uses less energy than processes such as fusion welding. Figure 6, taken from [Mishra and Ma, 2005] gives a more complete list of the advantages of FSW.

| Key benefits of friction stir welding | | |
|--|--|---|
| Metallurgical benefits | Environmental benefits | Energy benefits |
| Solid phase process | No shielding gas required | Improved materials use (e.g., joining different thickness) allows reduction in weight |
| Low distortion of workpiece | No surface cleaning required | Only 2.5% of the energy needed for a laser weld |
| Good dimensional stability and repeatability | Eliminate grinding wastes | Decreased fuel consumption in light weight aircraft, automotive and ship applications |
| No loss of alloying elements | Eliminate solvents required for degreasing | |
| Excellent metallurgical properties in the joint area | Consumable materials saving, such as rags, wire or any other gases | |
| Fine microstructure | | |
| Absence of cracking | | |
| Replace multiple parts joined by fasteners | | |

Figure 6: Key Benefits of FSW [Mishra and Ma, 2005]

Terminology in Friction Stir Welding

Recent work by Threadgill has focused on standardizing the language used to describe FSW. In this paper the syntax outlined in “Terminology in friction stir welding” will be used [Threadgill, 2007].

The FSW *tool* is the whole of the rotating device between the spindle and the material. The *probe* is the part embedded in the material, and the larger diameter *shoulder* is the part which rests directly on the material.

The “welding parameters” for FSW are the welding speed, and the tool rotation speed. These both affect the quality of the weld to a great extent and will be in later sections concerning weld quality and control.

The forces applied are described as X, Y and Z. The Z force, or axial force, is applied vertically downward through the tool, and is proportional to a number of other parameters but most directly to the plunge depth of the tool, although the rotation and weld speed influence this, and other force values. The X force is the force experienced “along the weld”, with positive X being in the direction of tool traversal. The Y force, or transverse force, is perpendicular to weld traverse. (See figure 1)

The final terminology to review is the “microstructural classification” [Threadgill, 2007]. Friction stir weld cross samples are typically classified into four regions (refer to figure 7).

A: Parent Material Area unaffected by weld process, either through heat or deformation

B: Heat Affected Zone (HAZ) Material affected only by heat

C: Thermo-mechanically Affected Zone (TMAZ) Material affected by both deformation and heat, may not be completely recrystallized

D: Nugget This is the recrystallized region of the weld [Threadgill, 2007]

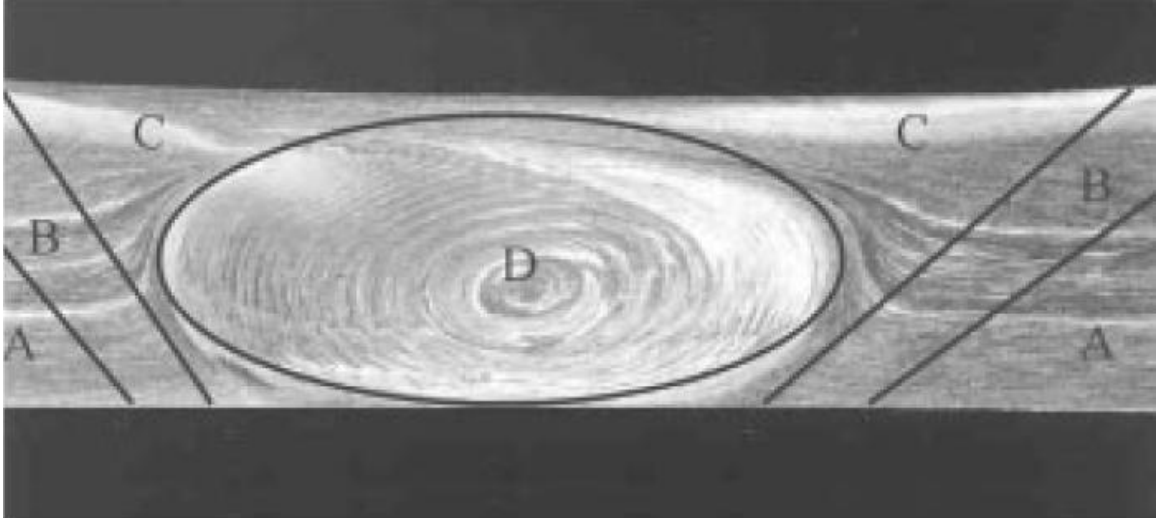


Figure 7: Friction stir weld regions [Threadgill, 2007]

FSW configurations

There are several ways that FSW joints can be fixtured. In figure 1, the two samples to be joined are butted against each other and the tool traverses this joint producing the weld. This is referred to as a butt joint. In this work, three different configurations are discussed: lap- T- and butt-joints. These are shown in figure 8.

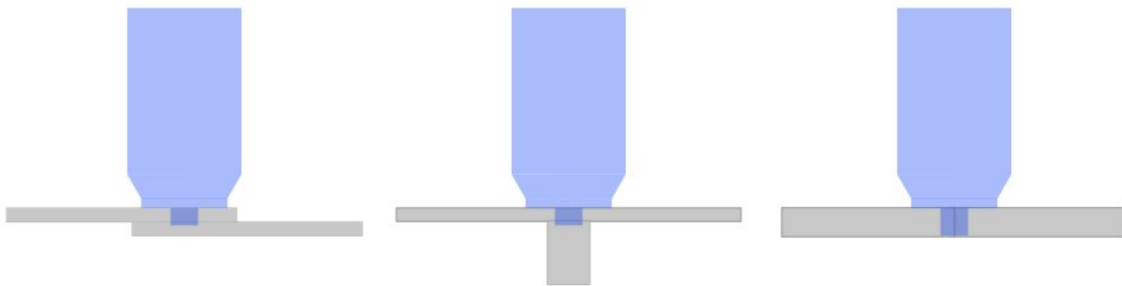


Figure 8: FSW Configurations from left to right: lap, t-joint and butt

The leftmost weld is a lap joint, where the material to be welded is laid one on top of the other. The probe penetrates through the upper material and just into the lower. The middle configuration is a t-joint, which is similar to a lap joint. In this case, there is a horizontal member on top and a vertical member underneath. The

probe penetrates through the horizontal member and just into the vertical member. To the right is the butt joint.

Faults in Friction Stir Welding

There are a number of advantages of FSW given in the previous section. Among these advantages are that FSW, being solid-state, overcomes the problems of porosity and hot cracking which are seen in fusion welds [Leonard and Lockyer, 2003]. However, there are a number of flaws and defects which do occur in FSW. In this section, a brief overview of these flaws is presented, followed by a review of the pertinent literature. The literature gives information about the types, causes and effects of faults in friction stir welding.

Brief look at defects in FSW

When discussing quality in FSW the paper “Terminology in Friction Stir Welding” uses the following definitions:

Imperfection A departure of a quality characteristic from its intended condition

Flaw An imperfection detectable by NDE (non-destructive evaluation)

Defect A flaw of such size, shape orientation location or properties as to be rejectable
[Threadgill, 2007]

From these definitions one can see that not all “flaws” are “defects”; classification depends on the requirements of the process [Threadgill, 2007].

In the FSW literature, there are in general four main flaw types:

Volumetric Flaws or Voids Are voids or gaps in the weld, possibly breaking through the surface. An example is shown in figure 9

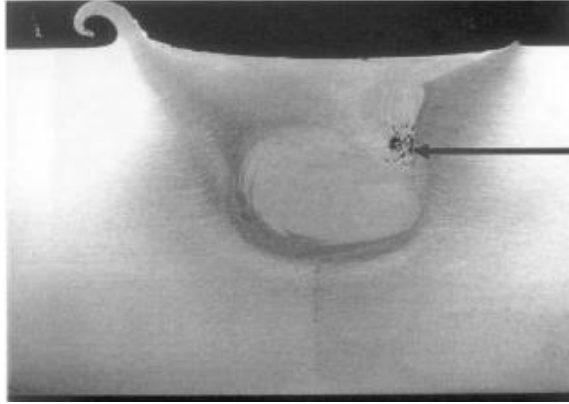


Figure 9: A void flaw from [Threadgill, 2007]

Weld Line Flaws or Root Flaws These flaws pertain to flaws associated with the original weld line. A typical case is lack of bond along the weld-line, or a portion of the weld-line left unwelded. This is shown in figure 10.



Figure 10: A weld line flaw from [Threadgill, 2007]

Joint Line Remnants This is the “distribution of oxide particles through the thickness of the aluminum” [Leonard and Lockyer, 2003]. It often results in a weaker bond.

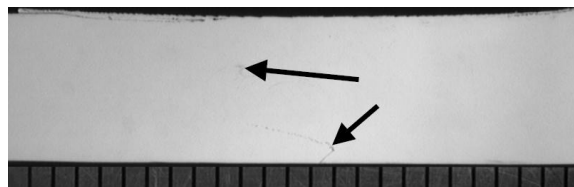


Figure 11: A joint line remnant from [Leonard and Lockyer, 2003]

Excessive Flash Flash is the metal ejected from the weld. It is often attributed to excessive heat input.

Literature review

Flaws in Friction Stir Welds

A good overview of flaws in Friction Stir Welding is the paper “Flaws in Friction Stir Welds”, which was presented at the 4th International Symposium on Friction Stir Welding in 2003 [Leonard and Lockyer, 2003].

The paper first points out that FSW has the advantage of not producing faults associated with fusion welding such as porosity and heat affected liquitation cracking. The paper then discusses and explains the flaws which do pose a problem for FSW and their causes. The flaws investigated in this paper were: voids, root flaws and joint line remnants. The authors attempted to induce these flaws by inserting gaps in between the weld samples, using insufficient plunge force, setting improper weld parameters (welding speed in this case) and finally by increasing the size of the oxide layers in the samples through anodisation.

This experiment lead to a very helpful conclusion in the form of the causes of these main flaws in Friction Stir Welding, shown in figure 12.

Defects formation in Friction Stir Welding of Aluminum Alloys

The paper “Defects formation in Friction Stir Welding of Aluminum Alloys” examines defect formation in the 5083-O, 2024-T3 and 6063-T6 alloys of aluminum [Leal and Loureiro, 2004]. The authors welded the specimens using varied weld speeds and axial forces. They found a tendency for defect formation in 2024 and 5083, but

| Flaw Type | Location | Causes |
|--------------------|--|---|
| Void | Advancing side at edge of weld nugget. | <ol style="list-style-type: none"> 1. Reduced forging pressure. 2. Welding speed too high. 3. Plates not clamped close enough together. Joint gap too wide. |
| Void | Beneath top surface of weld | Welding speed too high |
| Joint Line Remnant | Weld nugget, extending from the root of the weld at the point where the original plates butted together. | <ol style="list-style-type: none"> 1. Inadequate removal of oxide from plate edges. 2. Inadequate disruption and dispersal of oxide by tool. 3. Increase in welding speed. 4. Increase in tool shoulder diameter. |
| Root flaw | Weld nugget, extending from the root of the weld at the point where the original plates butted together. | <ol style="list-style-type: none"> 1. Tool pin too short. 2. Incorrect tool plunge depth. 3. Poor joint to tool alignment. |

Figure 12: FSW flaws and their causes from [Leonard and Lockyer, 2003]

not in 6061. Additionally, the welds in 2024 and 5083 had identical or superior hardness to the parent material whereas 6063 had a drastic reduction. They also made the following general observations:

- The increase in travel speed increases the frequency of defect formation
- The increase in axial force changes the position of the defect from the surface to the center of the weld

Effects of Friction Stir Welding Defects on 7075 Joint Strength and Fatigue Life

In “Effects of Friction Stir Welding Defects on 7075 Joint Strength and Fatigue Life”, the authors investigate the impact of certain problem conditions on the tensile strength and fatigue life of 7075 FSW samples [Barnes et al., 2006]. These problems were not in and of themselves defects, but more defect causing conditions, like those listed in figure 12. The five chosen preconditions were:

- Weld Gap

- Thickness Mismatch
- Lack of Penetration (using shortened pins)
- Worn Tool
- Minimum Recrystallized Grain Structure in extruded stiffener

The authors state that when choosing gap or thickness mismatch, they used values “slightly greater than those allowed in typical specifications.” With this guideline, the authors found that in terms of both ultimate tensile strength and fatigue life, only the lack of penetration had any statistically significant effect (see figure 13).

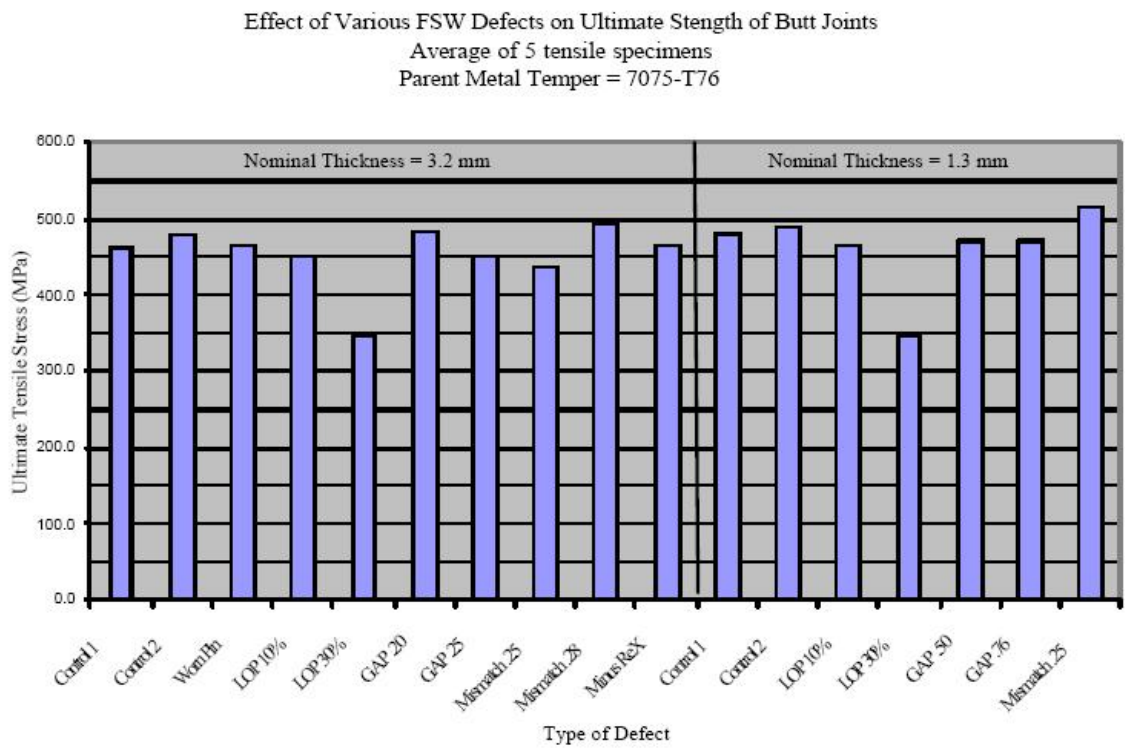


Figure 13: Effects of weld problems on ultimate strength of butt joints in FSW [Barnes et al., 2006]

Further, the authors found that lack of penetration was the only condition to create a noticeable flaw (a root flaw) visible in cross-sectioning (see figure 14).

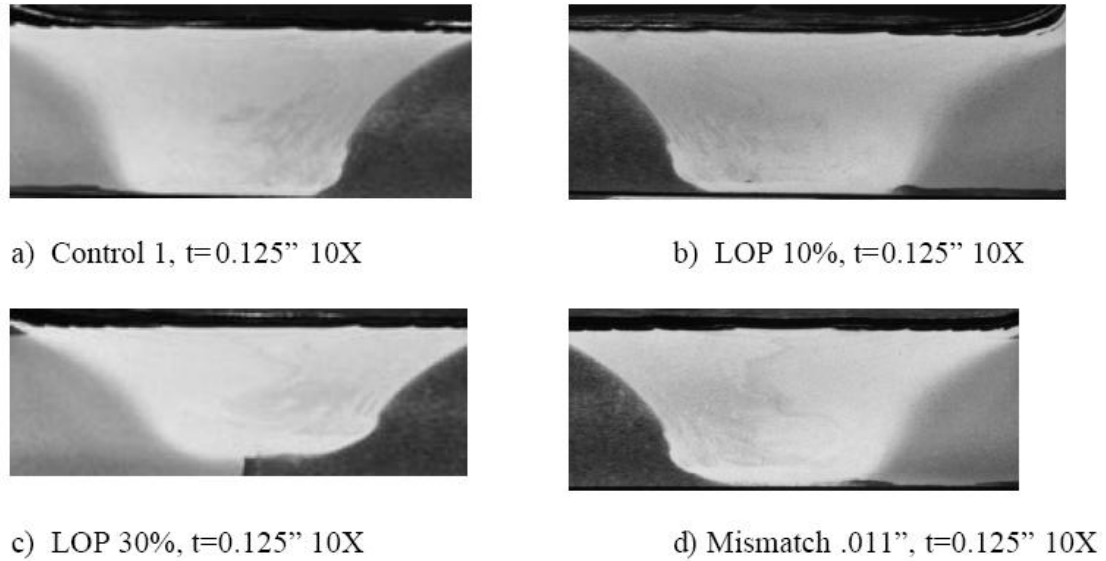


Figure 14: Cross sections of FSW butt joints with different flaw types present [Barnes et al., 2006]

The authors conclude that the FSW process, when proper parameters and tooling are selected is quite robust even when problems such as gaps, thickness mismatches and tool wear are present.

Fatigue of friction stir welds in aluminum alloys that contain root flaws

The paper “Fatigue of friction stir welds in aluminum alloys that contain root flaws” examined the effects of root flaws on butt weld samples made in 5083-O, 6082-T6, and 5083-H321 aluminum [Dickerson and Przydatek, 2003]. Welds were made both flaw free and with root flaws. The root flaws could not be detected non-destructively, but were demonstrated through cracking during bend tests (see figure 15). In these tests, the material is bent until a crack appears, and the angle of this bend is recorded.

The results of these experiments indicated the following:

- Root flaws less than $.35\text{mm}$ deep cause no identifiable degradation in mechanical performance compared to flaw free welds

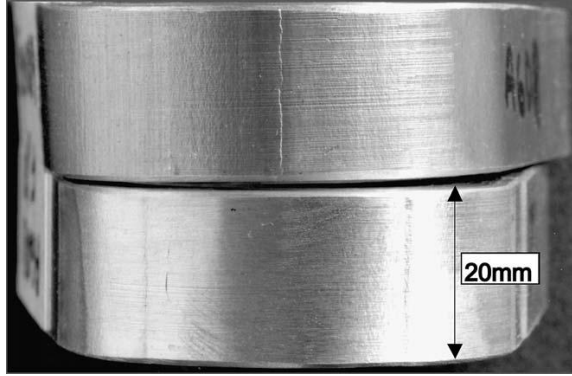


Figure 15: A bend test indicates a root flaw is present in a weld made in 6082-T6 aluminum [Dickerson and Przydatek, 2003]

- Root flaws in the 5083 and in the 6082-T6 welds did not induce loss in static or fatigue strength while the larger flaws in 5083-H321 caused reductions in both.
- SEM analysis of exposed root flaw surface showed partial bonding

The authors state that any root flaws deeper than 0.35mm or that affects tensile properties should be considered un-bonded.

Three defect types in friction stir welding of aluminum die casting alloy

This paper attempts to find optimal welding parameters in terms of welding and rotation speed given varied plunge forces [Kim et al., 2005]. The author discusses three flaws that develop in the non-optimal welds, namely: excessive flash; cavities (voids) caused by insufficient heating; and cavities formed by abnormal stirring.

The paper contains an interesting figure which shows the locations in the parameter space of the optimal conditions for FSW welding, as well as for producing their three defect types, for increasing plunge depths. See figure 16.

These results demonstrate the relationship between flaw-types and parameter settings. Additionally, the authors indicate that the size of the optimal region expands with increasing plunge force. A useful result for improving robustness.

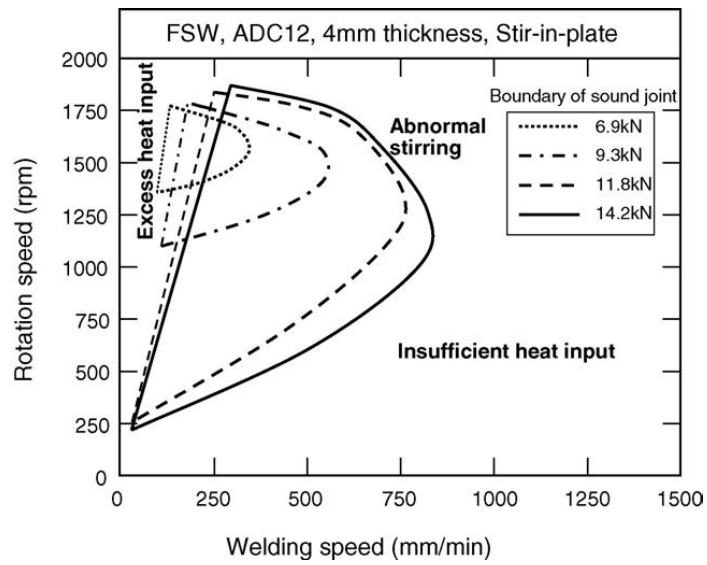


Figure 16: Range of optimum conditions for increasing plunge depths from [Kim et al., 2005]

Three-Dimensional Modeling of Void Growth in Friction Stir Welding of Stainless Steel

This paper reported on modeling to study the growth of voids in FSW [He et al., 2007].

Figure 17 shows some simulation from this experiment.

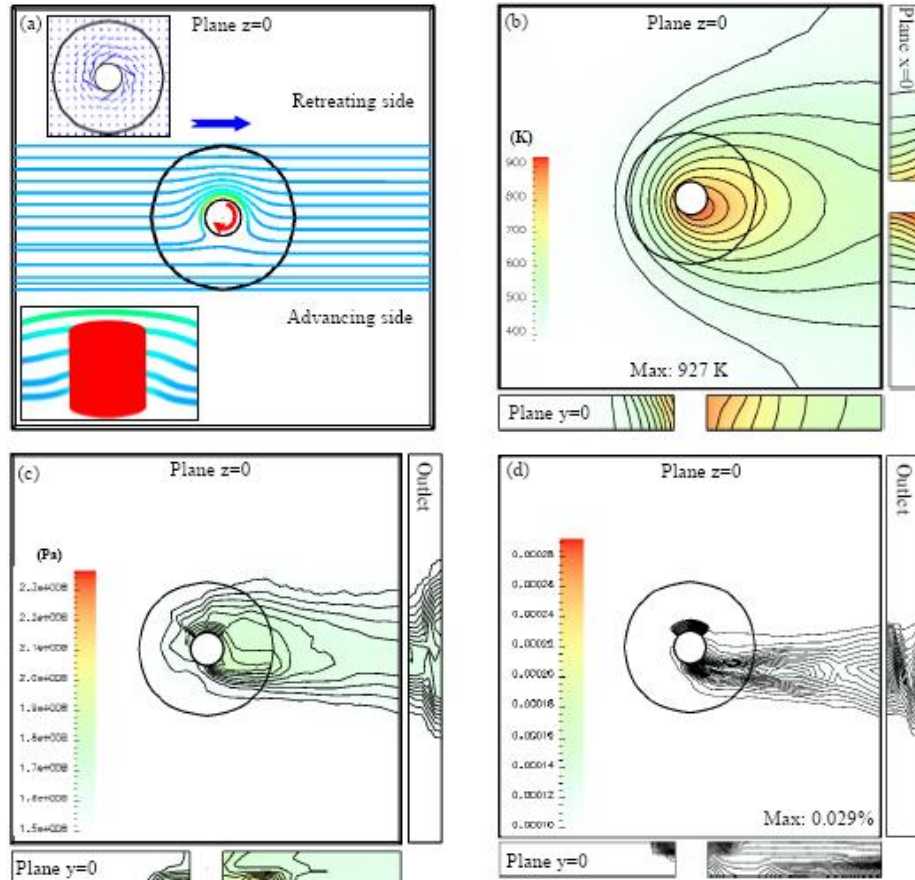


Figure 17: “Simulation results for pin rotational speed=5s-1, workpiece translational speed=1mm/s, with top tool shoulder active and no pin thread: (a) streamlines on the mid-plane (z=0), (b) temperature distribution, (c) strength distribution and (d) distribution of internal porosity.” [He et al., 2007]

The results obtained by this simulation are consistent with experimental measurements. Some conclusions are that:

- Increasing weld speed reduces heat input; this increases void formation.

- Increasing rotational speed raises weld the temperature, which reduces void growth. However this leads also to a general weld strength decrease.

Flaw Detection in Friction Stir Welding

Introduction

The flaws discussed in the preceding section can have a range of effects on the weld sample. As discussed, they can severely impact the tensile strength and fatigue strength of the weld, or they can be nearly inconsequential. Because it is possible for these flaws to undermine the integrity of the weld, it is often necessary to evaluate the weld to ensure that it is flaw free, or at least free of any consequential flaws.

This can be quite difficult. While some flaws may be easily observed by eye, others are not observable. Figure 18 below illustrates the difference of observability in fault types.

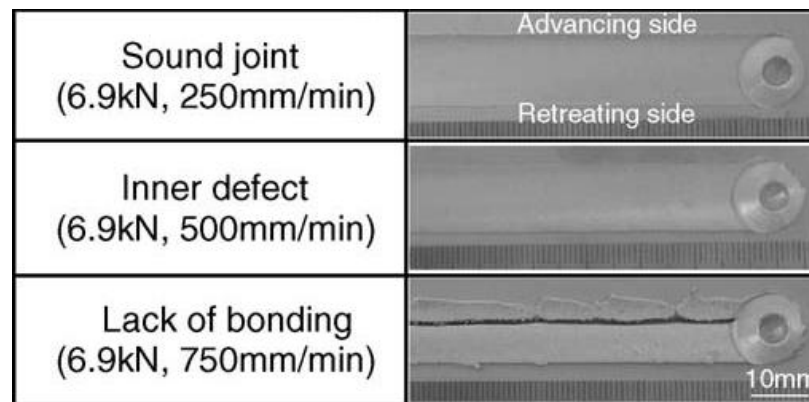


Figure 18: Flaw types from [Kim et al., 2005]

The discovery of flaws in FSW is not trivial and is therefore an active field of research within FSW. It can be subdivided into different paradigms.

Offline destructive weld inspections The most straight forward way of detecting flaws are through a number of standard mechanical testing techniques. These include tensile tests, root bend tests and cross-sectioning.

Offline non-destructive weld inspections This type of detection does not damage the weld, but is not performed during the weld process so if a defect is detected the sample must be rejected.

Online weld monitoring This is a very useful way of checking for flaws in FSW, because it allows for the possibility of correction if flaws are detected soon enough. This is the category where the monitoring research documented in this dissertation falls in.

Offline destructive weld inspection

Offline destructive inspection of welds is a more traditional way of inspecting weld joints and determining characteristics such as tensile strength, fatigue strength and to determine if the weld contains flaws. In this section the basic methods are reviewed. In the research documented in this dissertation, these methods are used to verify the results obtained non-destructively.

Tensile Testing

When this type of testing is used, the welds are machined into coupons and then pulled to the point of breaking by a tensile testing machine. Figure 19 shows what these machined coupons look like in Friction Stir Welding.

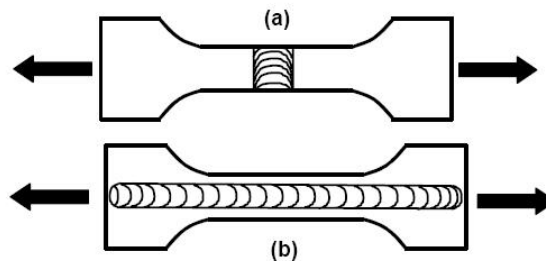


Figure 19: Tensile test coupons of type (a) transverse and (b) longitudinal [Khaled, 2005]

As shown in the above figure, the tension test can either run transverse or along the weld. From this test, one can learn the ultimate tensile strength, yield strength and elongation of the welded sample. These are important descriptors of weld quality and are tightly coupled to the presence of flaws or poor weld parameter selection.

Fatigue Testing

Fatigue testing, unlike tensile testing, tests the effects of repeated loading on the material. This provides important information about the capability to endure load applications over time. This sort of testing is reported in much of the literature.

Fatigue testing is not used in the research documented in this dissertation, but in the future it may be useful. The presence of flaws will likely impact the fatigue strength of the weld, so work in flaw detection will indirectly search for drops in fatigue strength.

In figure 20 taken from [Khaled, 2005], one method for extracting coupons from FSW welds is shown.

Bend Testing

Bend testing can be used as a means to detect root flaws [Dickerson and Przydatek, 2003] or to “provide qualitative information about longitudinal and transverse ductility [Khaled, 2005]. The test results can be reported in terms of the “maximum outer fiber elongation that can be sustained without cracking [Khaled, 2005]. Figure 15 shows two samples which have been bend tested.

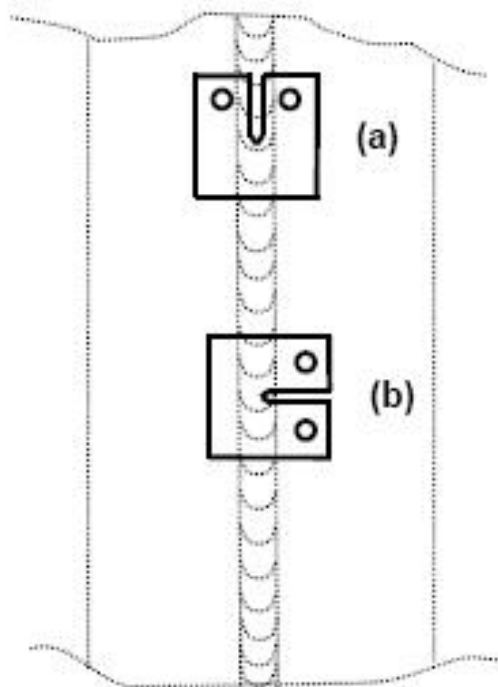


Figure 20: Fatigue test coupons [Khaled, 2005]

Testing for lap welds

According to [Khaled, 2005], most authors test lap welds using “single-lap-tension-shear-test to generate strength and S-N fatigue data for lap joints.” An illustration of the coupons used in this test are shown in figure 21.

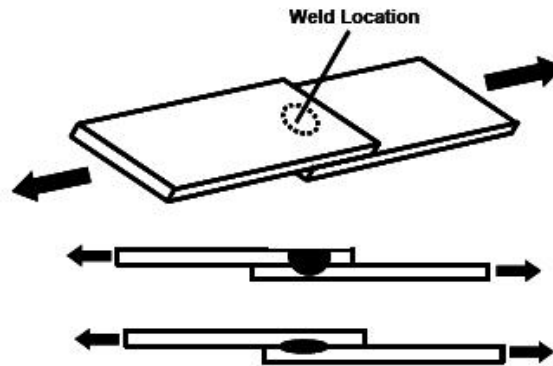


Figure 21: Lap joint strength and fatigue coupons [Khaled, 2005]

The coupons once machined can be tested using methods like the ones listed earlier for butt joints.

Offline non-destructive testing

In this section, the literature of off-line non-destructive testing is reviewed. Several papers were found which generally fit this category. However, these are not strictly off-line tests, as they could be incorporated into an online loop, as will be shown. However, in the usage described in the paper, the testing is done offline as a means of non-destructively searching for flaws.

This differs from tests which are intrinsically online because they monitor signals which are emitted during the weld process itself. These will be discussed later.

All three of the papers in this section use ultrasonic inspection to discover flaws in the material. The papers emphasize the ability to discover flaws which are buried in the material without having to destroy the specimen.

Non Destructive Detection of Flaws in FSW and their Metallographic Characterization

The paper “Non Destructive Detection of Flaws in FSW and their Metallographic Characterization” discusses the use of ultrasonic inspection to detect flaws in FS welds [Vugrin et al., 2004]. The flaws in this experiment were inserted by using aluminum samples which had larger than normal oxide layers deposited.

The “Non-Destructive Testing Resource Center” website gives a basic tutorial on Ultrasonic Testing [Center,]. With reference to figure 22, the transducer “generates high frequency ultrasonic energy”. Cracks or other discontinuities will reflect the signal back and this can be detected and used to find flaws in welds.

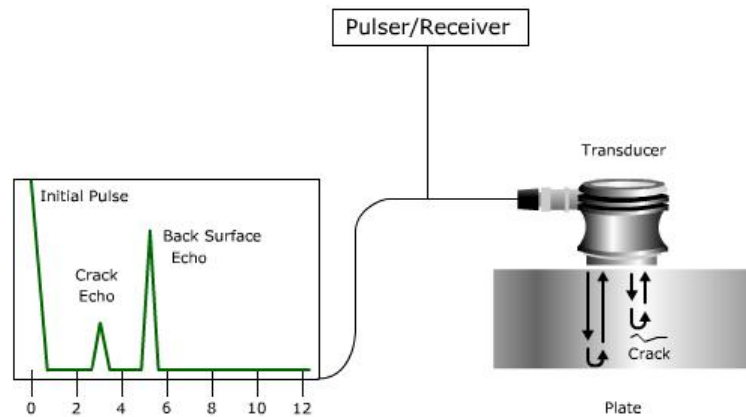


Figure 22: Ultrasonic testing of material [Center,]

The authors report that the ultrasonic inspection method when applied to FSW is capable of finding voids in the method described above. However, for lack of penetration and joint line remnants, it is necessary to apply the ultrasonic waves at an angle, as shown in figure 23

The authors state that this method is able to detect both voids and root flaws.

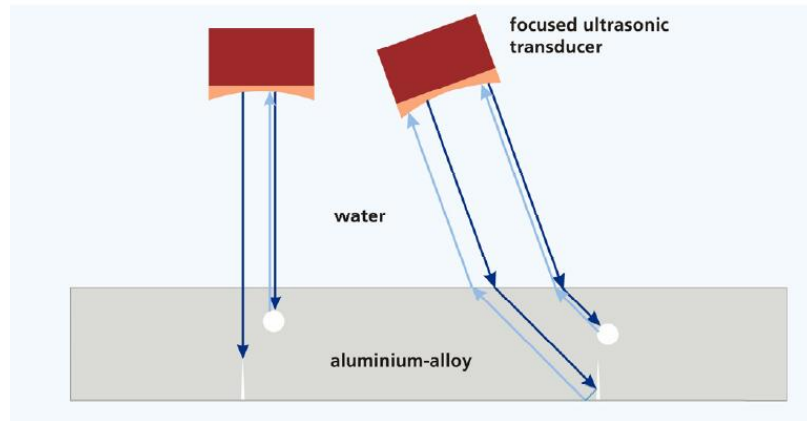


Figure 23: “Ultrasonic beam path for the detection of voids (shown on left) and the detection of the root flaw or the lack of penetration (shown on right) [Vugrin et al., 2004]

Further by “using a focused transducer with a high frequency . . . the detection of very small flaws was enabled.”

Some of the ultrasonic scans are shown in figures 24 and 25.

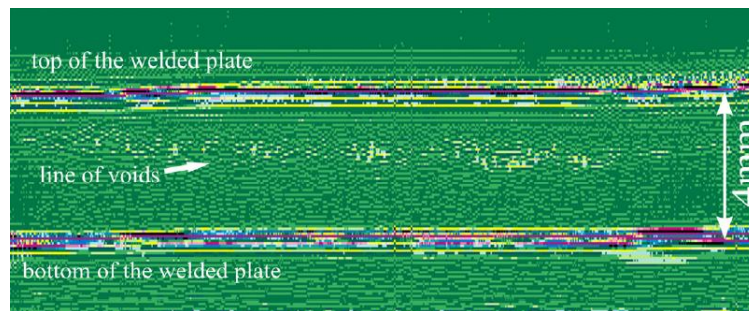


Figure 24: An ultrasonic scan of an FS weld from [Vugrin et al., 2004]

Ultrasonic Phased Array Inspection Technology for the Evaluation of Friction Stir Welds

The papers “Ultrasonic Phased Array Inspection Technology for the Evaluation of Friction Stir Welds” and “The inspection of friction stir welded aluminum plant”, both by Colin Bird of TWI, research into using ultrasonics for the detection of flaws in FSW is discussed [Bird, 2003] [Bird, 2004].

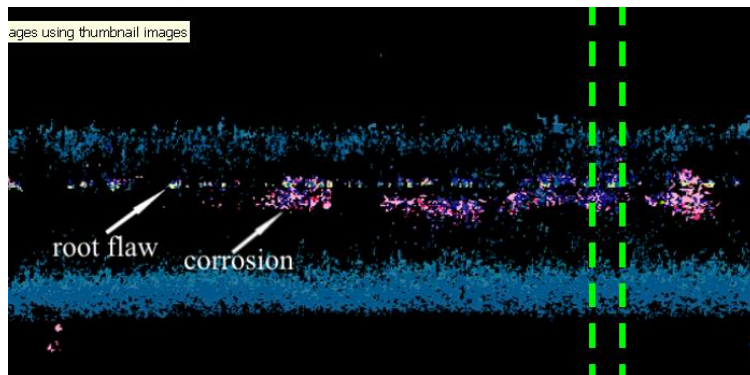


Figure 25: An ultrasonic scan of an FS weld from [Vugrin et al., 2004]

The author states that conventional flaws such as voids, or lack of penetration resultant flaws can be detected by the method outlined above. This is demonstrated in figures 26 and 27, which a cross-section of a weld with flaws, and its ultrasonic scan result.

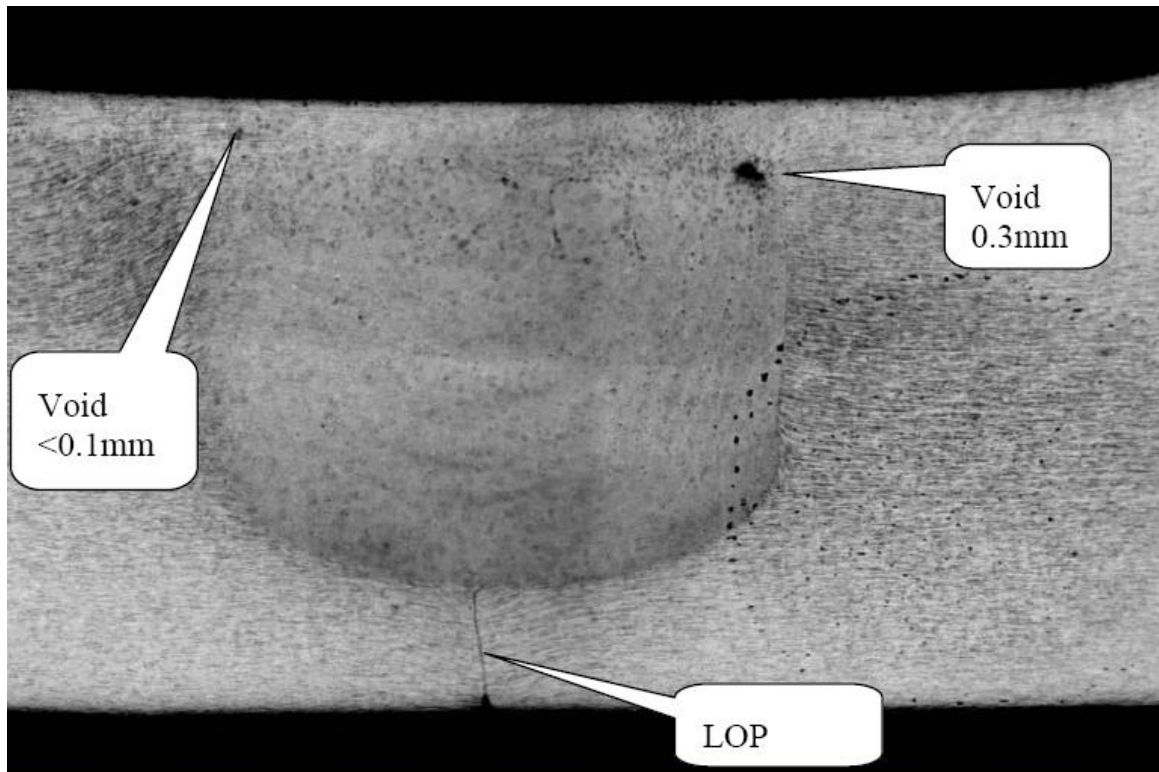


Figure 26: Material for Ultrasonic testing [Bird, 2003]

However, joint line remnant flaws, due to their fineness, required more research. The paper first investigates the use of velocity of ultrasonics and then frequency, but neither of these were capable of detecting the remnants.

However, the author does find a solution. First, the author states that: “where the weld nugget is correctly forged through to the weld root, entrapped oxide defects should not be present.” Therefore, if there was a method for non-destructively determining the depth of the “correctly stirred zone”, than that method would also ensure a “low probability of entrapped oxide.” [Bird, 2003]

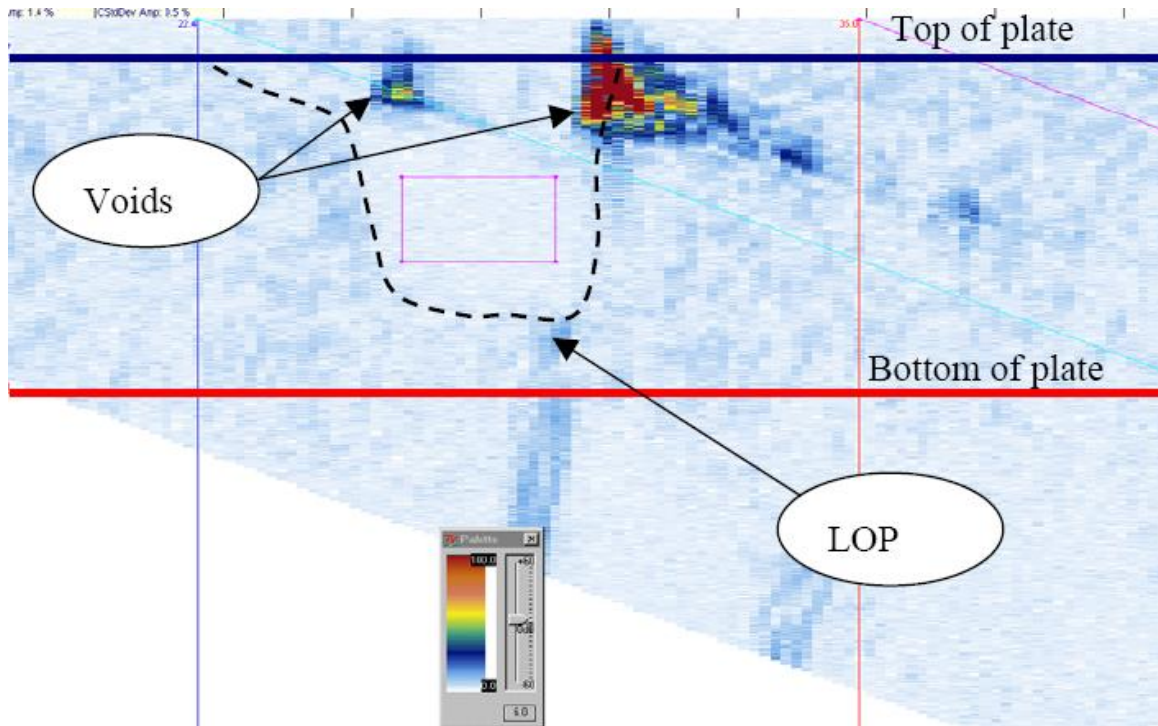


Figure 27: Ultrasonic testing of material [Bird, 2003]

This dual problem, that of detecting the correctness of the weld nugget, the author solves with ultrasonic noise distribution. The authors find that there was a “noise pattern associated with the FSW nugget” (see figure 28).

The authors then tried to determine a metric to compare welds with joint line remnants (based on an improperly forged nugget) vs. those with optimal depths. The chosen detection metric is the ratio of the parent plate noise against weld root noise. The results of this comparison are shown in figure 29.

The author concludes that this method is capable of “identifying possible entrapped oxide flaws with a through wall size greater 0.5mm and greater.”

Online monitoring of Friction Stir Welding

In this section, papers which attempt to monitor the quality of the FSW in-process are reviewed. These papers use signals which are generated during the welding process

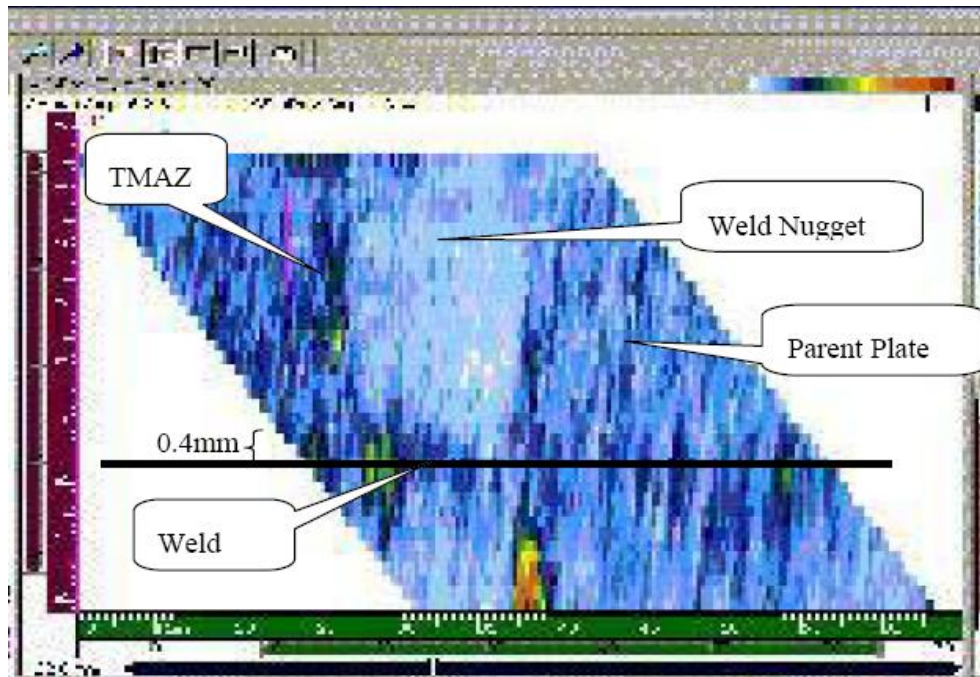


Figure 28: Ultrasonic image of FS weld [Bird, 2003]

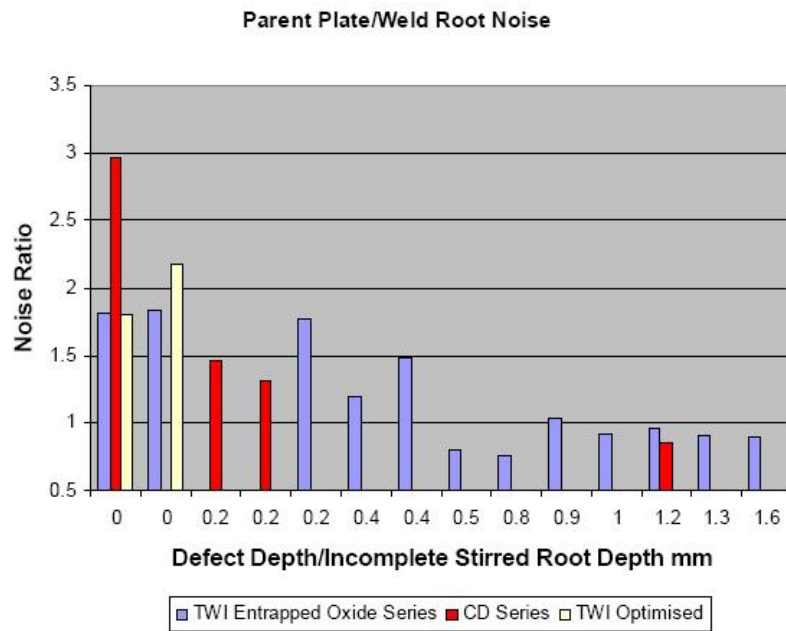


Figure 29: Comparisons of welds with different amounts of oxide [Bird, 2003]

itself to make inferences about the quality of the weld, and the presence or lack of flaws.

While the papers share the similarity of using in-process signals, they differ in which signals they rely on. These signals can be acoustic emissions, forces, temperature, electro-magnetic radiation, motor current and combinations thereof. In this section, the papers are grouped by signal employed.

Acoustic Emission

In the papers “Acoustic Emission in Monitoring Quality of Weld in Friction Stir Welding” and “Wavelet transform analysis of acoustic emission in monitoring friction stir welding of 6061 aluminum”, the authors discuss the use of acoustic emissions (AE) as a signal for the monitoring of the FSW process [Chen et al., 2003a] [Chen et al., 2003b].

Acoustic emissions are defined in [Huang et al., 1998] as “the stress waves produced by the sudden internal stress redistribution of the materials caused by the changes in the internal structure.” An AE based detection system, in general, works by monitoring the emissions of a work piece, and performing a certain amount of processing and then looking for features which might indicate a failure. This is shown in figure 30

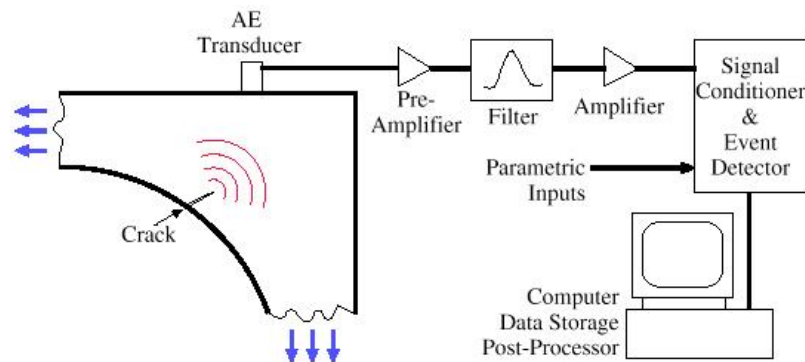


Figure 30: A typical AE setup [Huang et al., 1998]

The two papers by Changming Chen attempt to apply this method to Friction Stir Welding. The papers attempt to show that an AE detection system developed by the authors is sensitive enough to detect notches inserted into one side of 6061 Al butt welds. The experimental setup is shown in figure 31

In order to process the acoustic emissions, the wavelet transform is employed to decompose the time based AE signal into a weighted set of weighted wavelet functions. The wavelet function, like the Fourier Transform, transforms a signal into its frequencies. However, it does not use a constant bandwidth, but instead uses

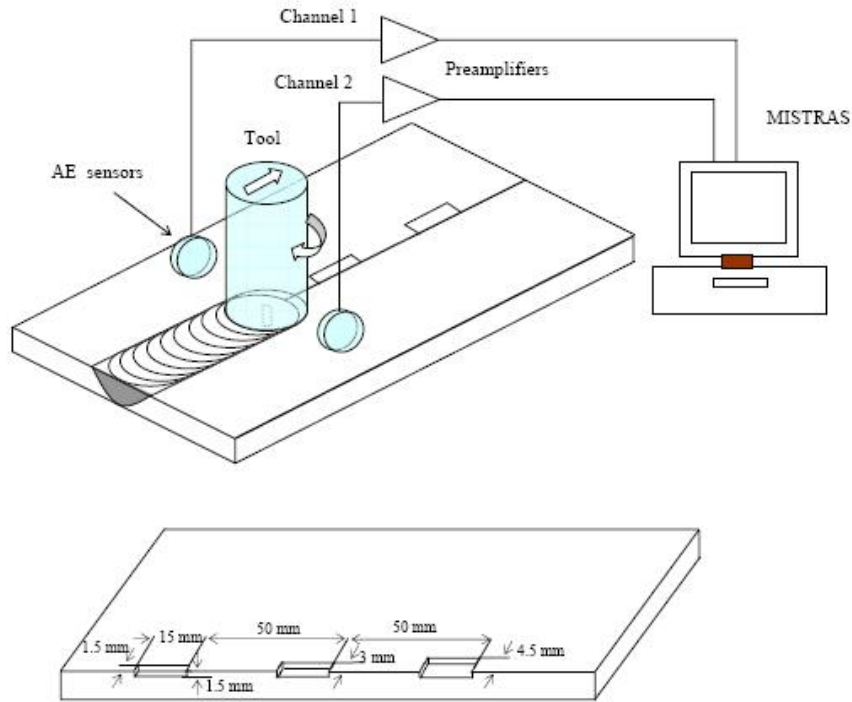


Figure 31: Setup for Acoustic Emissions detection in [Chen et al., 2003b]

separate bandwidths for different frequencies. This makes it “more appropriate for the analysis of complex signals such as transient and abrupt changes that are generally the symptoms of defects or sudden changes of the processing state.” [Chen et al., 2003b]

In looking at the result of applying the wavelet transform to the AE signals collected from the experiment illustrated in figure 31, than the results in figure 32 are obtained.

Notice that the spikes correlate to the inserted notches. This paper demonstrates one possibility for a method of monitoring weld quality in-process.

Electromagnetic Radiation

The paper “A study on electromagnetic property during friction stir weld failure” examines the use of electromagnetic radiation in the analysis of FSW quality [Muthukumaran et al., 2006].

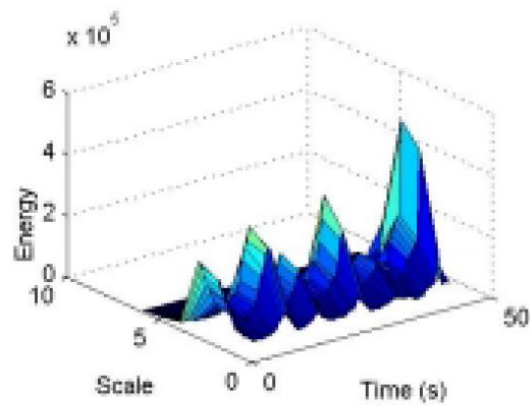


Figure 32: Wavelet transform of the AE signals from weld with gaps inserted [Chen et al., 2003b]

The research done for this paper focuses mostly on a post-process use of this technique, but it also states that the the method could be useful as “online condition monitoring”. “A stress-induced electromagnetic radiation (EMR) occurs during the transient stage of elastic to plastic deformation of metals and alloys under tension, compression, torsion and impact traction”. This would imply the method used as post-process has clear implications to an online system.

For this experiment however, FSW samples were made in advance and were machined into Tensile test samples. The samples were then loaded to failure while the electromagnetic radiation was recorded. This signal was the transformed into the frequency space using the Fast Fourier Transform. Finally, the fundamental frequency of the Fourier spectra was deduced for each sample. This leads to the results shown in figure 33.

| Specimen no. | Tool diameter (mm) | Tool rotation speed(rpm) | Traverse speed (mm/min) | Rake angle | Edge preparation | Fundamental frequency (KHz) |
|--------------|--------------------|--------------------------|-------------------------|------------|------------------|-----------------------------|
| 1 | 13 | 900 | 125 | 0 | Manual | 1.01 |
| 2 | 13 | 900 | 160 | 1 | Manual | 1.02 |
| 3 | 13 | 900 | 200 | 2 | Wire cut EDM | 0.6 |
| 4 | 13 | 1120 | 125 | 1 | Wire cut EDM | 0.797 |
| 5 | 13 | 1120 | 160 | 2 | Manual | 0.598 |
| 6 | 13 | 1120 | 200 | 0 | Manual | 0.752 |
| 7 | 13 | 1400 | 125 | 2 | Wire cut EDM | 0.589 |
| 8 | 13 | 1400 | 160 | 0 | Manual | 0.575 |
| 9 | 13 | 1400 | 200 | 1 | Manual | 0.612 |
| 10 | 15 | 900 | 125 | 1 | Manual | 0.589 |
| 11 | 15 | 900 | 160 | 2 | Manual | 1.18 |
| 12 | 15 | 900 | 200 | 0 | Wire cut EDM | 0.184 |
| 13 | 15 | 1120 | 125 | 0 | Manual | 0.398 |
| 14 | 15 | 1120 | 160 | 1 | Wire cut EDM | 0.401 |
| 15 | 15 | 1120 | 200 | 2 | Manual | 0.797 |
| 16 | 15 | 1400 | 125 | 2 | Manual | 0.672 |
| 17 | 15 | 1400 | 160 | 0 | Wire cut EDM | 0.376 |
| 18 | 15 | 1400 | 200 | 1 | Manual | 0.484 |

Figure 33: Table comparing welding parameters and fundamental frequencies [Muthukumaran et al., 2006]

This result illustrates a correlation between welding parameters illustrated in figure 34, which plots rotation speed and rake angle against fundamental frequency.

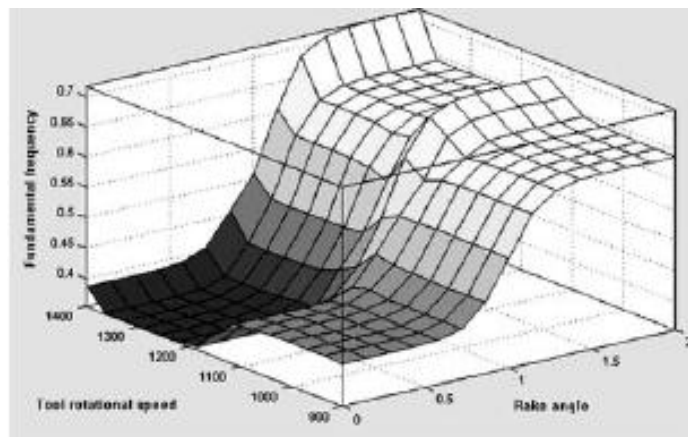


Figure 34: “Effect of tool rotational speed and rake angle on fundamental frequency”
[Muthukumaran et al., 2006]

Image Processing

The paper “Condition monitoring of first mode of metal transfer in friction stir welding by image processing techniques” demonstrates the use of visual inspection as a means of online quality inspection [Sinha et al., 2006].

In general, this method monitors the surface of the weld. The authors show this method has the ability to recognize pin failure and also lack of penetration. The way that this is done is by characterizing the surface features according to brightness gradient. So for example, a good weld has a fairly regular contours after the image of the surface has been brought to grayscale, contrast enhanced and contoured (see figure 35).

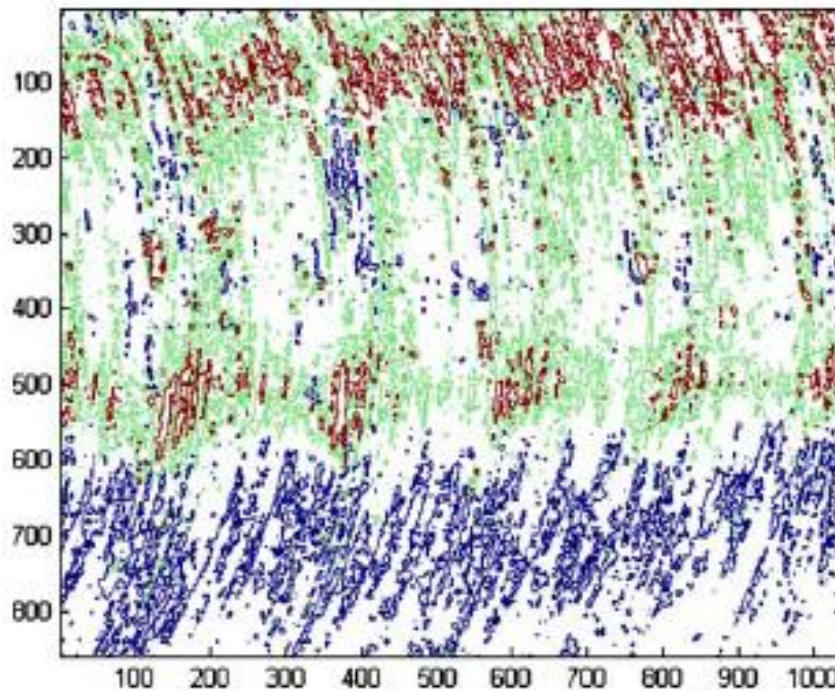


Figure 35: Regular contours from a good weld [Sinha et al., 2006]

Where a weld with lack of penetration (figure 36) leads to a “highly fractured“ contour, as shown in figure 37

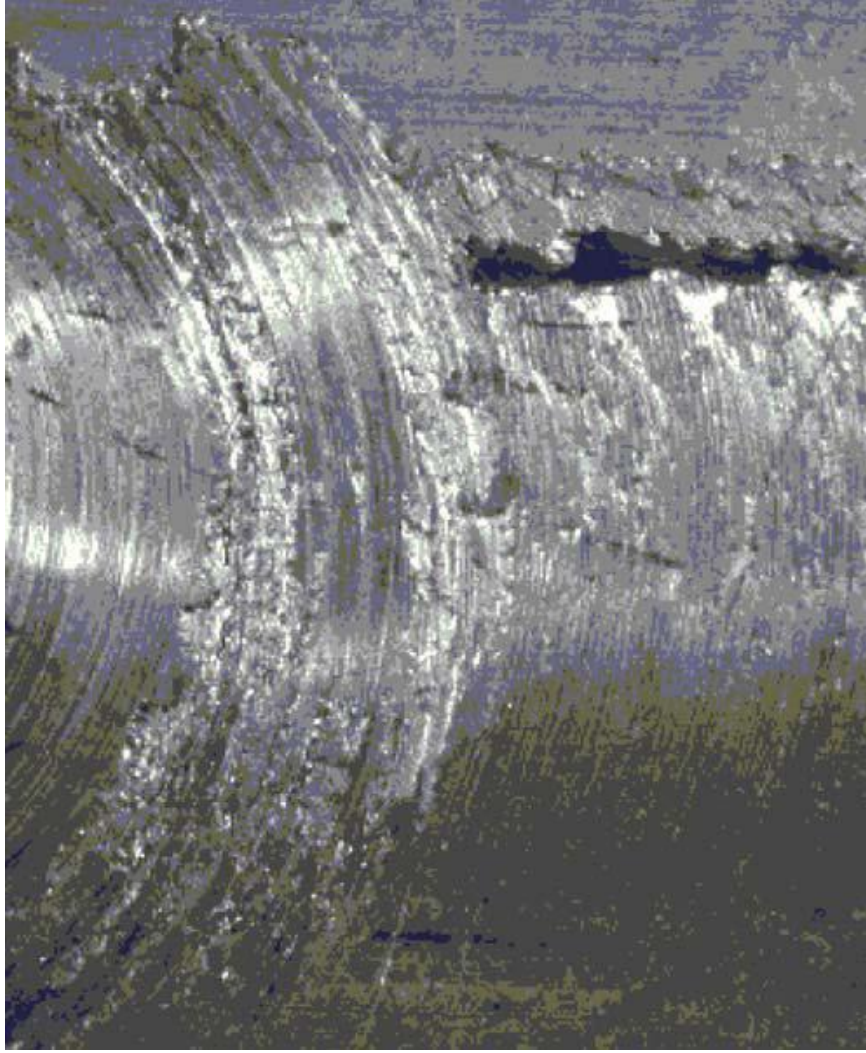


Figure 36: A weld run with lack of penetration [Sinha et al., 2006]

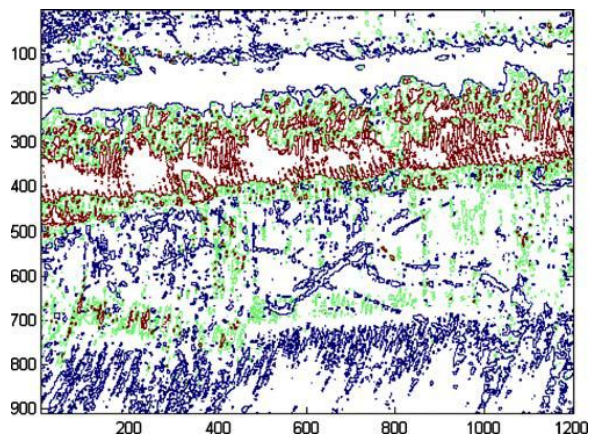


Figure 37: Contours from weld with lack of penetration [Sinha et al., 2006]

Force signals

Several papers in the literature use force as the feedback signal in flaw detection. These will be reviewed in this section. A special subset of these papers develop a load control algorithm using the vertical force. These papers will be reviewed in the FSW control section.

Neural Network Evaluation of Weld Quality using FSW Feedback Data

The paper “Neural Network Evaluation of Weld Quality using FSW Feedback Data” uses the frequencies of the recorded force data to discover flaws in the weld [Boldsai Khan et al., 2006a]. This is not unlike the use of the frequencies contained in the acoustic emissions or of the electromagnetic radiation.

In this work, FS welds were made with good and bad parameter sets and were grouped into two categories. In one, the samples were divided into those with and those without flaws. In the other, the samples’ tensile strength were rated high, medium or low.

The experiment then went as follows:

1. First the FSW samples were run and the X, Y, Z forces, and the the torque, were recorded.
2. Next the frequency spectra of the samples was computed for each signal (X, Y, Z, Mz)
3. These frequency spectra were binned into 32 groups (dimensionality reduction)
4. The samples were further broken down into training and testing sets
5. A neural network (a machine learning technique to be discussed in a later chapter) was trained on the training set of data to recognize either flaw presence or else tensile strength.

6. The trained neural network was then tested on the testing set.

The accuracy of these experiments is reported in figures 38 and 39

| Metallurgical Classification | | | | |
|-------------------------------------|-----------------------------|----------------------------|----------------------------|---------------------------|
| | Percent correct Training | Percent correct Testing | Number correct Training | Number correct Testing |
| X Force | 100% | 99.3% | 188/188 | 150/151 |
| Y Force | 100% | 100% | 188/188 | 151/151 |
| Z Force | 100% | 92.7% | 188/188 | 140/151 |
| Torque | 100% | 97.3% | 188/188 | 147/151 |

Figure 38: Flaw detection classification [Boldsai Khan et al., 2006a]

| Tensile Strength Classification | | | | |
|--|-----------------------------|----------------------------|----------------------------|---------------------------|
| | Percent correct Training | Percent correct Testing | Number correct Training | Number correct Testing |
| X Force | 97.5% | 90% | 184/188 | 136/151 |
| Y Force | 95.7% | 88.7% | 180/188 | 134/151 |
| Z Force | 100% | 82.2% | 188/188 | 125/151 |
| Torque | 97.9% | 78.1% | 184/188 | 118/151 |

Figure 39: Tensile strength classification [Boldsai Khan et al., 2006a]

The conclusions of this paper are that there is a good success rate for identification of flaws in sample, and of weld tensile strength using the method outlined in this paper.

Analysis of the FSW force footprint and its relationship with process parameters to optimize weld performance and tool design

The paper “Analysis of the FSW force footprint and its relationship with process parameters to optimize weld performance and tool design” [Hattingh et al., 2004] looks at the use of recorded forces as a means of monitoring the weld process.

The authors record the axial force and torque, but in addition record a “force footprint”. This is the recording of a force which is aligned with the rotating tool through one revolution. The author then demonstrates that this recorded force footprint holds information about the energy put in to the weld, tool geometry and weld process parameters (see figure 40).

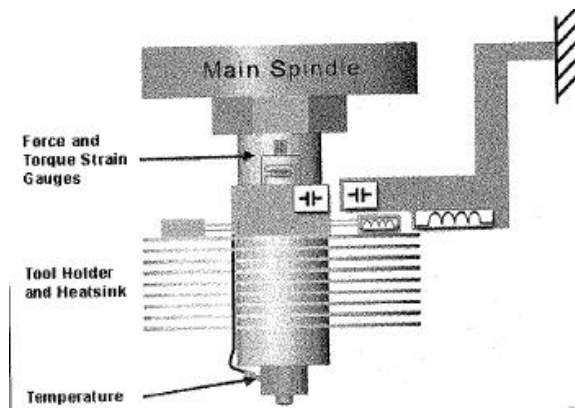


Figure 40: An FSW monitoring system [Hattingh et al., 2004]

The recorded force footprint is shown in figure 41 for a smooth tool (left) and one with a feature on one side in line with the force reading (right).

Figure 41 shows how the force footprint changes with the tool geometry. Further, figure 42 demonstrates how the footprint changes with the weld parameters.

The authors demonstrates that the recorded forces can be shown to vary with changing tool geometry and process parameters.

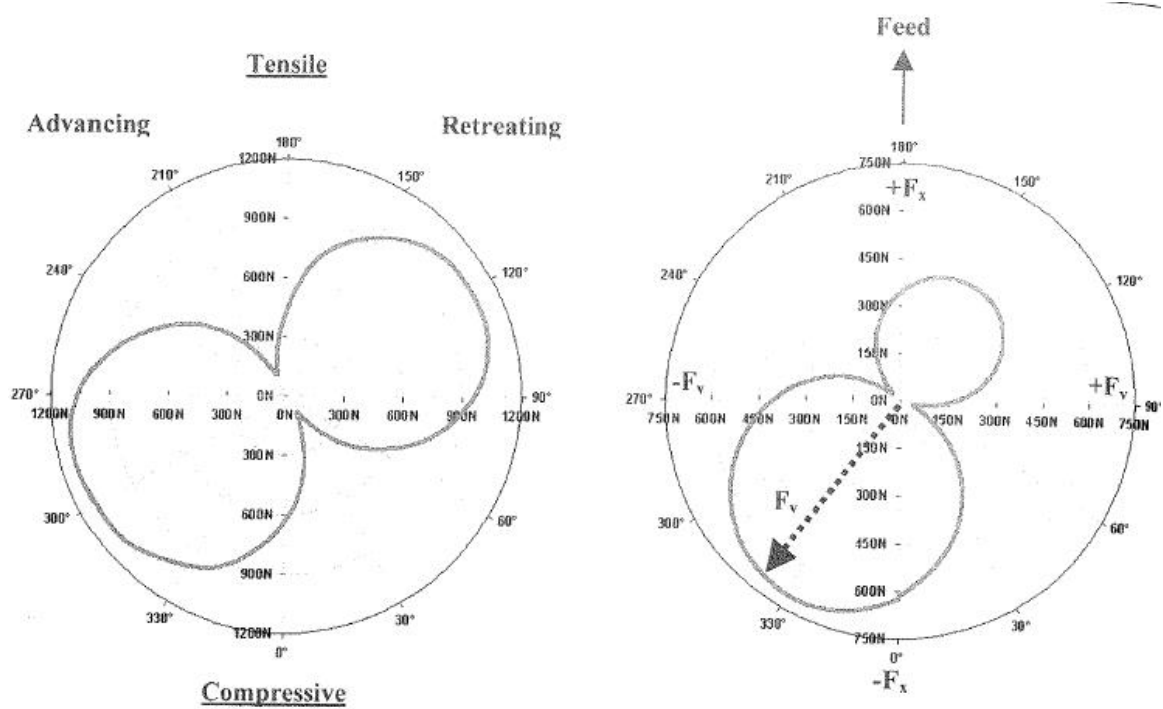
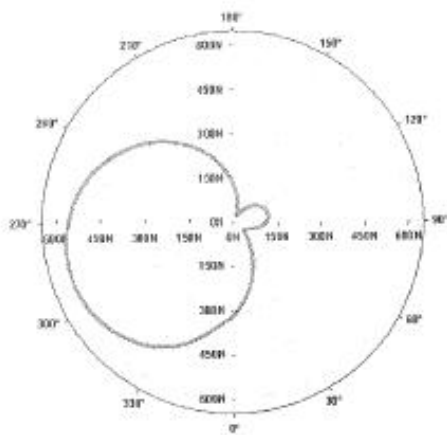
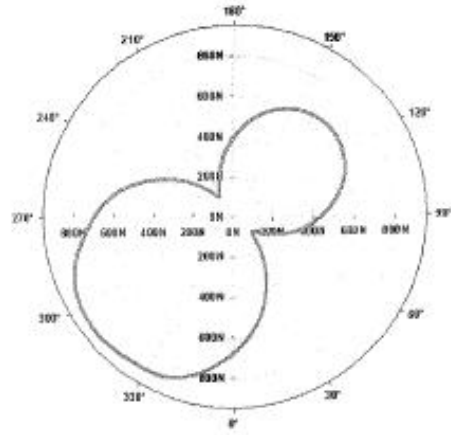


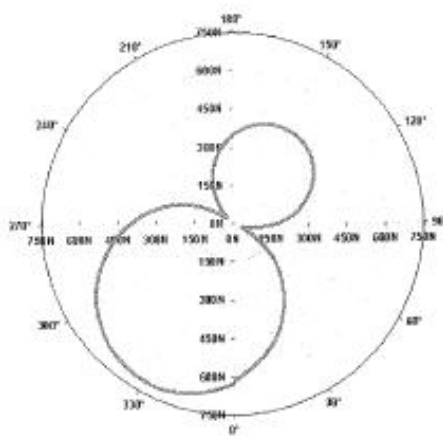
Figure 41: FSW “force footprints” obtained for two different tool geometries [Hattingh et al., 2004]



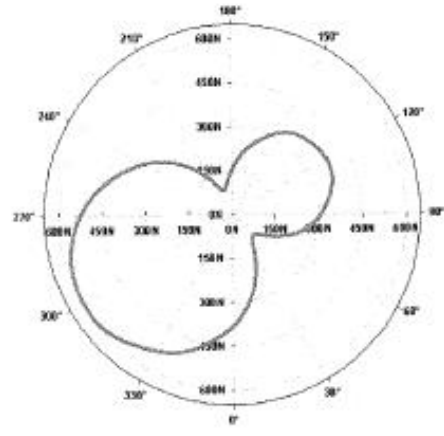
a) Test 1 (300 rpm, 120 mm/min)



b) Test 2 (600 rpm, 120 mm/min)



c) Test 3 (450 rpm, 80 mm/min)



d) Test 4 (450 rpm, 160 mm/min)

Figure 42: FSW “force footprints” shown changing with the weld parameters [Hattingh et al., 2004]

Development of a low cost friction stir welding monitoring system

The paper “Development of a low cost friction stir welding monitoring system” documents the LOSTIR device as a means of FSW monitoring [Beamish et al., 2006].

The LOSTIR device is similar to the one illustrated in figure 40, it monitors tool torques, forces and temperatures. The device is shown in figure 43

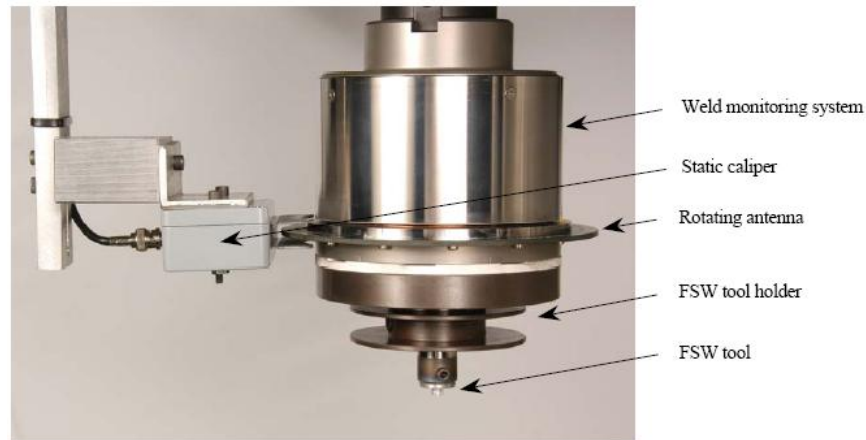


Figure 43: The LOSTIR device [Beamish et al., 2006]

In order to demonstrate the use of this device for monitoring, the authors performed an experiment where samples were made with the following flaws: tool wear, lack of penetration, joint line gap and void formation. Figure 44 shows the recorded axial forces for this experiment.

Using process forces as a statistical process control tool for friction stir welds

In the paper “Using process forces as a statistical process control tool for friction stir welds” force signals are used in an attempt to monitor quality of weld and flaw detection [Arbegast, 2005]. The author looks at both direct force observation and frequency based observation of forces as well. The paper examines possible algorithms for using force signals as a process control input. As in earlier papers, correlations are noted between recorded force levels and void formation due to poor parameter

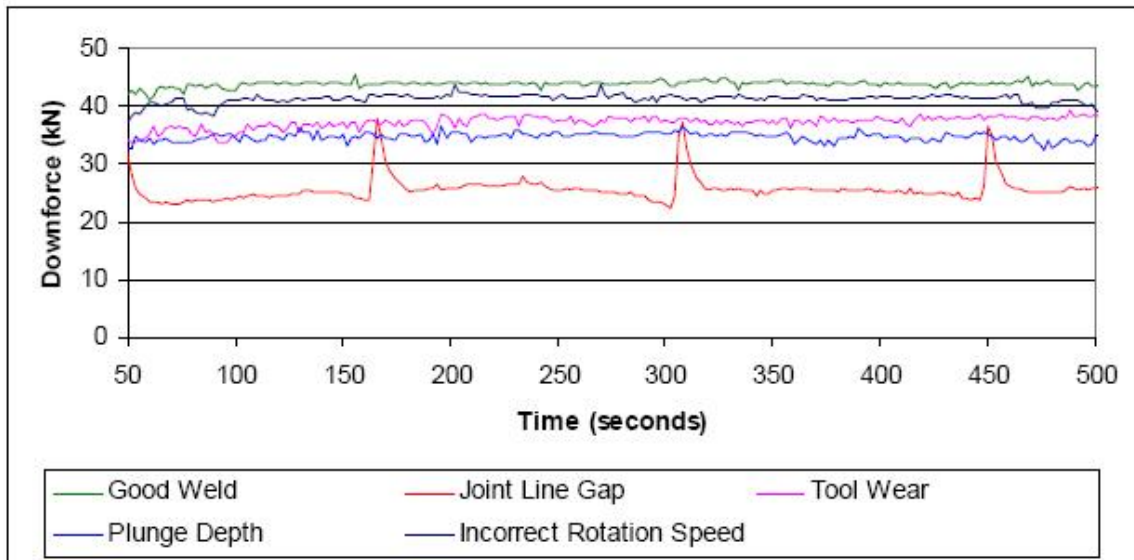


Figure 44: Influence of weld parameters on down-force [Beamish et al., 2006]

selections. This paper also documents an FSW control approach dubbed *Normalized Cumulative Fourier Area Analysis*. The essential workings of this technique is:

The X- Y- and Z- force data is analyzed in frequency space and normalized to the spindle rotation speed and the amplitude of the signal at the normalized spindle frequency. The cumulative area under the normalized frequency curve at very low frequencies is calculated using numerical integration techniques. For FSW producing volumetric indications, the rate of rise of this cumulative area curve is fast indicating a large degree of low frequency events. For FSW which are not producing volumetric indications, the rate of rise is small [Arbegast, 2005].

This method is stated to be the best statistical process control tool - based on this study - to “evaluate the weld quality either ‘post welding’ or in ‘real time’” [Arbegast, 2005].

Control of Friction Stir Welding

In this section the literature which pertains to control in Friction Stir Welding is reviewed. Most of the literature found pertains to load control [Loftus et al., 1999] [Kinton and Tlusty, 2000] [Stotler and Trapp, 2007]. However, at least some papers deal with broader control issues.

Non-load control papers

Software Architecture for Real-time Sensor Analysis and Control of the Friction Stir Welding Process

The paper “Software Architecture for Real-time Sensor Analysis and Control of the Friction Stir Welding Process” attempts to describe a control system for Friction

Stir Welding [Kruger et al., 2004]. It builds on the previous paper in that it includes the “force footprint” as one monitoring measurement using the device illustrated in figure 40, in addition to other variables including: motor currents; speed; torque; temperature; linear displacement; tool temperature; torque; axial, radial and tangential forces.

The paper presents the following diagram as an overview of the total control architecture (shown in figure 45)

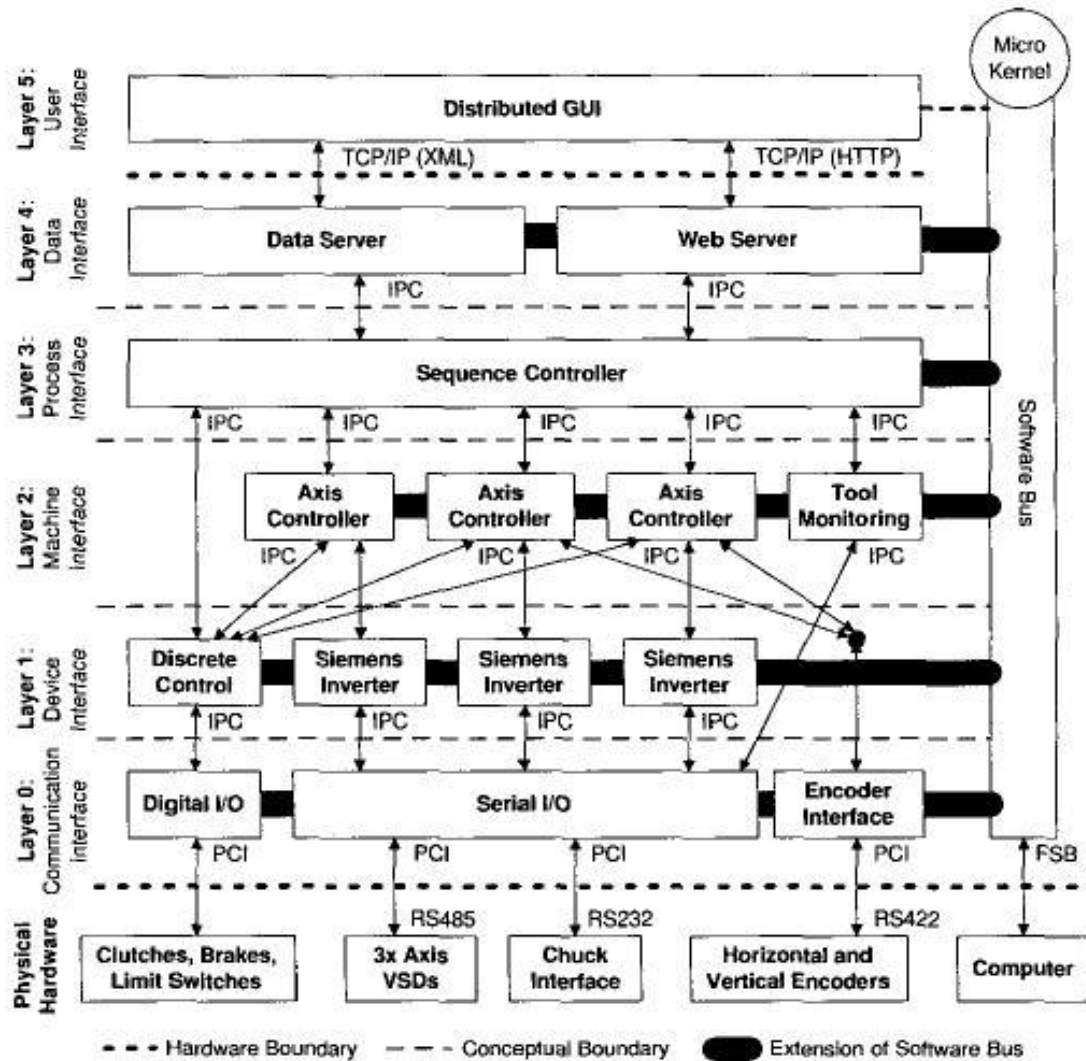


Figure 45: FSW control architecture from [Kruger et al., 2004]

As can be seen, a total control system for FSW could be a very complicated process.

Load Control Papers

Software Architecture for Real-time Sensor Analysis and Control of the Friction Stir Welding Process

The paper “Software Architecture for Real-time Sensor Analysis and Control of the Friction Stir Welding Process” describes a system developed with load control [Loftus et al., 1999]. The system is an in-house developed Visual Basic FSW control system (like the one used in the VUWAL). A screenshot of this system is shown in figure 46

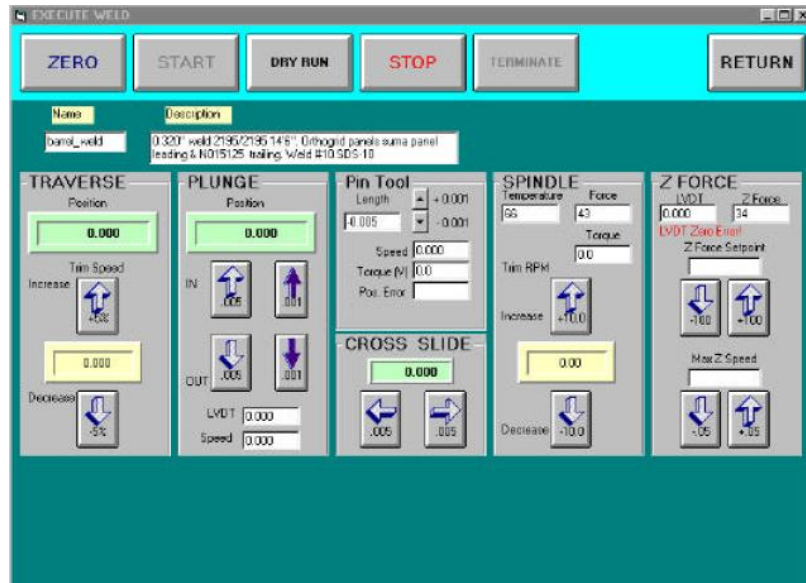


Figure 46: Computer screen for welding control and monitoring used in the paper [Loftus et al., 1999]

The system discussed in this paper uses the force recorded in the axial direction as its feedback signal. It maintains this as a constant by adjusting the plunge depth, while staying in safe regions of plunge depth. This is a natural means of automated welding with load control in FSW.

Method and apparatus for controlling down-force during friction stir welding

In the patent “Method and apparatus for controlling down-force during friction stir welding”, the inventor discusses a very similar method for load control as the one outlined above [Kinton and Tlusty, 2000]. The main control loop, shown in figure 47 illustrates this.

Friction stir welding travel axis load control method and apparatus

The patent “Friction stir welding travel axis load control method and apparatus” is similar to the above patent in that it strives to maintain a constant load [Stotler and Trapp, 2007]. However, it differs in that it actuates control by increasing or decreasing the travel speed. It does this while attempting to maintain a constant load on the tool. This is demonstrated in figure 48

Summary

The papers in this section represent what currently exist for control of FSW. The majority can be summarized in one of two ways:

1. Maintain constant axial force by adjusting the plunge depth
2. Maintain constant travel force by adjusting travel speed

Because it has been reported that two of the most critical parameters after tool design are travel speed and plunge depth, or the forces derived from them, these are both very sensible strategies.

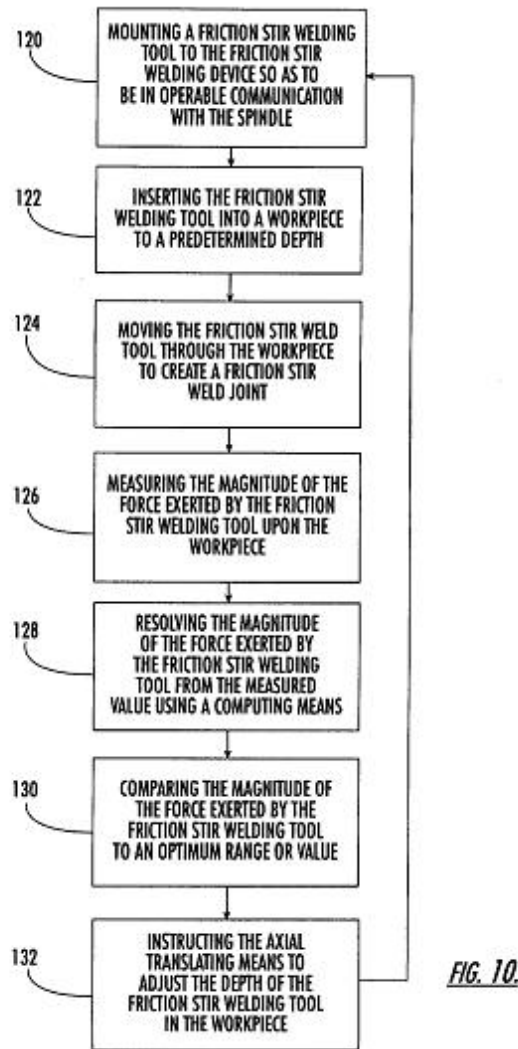


Figure 47: Load control loop from [Kinton and Tlustý, 2000]

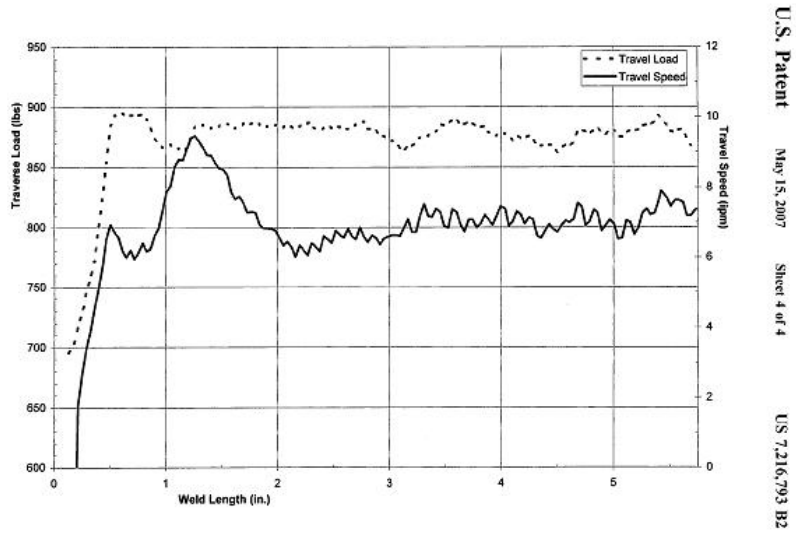


Figure 48: Travel load and travel speed from [Stotler and Trapp, 2007]

CHAPTER IV

BACKGROUND LITERATURE REVIEW: DETECTION AND CLASSIFICATION TECHNIQUES

The mathematics of detection and classification is used throughout this research, and a review of the methods employed is provided in this chapter.

Principal Components

Overview

For the summary of Principal Components “Multivariate Statistical Methods” will be used as the primary source [Manly, 1986]. However, it should be pointed out that this is a rather old technique, which is often dated back to a 1901 article by Karl Pearson [Manly, 1986] [Pearson, 1901]. Additionally, the book “A user’s guide to principal components” was helpful in pointing out applications and use of principal components [Jackson, 2003]. Finally [Montgomery et al., 2001] was used for statistical background.

A summary of what happens in principal components is that it performs a transformation where data points in an input space are mapped to another space which has some useful analytical properties. To explain in terms of the research in this dissertation, assume that the input space is a vector which contains force values. It might look like a vector of values as shown in figure 49.

Assume a vector like this is used for each sample in an experiment with control welds and welds with increasing amount of problem scenarios. One could analyze this data using traditional statistical techniques such as comparing the mean values of the vectors, finding the distance between the vectors and so forth. But one can not plot 9-dimensional data.

| |
|-----------|
| Feature 1 |
| Feature 2 |
| Feature 3 |
| Feature 4 |
| Feature 5 |
| Feature 6 |
| Feature 7 |
| Feature 8 |
| Feature 9 |

Figure 49: An input vector

Principal Components Analysis (PCA) allows us to map this vector from this “input space”, where each element of the vector is the coefficient of an input, into a space where each dimension is Principal Component. The advantages of this transformation are that:

1. The dimensions are uncorrelated.
2. The dimensions are ordered by variance [Manly, 1986]

PCA produces a linear transformation that maps each input vector to a vector of equal length, which has the properties given above. The advantage of the the uncorrelated data is that now each vector can be thought of as “measuring different ‘dimensions’ in the data” [Manly, 1986]. The advantage of the ordering of variance is that often times it is found that a large majority of the variance in the experiment is contained in the first few components. This implies that that lower variance components can be considered negligible. Thus, a larger dimensional system can be reduced to a smaller dimensional system without much loss of information. This often helps because higher dimensional vectors can than be plotted against their principal components which can often times give good insight [Manly, 1986].

For the example input vector in figure 49 this might look something like figure 50

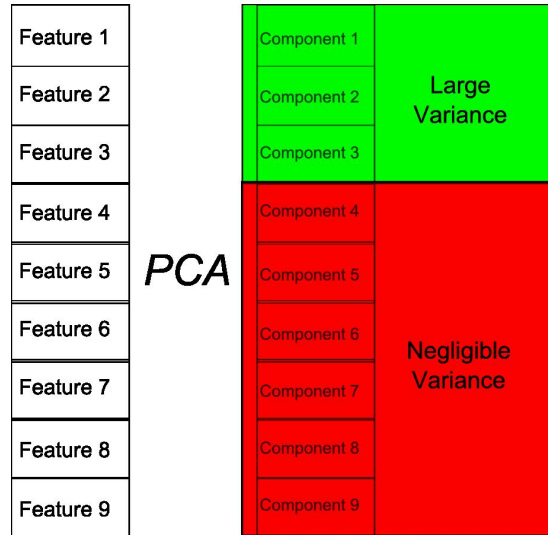


Figure 50: After applying PCA

This illustrates PCA's transformation of a 9-dimensional space where the elements of the array are likely correlated (for instance if one is x-force and one is y-force) to an effective 3-dimensional space, where each dimension is uncorrelated.

Mathematical technique of PCA

PCA is carried out using a rather straightforward method. Assume n samples of input vectors, each of size p . The first step is to find the mean and variance of each of the elements across all the samples. Then normalize each element of each sample using these values. This prevents any one element from dominating on the basis of its unit giving larger values. Next the covariance matrix is computed of these input samples. It is a $p \times p$ matrix. Because all the variables have been normalized, all the diagonal elements (representing the variances of each variable) is 1 and the matrix is a correlation matrix.

The next step is to compute the eigenvalues and eigenvectors of this correlation matrix. These eigenvectors are the principal components, and their corresponding eigenvalues indicate the variance “explained” by the eigenvector or component. Eigenvalues and vectors are computed using a statistical package or algorithm.

Linear Discriminant Analysis

Linear discriminant analysis (LDA) is a method related to PCA. However, it differs in that the algorithm assumes that there are two groups of data points, and that the classification of the data points is known. LDA is often credited to R. A. Fisher [Fisher, 1936] [Manly, 1986]. For this section the primary source will be “Recent developments in discriminant analysis on high dimensional spectral data” [Mallet et al.,].

In PCA, a linear function was derived which found coefficients for the “principal components” of the input vectors. These principal components were uncorrelated. Additionally, they were ordered by variance, so that the first component contained the maximum variance of any axis through the space. The second component contained the maximum variance for any axis uncorrelated to the first component and so on.

In LDA, it is assumed that there are two groups and a linear function of the input vectors which maximize the separation of these two groups is sought. The solution in LDA is to find the vector of discriminant coefficients which maximize the “between class scatter” and minimize the “within class scatter”.

Computation of LDA

LDA, like PCA, will yield p discriminant vectors, where p is the dimensionality of the input vectors. If a new vector is built up where each element is the result of the dot product of each discriminant vector and the input vector, this would effectively

be once again transforming the data to a new space, where dimensions are uncorrelated. Also, similar to PCA, each discriminant will be ordered by the measure of the discriminant criteria [Mallet et al.,].

So, for each discriminant a vector \mathbf{v} is sought which will compute a value vector \mathbf{z} of “discriminant scores”. Assuming the matrix X contains all the input vectors this would look like:

$$\mathbf{z} = X\mathbf{v}$$

According to the literature, to achieve this goal for maximal class separation maximize:

$$\mathbf{v}^T S_B \mathbf{v}$$

With the constraint that:

$$\mathbf{v}^T S_W \mathbf{v} = 1$$

Where S_B is the “between class covariance” and S_W is the “within class covariance” [Mallet et al.,]. These are defined as follows:

$$S_B = \frac{1}{n} \sum_{k=1}^K n_k (\bar{\mathbf{x}}_k - \bar{\mathbf{x}})^T (\bar{\mathbf{x}}_k - \bar{\mathbf{x}})$$

$$S_W = \frac{1}{n} \sum_{k=1}^K \sum_{i=1}^{n_k} (\bar{\mathbf{x}}_i^{(k)} - \bar{\mathbf{x}}_k)^T (\bar{\mathbf{x}}_i^{(k)} - \bar{\mathbf{x}}_k)$$

$\bar{\mathbf{x}}_k$ is the mean vector of class k and $\bar{\mathbf{x}}$ is the overall mean. This reduces to solving (assuming S_W is invertible):

$$(S_W^{-1}S_B - \lambda I)\mathbf{v} = 0$$

Which is now an eigenvalue/eigenvector problem which can be solved computationally.

Support Vector Machines

Support vector machines represent one of the more sophisticated techniques employed in this research. For this review the book “Support Vector Machines for Pattern Classification” [Abe, 2005], as well as the paper “Support Vector Machines: Hype or Hallelujah?” [Bennett and Campbell, 2000] and also a chapter from the book “Handbook of Engineering Statistics” [Pham, 2006] are used.

SVM basic theory

As in earlier methods input vectors of sensor data represent force readings. Each vector corresponds to a particular weld, whether it be a good weld or else one where some flaw or problem has been included. Assume that M of these vectors which are divided between 2 classes, SVM theory starts by trying to find some decision function D :

$$D(\mathbf{x}) = \mathbf{w}^T \mathbf{x} + b$$

Where $D(\mathbf{x})$ is negative for one class and positive for the other. If it is assumed that the data are linearly separable then the equation can be re-setup so that $D(\mathbf{x})$ is ≤ -1 for one class and is ≥ 1 for the other.

The equation:

$$D(\mathbf{x}) = \mathbf{w}^T \mathbf{x} + b = c$$

is the equation of a hyperplane. In essence, one is attempting to find a decision hyperplane which divides the sample. There are often a number of hyperplanes which would accomplish this (see figure 51)

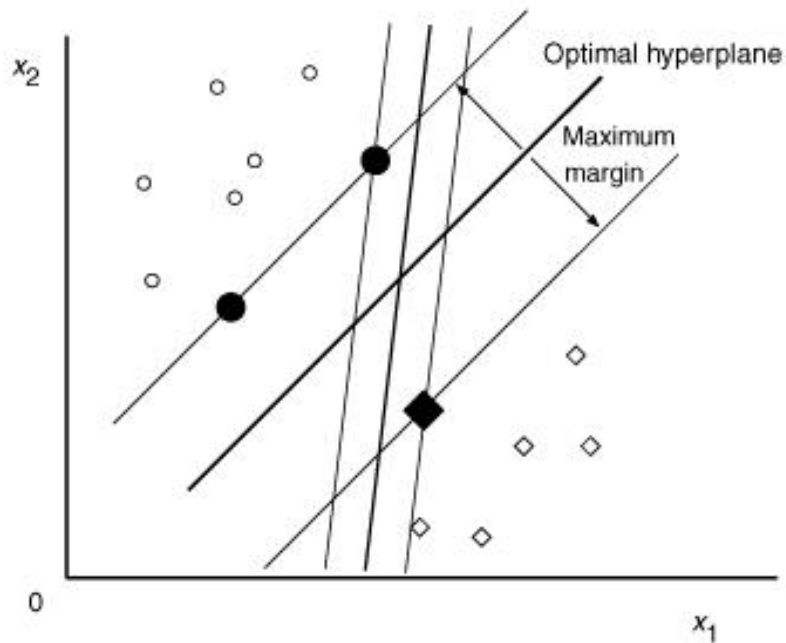


Figure 51: Hyperplanes [Abe, 2005]

Notice from the figure that one hyperplane (notated the Optimal hyperplane) has the maximum margin between itself and the nearest instances (referred to as Support Vectors). The essential algorithm of Support Vector Machines solves for this optimal hyperplane. This is done through an optimization of a constrained equation. For the complete algorithm refer to [Abe, 2005].

Advantages

As can be seen by a quick search in the literature, SVMs are finding applications in a number of fields. Publications regarding SVMs and their applications are numerous. SVMs have a number of advantages versus related techniques like multilayer neural networks such as:

1. “Maximization of generalization ability”
2. “No local minima”
3. ”Robustness to outliers” (from [Abe, 2005])

Extensions to SVMs

The SVM described earlier in this chapter is the most basic instance. It deals with data which are linearly separable into two classes. However, it is important to point out that there are extensions to this basic setup to handle more complicated data should the need arrive.

One of these extensions is the inclusion of a cost function. This allows for a “soft margin” during training where it is allowed that some training vectors are on the wrong side of the decision function. This is necessary if the data is not completely linearly separable or if there are spurious points.

Another extension is the use of kernel functions to allow for non-linear hyperplanes. Common kernels used are radial basis and sigmoidal. Additionally, a number of mechanisms exist for dealing with multi-class problems. One example would be a one-against-all Support Vector Machine. Finally, adaptations exist to allow the output of the SVM to be a regressive function, rather than a classification.

These extensions combined with the innate qualities of the SVM make it a very useful statistical tool.

K-means clustering

K-means clustering is an unsupervised learning technique and is a form of clustering. It can be used to attempt to learn where data is organized into “clusters”, without prior specification of class membership. In [Jain et al., 1999] it is described as the “simplest and most commonly used algorithm using a squared error criteria”.

Algorithm

The essential algorithm ([Jain et al., 1999]) works in the following way. Assume there are n sample instances to cluster. First, the number clusters to use must be chosen. Assume k clusters ($k \leq n$). Then first randomly assign k cluster centers to the points in the hypervolume containing the sample instance. Next each sample instance is assigned to the nearest cluster center. For each cluster center, relocate the center as the center of the sample instances currently assigned to it. Then reassign instances based on the new center locations. These steps are repeated until some convergence criterion is met.

The algorithm is illustrated in figure 52 where the term “points” is used in place of “sample instances” ([Wikipedia, 2007]).

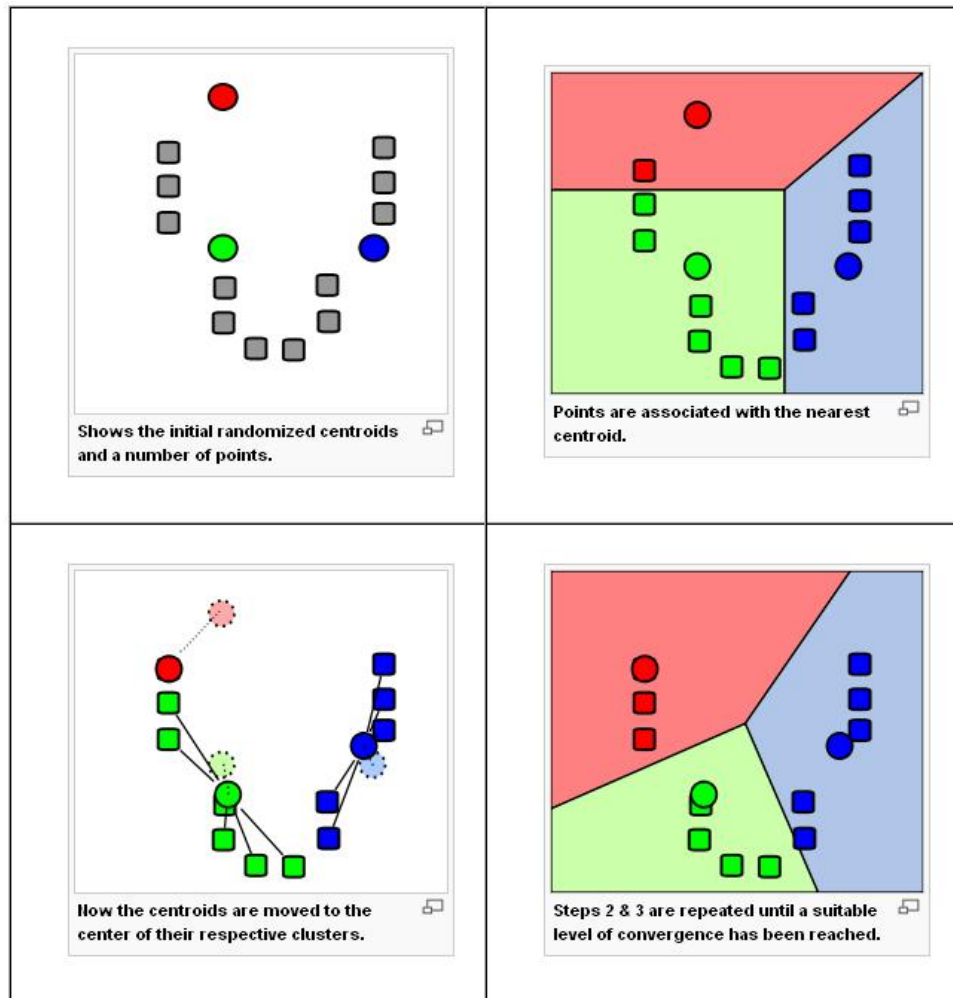


Figure 52: K-means clustering from [Wikipedia, 2007]

Neural Networks

Neural networks have been applied in the literature of FSW monitoring and control. One example of the use of Neural Networks is [Boldsai Khan et al., 2006a] (reviewed earlier in this paper) for the evaluation of weld quality. Additionally the paper “Artificial neural network application to the friction stir welding of aluminum plates” uses neural networks as a means of discovery of the correlation between weld parameters and resultant mechanical properties [Okuyucu et al., 2005]. Finally, in the patent “Method and apparatus for in-process sensing of manufacturing quality”, a neural network is successfully used to monitor weld joint quality using acoustic emissions applied to the inputs of a neural network [Hartman et al., 2005].

A Brief Description of Neural Networks

For this description the paper “Artificial neural networks: a tutorial” is used [Jain et al., 1996]. An artificial neural network can be viewed as a “weighted directed graph”; the nodes being artificial neurons and the weighted edges are the connections between nodes. Figure 53 shows an example of this sort of network.

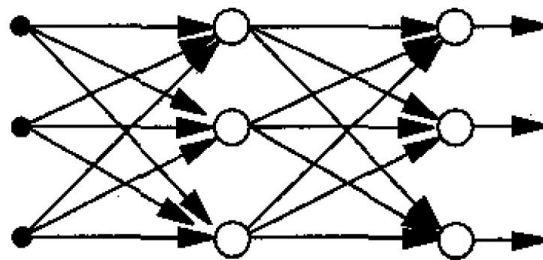


Figure 53: A basic feed-forward neural network [Jain et al., 1996]

In a typical setup, each node can be described by the following equation

$$y = \theta\left(\sum_{j=1}^n w_j x_j - u\right)$$

Where θ represents a type of step function. This result generally relates that if the weighted sum of a neuron's inputs exceeds a threshold u , the neuron "fires" or has a high activation which is fed on to either the input of another neuron, or else to an output. The first row of the network receives the inputs, and the last row produces the outputs. There are a large number of variations on this basic theme. The described fundamental network is often called a "multilayer perceptron".

The information in the network is stored in the weights. These are learned by known examples, when inputs can be fed into the inputs and the output of the network compared with the known correct output. The difference between the produced output and the desired output is compared and "fed back" through the network to update the weights in a common algorithm known as "back-propagation".

A more advanced Neural Network, is the general regression neural network. [Specht, 1991]. This is of the family of radial-basis neural networks and has been shown to quickly converge to a smooth nonlinear regression function, even given sparse data.

Neural networks have been used in a large number of fields, including Friction Stir Welding.

Part II

Journal Publications: Published and Under Review

CHAPTER V

PAPER 1A: IN-PROCESS GAP DETECTION IN FRICTION STIR WELDING (SENSOR REVIEW)

Paul A. Fleming, David H. Lammlein, D. M. Wilkes, Katherine A. Fleming, Thomas S. Bloodworth, George E. Cook, Alvin M. Strauss, David R. DeLapp, Thomas J. Lienert, Matthew T. Bement, and Tracie J. Prater

Sensor Review, Vol. #1, 2008

Abstract

Friction Stir Welding (FSW) is a recently-developed technique where metals are joined together through mechanical stirring. FSW, often performed by robotic welders, is being used in an increasing number of industries such as aerospace, maritime and transportation. FSW has proven to be very effective and has replaced fusion welding and riveting in a number of manufacturing processes. In order to increase FSW's applicability, it is important that methods for control, fault avoidance, and detection be implemented reliably. Unfortunately, a number of faults occurring in FSW are difficult to detect. A worm-hole fault for instance occurs entirely below the weld surface. What is needed is a non-destructive testing system which can detect fault occurrences in real time and take corrective action. In this work, the use of force feedback is investigated as a means of monitoring gaps in Friction Stir Lap Welding (FSLW). Results are presented which indicate that although the gaps cannot be seen visually before or after the weld, forces can be used to discern even small gaps between the metals.

Introduction

Friction Stir Welding

Friction Stir Welding (FSW) is a relatively new welding technique where the samples are joined through mechanical stirring. Figure 54 shows the basic workings of FSW.

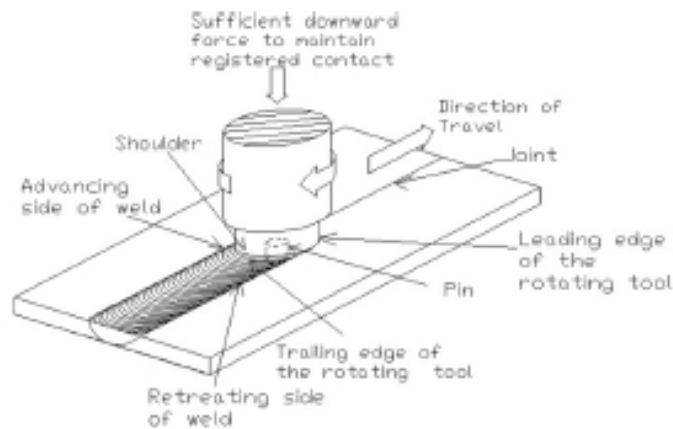


Figure 54: Outline of friction stir welding [Cook et al., 2004]

The tool pin in the figure is rotating while traversing the material to be welded. The shoulder of the tool generates heat which allows the material to be plasticized but not melted. FSW has a number of advantages over fusion methods including[Cook et al., 2004]:

- Excellent mechanical properties
- No filler material, non-consumable tool
- No fumes, porosity or spatter
- Ability to weld alloys difficult for fusion methods

Because of its advantages, FSW is currently employed in a number of industries including: Aerospace, Maritime, Railroad and Automobile. However improved control

and fault detection/avoidance are an important component for the continued expansion of FSW.

Automation of FSW for robotic welding

In this research, we examine a paradigm for monitoring the FSW process. We are interested in this in order to improve the robustness and reliability of automated FSW.

One of the challenges in fault avoidance in FSW is fault detection. Some of the faults associated with FSW are difficult to observe non-destructively. A "worm-hole" fault, which is a void in the weld line, may exist completely below the weld surface and therefore be unobservable to a human inspector. These faults can severely weaken the integrity of the weld. For this reason, the development of an in-process monitoring system is essential for both quality control and process yield. In-process detection of faults in FSW is not trivial. A number of techniques for detecting weld quality and faults have been published, and many involve high quality sensors and advanced machine learning techniques.[Boldsai Khan et al., 2006b][Chen et al., 2003c] "First-order" sensing, the observation of the weld visually or direct observation of process signals, often does not provide evidence of fault occurrence. However, if the signals are first processed using modern signal processing and machine learning techniques, fault detection can be achieved. This means that feedback control for FSW is a two-step process. The raw signal data obtained from either dynamometers, acoustic emission sensors or accelerometers must first be applied to a computational unit which can quickly detect faults, or rank fault likelihood, and this information can in turn be accounted for by a process controller. In FSW, the controller can attempt to affect change by adjusting the tool rotation speed, sample traversal speed or plunge depth if it is possible to correct the for the detected fault, or else alert the operator of fault occurrence. This scheme is represented in the control loop shown in figure 55. In

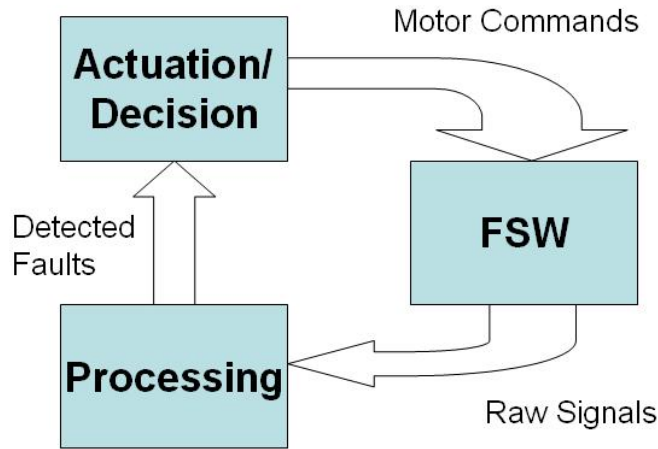


Figure 55: Control Loop in FSW

order for a successful feedback loop, fault detection schemes must be developed for all faults, and for all weld processes. In this paper, an investigation into the possibility of using force readings as a signal for the detection of gaps is presented. Gaps, caused by poor fit-up between samples to be welded, are spaces in the weld joint prior to welding. The presence of poor fit-up, like poor weld parameter selection, is not a fault in and of itself, but rather a fault causing condition. In [Leonard and Lockyer, 2003], gaps are listed as a potential cause of void (worm-hole) formation.

Experiment Setup

Friction Stir Lap Welding

As an experimental test bed, Friction Stir Lap Welding (FSLW), which is the joining of two metal sheets placed one on the other by FSW is used. Current applications of FSLW include hermetically closed boxes, wheel rims and car back supports[Ericsson et al., 2007]. A problem-causing condition could be the existence of a gap between the weld samples. Kawasaki et al. [Kawasaki et al., 2004] discuss the difficulties of FSW overlap

welds with gaps. In this work, this sample problem is used to investigate the previously discussed control system. Specifically, the application of signal processing and machine learning techniques provides the ability to detect these faults.

Material and Equipment

The samples used were 1/8" thick 6061 Aluminum. Two samples were mounted and clamped directly one on the other as shown in figure 56. All welds were run with a spindle speed of 2000 rpm, and a traversal speed of 16 ipm. These values were shown to be effective FSLW parameters in the paper "Lap Joints produced by FSW on flat aluminum EN AW-6082 profiles", and worked well for this research[Mishina and Norlin, 2003]. The tool used was a 01 steel tool, with a 5/8" shoulder and threaded cylindrical .16" long pin. Gaps were created in the samples

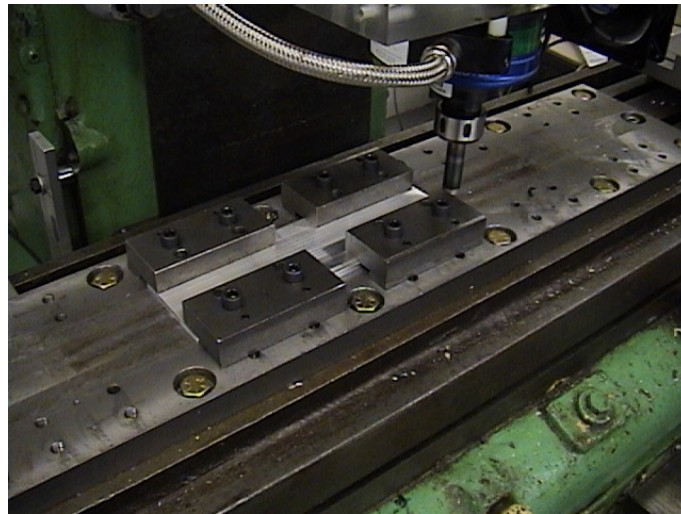


Figure 56: Samples clamped in position

using a milling machine. The gap depths used are: no gap , 0.0004" , 0.0008" , 0.0012" , 0.0016" , 0.0020" , 0.0030" , 0.0040" and 0.0050". The gaps were applied to one plate and a normal plate was placed and clamped on top for experimental welds. The plates are shown in figure 57. Force signals were collected with a Kistler Dynamometer at

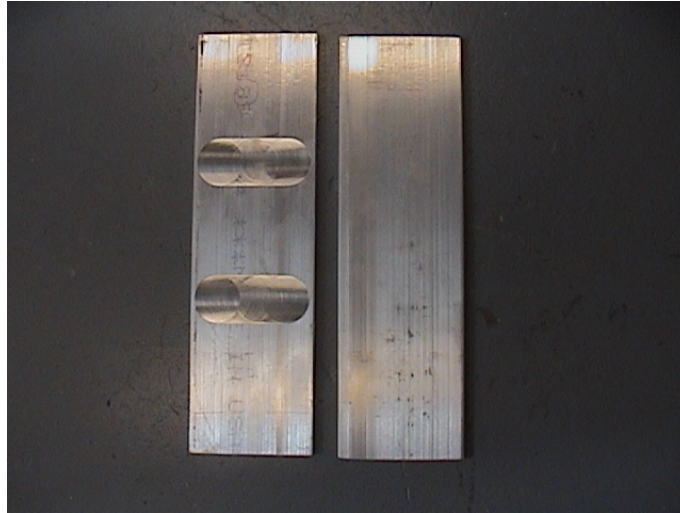


Figure 57: Inserted Gap of 0.0008"

1000Hz.

Results

Initial Results

After welds were completed, a visual inspection of the weld surface was carried out to determine if there were clear visual cues of the inserted gaps. In figure 58a, the surface of the weld with 0.0050" gaps inserted is shown to look normal, with no obvious trenches, flash or other surface features. The close up in figure 58b is looking at the surface over the gap at close range to illustrate the lack of any clear signs of defects on the surface.

Collected Force Signals

A graph showing typical axial forces for the different gap depths is shown in figure 59a.

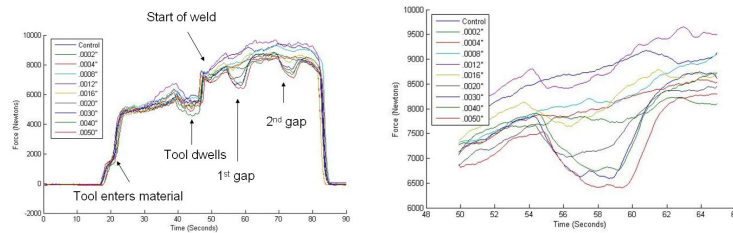
One can see that for gaps of depth 0.002" or greater a large noticeable drop in axial



(a) Weld Surface

(b) Zoomed In

Figure 58: Surface of weld with 0.0050" gap



(a) Axial Forces

(b) Zoomed In on First Gap

Figure 59: Axial forces

force can be expected. This can be further emphasized by examining the gap section in greater detail in figure 59b. From this we observe that the gap produces a 1000 Newton reduction in force when the gap is larger than .002". There are smaller but still noticeable reductions up until 0.0012". These sudden drops in force are a good cue for an automated welding system that it is welding over a gap in the material, with the amount of force proportional to the severity of the gap. However, it is also possible that this information, left unprocessed, may be insufficient for accurate detection of gaps. Forces can vary from other causes. Also, when the gaps are smaller, the change in force appears insufficient for discrimination.

Feature Extraction

In order for an automatic robotic welding system to detect faults given these force signals, the processing block in the control loop must extract meaningful information from the data. Simply providing the force signals may not give a robotic controller an indication of how to proceed. Feature extraction, which means representing the larger data set by a smaller representation which more effectively and purposefully describes the data helps a classifier develop a decision making process[Fukunaga, 1972]. In the case of this experiment, by converting the data into the frequency domain and then applying techniques such as Principal Component Analysis and Linear Discriminant Analysis, low dimensional subspaces are found in which the data is nearly linearly separable, making categorization straightforward.

Frequency analysis

The frequency domain provides a rich source of information for analysis. It is quite possible that gaps will create "chatter" or amplify existing frequencies with increased oscillation. The Fourier transform can be used to determine the spectral density of the force signals. This allows for comparison of the frequency components of the collected force signals. Since the forces are sampled, a good method for the computation of the Fourier transform is the Fast Fourier Transform, a computational method, which is implemented in Matlab[Lathi, 1998]. One issue with the Fourier Transform is that either the frequency spectra for the entire signal must be computed, or else the signal must be windowed. Windowing involves selecting portions of the time signal in order to get a perspective of what the frequency spectra is at a given moment in time. For this experiment, the force signals are each windowed over the gap regions, to examine differences in spectra over gaps, rather than over the whole weld. The only exceptions

are the control welds, which have no gaps, so more of the weld is used. However the window size is constant in all cases, approximately 2 seconds long.

Principal Component Analysis

As stated earlier, it is important to find a compact, or low-dimensional representation of the data. In this experiment, the collected data is represented by frequency spectra of welds run with and without varying gaps inserted. If we consider spectra with 100 frequency bins, that implies that each sample is described by a point in a 100-dimensional space. Principal Component Analysis (PCA) attempts to project these points on to a lower dimensional space, chosen according to which dimensions maintain the highest variance. This is accomplished by diagonalizing the covariance matrix of the data. This operation reduces the redundancy found in data, resulting in a new, and more meaningful low-dimensional data-set[Shlens, 2005]. Although it is not necessarily the best representation from a statistical perspective, PCA is used to project all the samples on to a two dimensional space. The results of this are informative.

Shown in figure 60 are the resulting dimensional representations of the weld samples after PCA with the projections of the control welds represented by red x's and the gap welds by black circles. The figures are split to show the results when the principal components are computed with a varying amount of gap sizes included. Notice that after 0.004" gaps the representations become linearly separable. This is actually a very good result considering the fact that PCA is an unsupervised technique, meaning that no information about the classes of the data was provided to the algorithm to encourage this separation. It occurred naturally due to the fundamental differences of the data being analyzed by PCA.

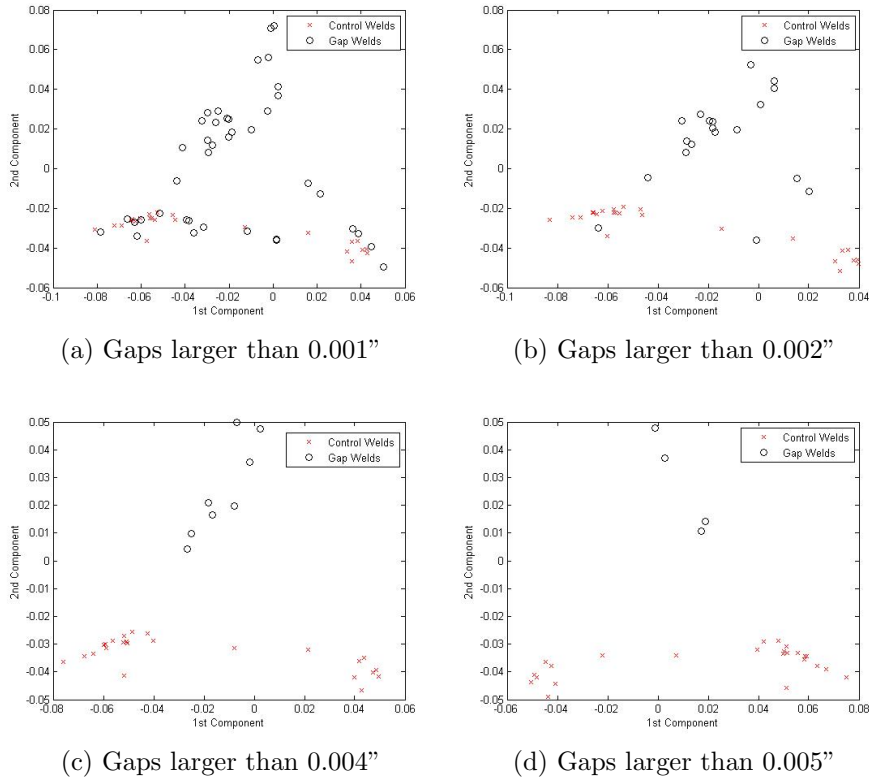


Figure 60: Principal Component Projections

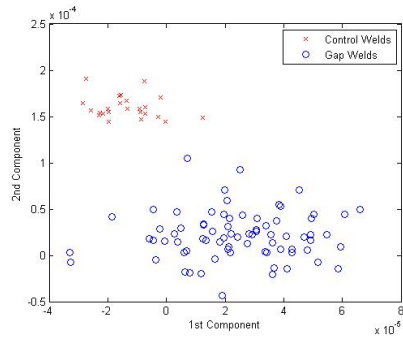
Linear Discriminant Analysis

Linear Discriminant Analysis, or Fisher’s Linear Discriminant, is also a dimensionality reduction technique. However, unlike PCA, it is given *a priori* knowledge of the classes of the samples and then finds a lower-dimensional projection that maximizes the class separability. This is accomplished by solving equations which maximize between-class scatter and minimize within class scatter. The results of applying this are shown in figure 61.

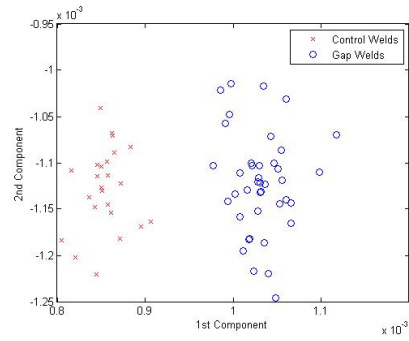
From figure 61, it can be seen that even if the gap is 0.0002”, LDA provides a 2-dimensional representation of the data where control welds and gap welds are linearly separable.

Conclusions and Future Work

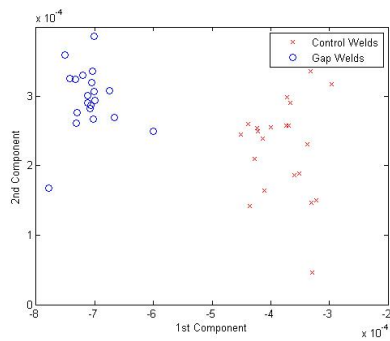
This research demonstrates two methods which could be used in designing an automatic fault detection/avoidance system for Friction Stir Welding. Statistical methods can be used as a pre-step to derive representations of force data which provide good insight into the state of the current weld. Deriving these representations may take some time off-line, but the projections can be then done quickly on-line. This can in turn be used to devise a complete real time fault avoidance control which would allow reliable and robust robotic friction stir welding.



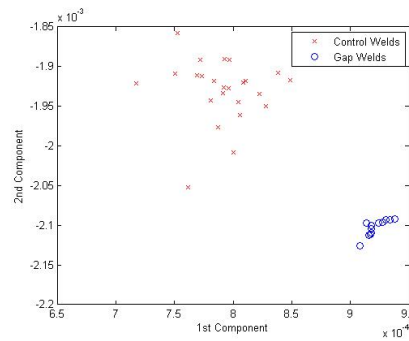
(a) Gaps larger than 0.0002"



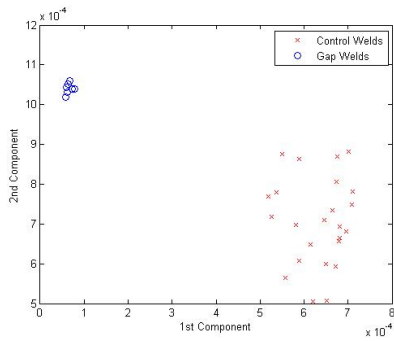
(b) Gaps larger than 0.001"



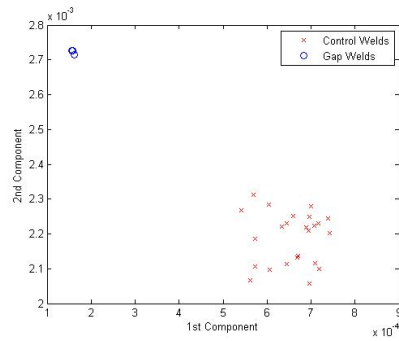
(c) Gaps larger than 0.002"



(d) Gaps larger than 0.003"



(e) Gaps larger than 0.004"



(f) Gaps larger than 0.005"

Figure 61: Linear Discriminatory Analysis

CHAPTER VI

PAPER 1B: AUTOMATIC FAULT DETECTION IN FRICTION STIR WELDING (MS&T 2007)

Paul A. Fleming, Katherine A. Fleming, D. Lammlein, D. M. Wilkes, Thomas S. Bloodworth, George E Cook, Alvin M. Strauss, David DeLapp, and Tracie Prater.

Proceedings of Materials Science and Technology, Detroit, MI, 2007.

Abstract

Friction Stir Welding (FSW) is a relatively new welding technique where metals are joined through mechanical stirring. Due to its numerous advantages over older welding methods, it has been implemented in an increasing number of industries. However, there are remaining challenges to be overcome in FSW. One of the most serious is its reliance on accurate weld parameters. Additionally, faults or poor quality welds can develop from problems not easily detectible by an operator or robotic welder. In our work, we pursue automatic means of detecting fault occurrences and other quality problems. Force signals are collected from control welds run in aluminum as well as welds containing gap faults. Signal processing techniques, specifically Support Vector Machines (SVMs), are then used to correctly detect fault occurrences. Results demonstrate the ability for in-process fault detection of FSW.

Introduction

Friction Stir Welding (FSW), a welding technique that joins metals through mechanical stirring, is finding applications in an increasing number of industries. A diagram showing the essential workings of FSW is shown in figure 62. A cylindrical

tool is rotated while traversing along the weld line. The material is plasticized-but not melted-and stirred together. The advantage of this type of welding over traditional fusion techniques include excellent mechanical properties, no filler material, a non-consumable tool, and no fumes, porosity or spatter.[Cook et al., 2004]

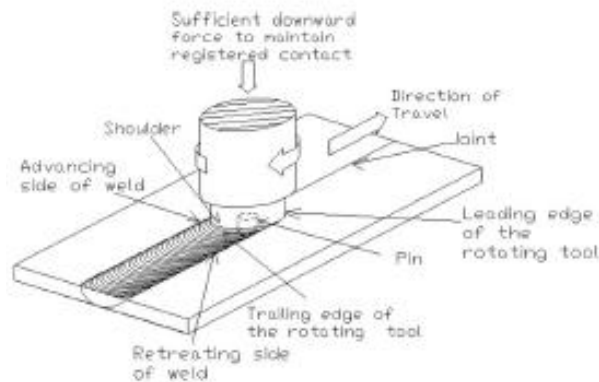


Figure 62: Friction Stir Welding Basic Diagram [Cook et al., 2004]

Robotic control and automatic fault detection

One of the challenges involved with FSW is fault detection. Faults such as tool misalignment and excessive flash can reduce the quality of the weld. If these faults are observed on a weld, the piece will be defective unless the fault is detected in-process early enough to allow for correction. A complete robotic FSW system must include a means for detecting faults and a feedback loop for correcting them. In this work, we present one method for fault detection using the frequency spectra of collected force signals. For our experimental test bed we use Friction Stir Lap Welding.

Friction Stir Lap Welding

In Friction Stir Lap Welding, the materials to be welded together are laid one on top of the other and the FSW tool is plunged through the top material into the second. Current uses of this type of FSW include hermetically closed boxes, wheel rims, and car back supports.[Ericsson et al., 2007] Our set-up for Friction Stir Lap Welding is shown in figure 63.

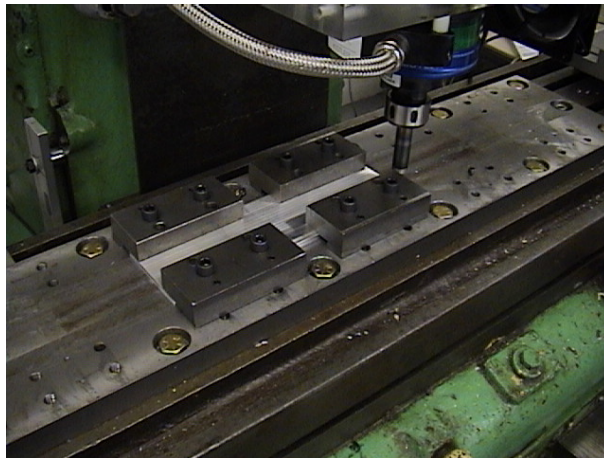


Figure 63: Friction Stir Lap Welding Setup

Gap Detection and Ranking

In order to demonstrate the possibilities for fault detection in FSW using force signals, we used the specific problems of gap occurrence in lap welding. A gap can occur between the two samples welded together and can lessen the integrity of the weld. The paper “Application of friction stir welding to construction of railway vehicles” gives examples of the difficulties of gaps in lap welding.[Kawasaki et al., 2004] In the experiments performed for this paper, some samples that contain no gaps are run while other samples have 0.0002” to 0.005” gaps milled into portions of the lower sample. Force signals are collected using a Kistler Dynamometer during the weld. The frequency spectra of these signals are then determined using the Fast Fourier

Transform. Finally, SVMs are used to determine whether the gap faults can be detected and classified given the frequency spectra of the collected force signals.

Support Vector Machines

A Support Vector Machine (SVM) is a machine learning algorithm which traditionally works by mapping input feature vectors into a feature space and then determining a decision plane in that feature space. One of the key benefits of this technique is its good generalization.[Corinna and Vapnik, 1995] Additionally, SVMs can be considered more transparent than a neural network and therefore may provide more physiological insight. This may help correlate the work presented here with related research in modeling of FSW and FSW fault development. For this work, an implementation of SVMs written for MATLAB was used.[Canu et al., 2005]

Experimental Setup

In the experiments, force signals were collected from samples containing no gaps and those with gap depths measuring 0.0002", 0.0004", 0.0008", 0.0012", 0.0016", 0.002", 0.003", 0.004", and 0.005". The first experiment (Gap Fault Detection) was performed in order to determine whether or not a SVM classifier could be built from the collected frequency spectra of the axial forces which could differentiate between welds that contained gaps and those that did not. Additionally, the performance of the classifier with respect to the depth of the gaps was calculated. The second experiment (Gap Fault Ranking) involved determining whether a classifier could be built which could rate the severity of the detected gaps using the same signal data. A variation of SVM called Support Vector Regression was used in this case.

Results

Gap Fault Detection

In the case of gap fault detection, the frequency spectra of the various runs were computed and used as input vectors for a SVM. It was discovered that because the spectra contained a large number of frequencies, good performance was only achieved if the results were "binned" (placing the averages of regions of frequencies into bins to reduce the dimension of the spectra). Classifiers were built using different-sized subsets of the data. Specifically, some classifiers were built and tested using all of the collected data, while others were built and tested using only the control and larger gaps in order to compare the effectiveness of the classifier given very small gaps (0.0002"). For this first experiment, ten-fold cross validation was used to determine the effectiveness of the classifier. The data was randomly divided into ten groups; the classifier was then trained on nine of the groups and tested on the tenth. This was done for each of the ten groups and the average accuracy is computed. Training a SVM involves presenting the input vectors (the binned frequency spectra) and the labels (either gap or no gap) for each run and finding the decision plane in the feature space. This decision plane is then used for classification. Testing then means using the SVM to classify a given input vector (frequency spectra) and comparing it to a known label. The ten-fold cross validation process was performed five times and the overall accuracy was then computed. Accuracy results for different bin sizes are shown in figure 64. As can be seen from this figure, over and under-binning resulted in the worst performance. The partitioning of the data into 200 bins yielded the best overall results. Figure 65 shows the detection accuracy for a 200-bin partition.

These results indicate that high degrees of accuracy in detecting the presence of gaps between the weld samples are obtainable using the method presented above. More specifically, perfect detection accuracy was achieved when gap size was 0.004"

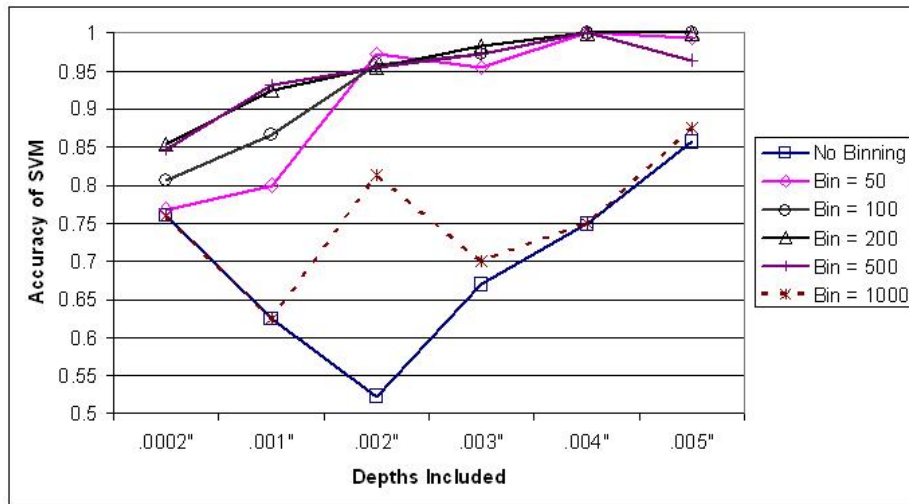


Figure 64: Accuracy Results of SVM given varying bin counts

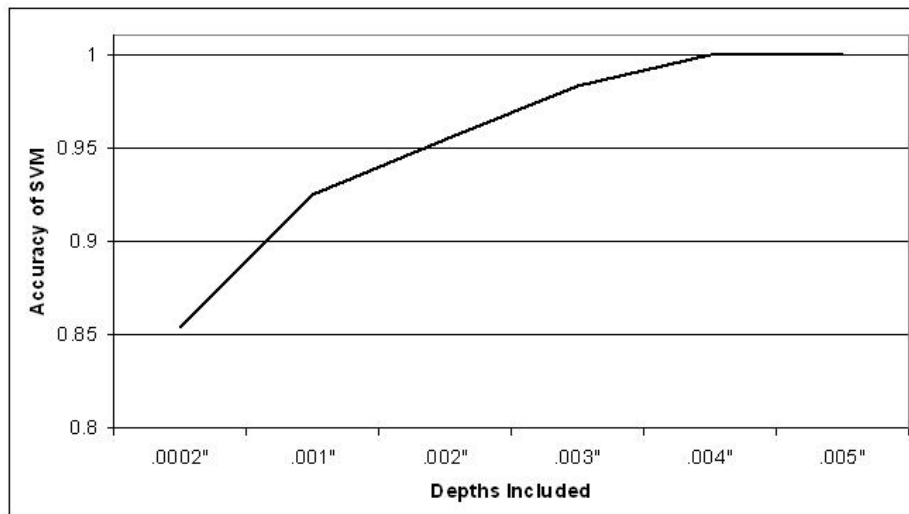


Figure 65: Accuracy of SVM with 200 Bins

and above. Although the training of an SVM might consume some amount of time, its implementation amounts to a simple algebraic computation and can be done quickly. This would indicate that using SVMs to interpret collected force frequency spectra data can reliably detect even small gap faults. Furthermore, this can be done in real time.

Conclusion

A method for the detection of gap faults in friction stir lap welding was presented. This SVM-based method identifies the presence of gaps. The results presented in this paper show the effectiveness and accuracy of this technique, which can be used in a variety of other FSW fault detection scenarios. Future research will aim to apply this SVM classification technique to such scenarios.

CHAPTER VII

PAPER 2: MISALIGNMENT DETECTION AND ENABLING OF SEAM TRACKING FOR FRICTION STIR WELDING

Paul A. Fleming, David H. Lammlein, D. M. Wilkes, George E. Cook, Alvin M. Strauss, David R. DeLapp, and Daniel A. Hartman

Science and Technology of Welding and Joining, Vol. 14, #1, 2008.

Note: The journal required for this paper to be reduced in length for publication. However, the full version originally submitted is provided in this dissertation because it provides more information.

Abstract

This paper describes a technique for determining the position of a friction stir welding (FSW) tool with respect to the weld seam during welding. Forces are used as a feedback signal and a general regression neural network is trained to predict offset position given weld forces. Experimental results demonstrate the accuracy of the developed position predictor. This technique is proposed for online misalignment detection or as a position estimator for in-process tracking of the weld seam for FSW and robotic FSW.

Introduction

Friction stir welding

Friction stir welding (FSW) is a method of welding where material is joined by a rotating tool which traverses along the joint line.[Mishra and Ma, 2005] It was first patented in 1991 by The Welding Institute and has since found an increasing number of applications.[Thomas et al., 1991b] The basic process of FSW is shown in figure 66.

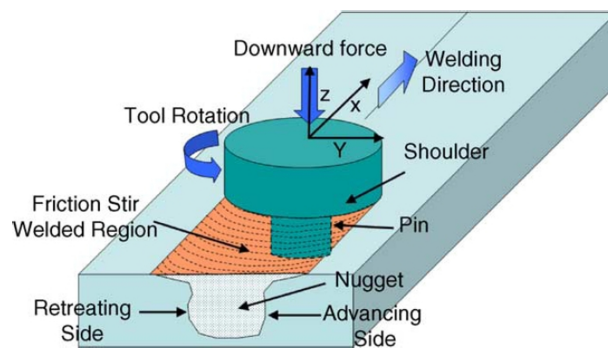


Figure 66: The essential schematic diagram of FSW from [Mishra and Ma, 2005]

figure 66 illustrates an FSW butt-joint, where the materials to be joined are aligned together end to end. The FSW tool, consisting of a pin (or probe) and shoulder rotates and traverses the joint, applies heat through friction and plastic deformation and stirs the material together.[Mishra and Ma, 2005] The two sides of the weld are named according to whether the side of the tool is rotating with the welding direction (advancing side) or against (retreating side). This nomenclature is used throughout this paper.

Butt-welds however are only one type of joint to which FSW can be applied. A number of other joint types have been shown to be amenable to FSW, including: single lap welds and multi-lap welds, 2 and 3 piece T-joints, edge butts and corner fillet welds.[Dawes and Thomas, 1995] Figure 67 illustrates two of these other joints used in FSW: lap welds and T-joints. In these types of FSW, the probe penetrates

through the upper member and into the lower member, stirring the material together to form the joint.

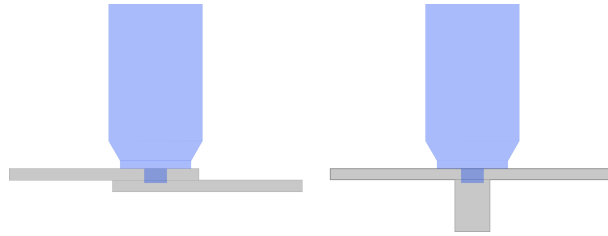


Figure 67: Lap FSW (left) and T-joint FSW (right)

FSW alignment and seam tracking

This paper develops techniques for misalignment detection in FSW. This technology could be useful as a means of in-process monitoring to ensure the tool is properly aligned throughout the weld. Additionally, this could be incorporated as feedback to implement seam tracking for FSW. Typically in the FSW literature, the weld seam is linear and the FSW process is rigidly clamped so that the alignment of the tool to the seam can be set at the start of the weld and will remain aligned throughout the weld. However, there are also technologies capable of implementing non-linear weld-seams. Robotic FSW is one such technology. The apparatus described in Nelson et al. is another, which allows a sheet of metal to be guided through FSW either by an operator, or else by controlled actuators.[Nelson et al., 2007] These technologies do not intrinsically follow the weld seam, and rely on operator control either by hand or joystick, preprogrammed welding paths or computer vision to track the non-linear weld seam. The technology described in Heideman et al., which uses a tactile sensor at the end of a robotic manipulator to trace and record a 3-dimensional weld seam, could be used to learn the weld seam geometry ahead of time and be used as the programmed input to the above technologies.[Heideman et al., 2000]

In all FSW joint types, the alignment of the FSW tool with respect to the weld

seam is important to ensure good weld quality. In butt welds, an improperly aligned tool can result in root flaws.[Leonard and Lockyer, 2003] In extreme cases, a severe mis-alignment will result in no weld at all if the tool is entirely located in only one sample. In general however, the effect of misalignment and its severity is dependent on weld configuration and other parameters.

T-joints are particularly susceptible to misalignment because the weld line is not observable from above. In T-joints, the effects of offset depend upon the dimensions of the material used, the dimensions of the FSW tool employed and the clamping methods used. In one method of clamping for T-joints, steel blocks are clamped alongside the vertical member and under the horizontal member. These blocks provide rigidity for the vertical member. Additionally, if the corners of the blocks near the weld are sharp and fill all the space alongside the area of contact, then they do not allow material to be extruded. However, it has been shown that machining a radius into this corner and allowing material to be ejected into a small fillet can improve weld quality.[Erbsloh et al., 2003]

One case in which the weld is particularly sensitive to offset is the “open-air” clamp, where there is effectively open space alongside the contact plane of the horizontal and vertical member. In this case, if the probe is offset from the center of the vertical member, material is ejected into this space leaving voids in the weld. The three clamping techniques for T-joints just discussed are illustrated in figure 68.

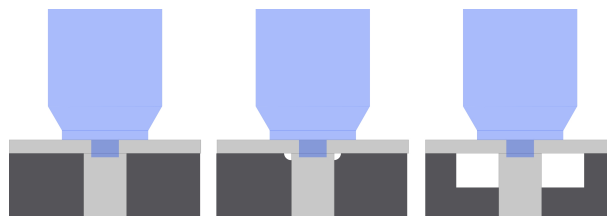


Figure 68: T-Joint clamping methods illustrated, from left to right: full clamps with no fillet, with fillet and “open-air”

In this work, T-joint FSW with “open-air” clamping is used as a test-bed to

demonstrate misalignment detection. This fixturing setup is selected both because of its sensitivity to offset and its practical implications in industry. An “open-air” clamp simulates all clamping configurations where clamps are designed without consideration of material containment. However, it is expected that other users may prefer clamps with small fillets, as was done in Erbsloh et al. and Fratini et al. [Erbsloh et al., 2003][Fratini et al., 2006] The approach outlined in this paper is applicable to these clamping schemes as well.

Force as a process feedback mechanism

In this work, force values are used to determine offset position. Using force as a feedback signal is typical in the literature of monitoring and control of friction stir welding. Boldsaikhan et al. use the frequency content of the dynamic force signal to discover metallurgical defects and evaluating tensile strength during the welding process. [Boldsaikhan et al., 2006a] Hattingh et al. demonstrate a relationship between forces experienced by the tool and process parameters such as welding and rotation speeds, as well as tool geometry. [Hattingh et al., 2004] Fleming et al. investigate the use of force monitoring for in-process detection of gaps between the material to be joined. [Fleming et al., 2008c]

Additionally, axial forces are typically monitored and controlled to ensure weld quality (load control). [Kinton and Tlusty, 2000] [Stotler and Trapp, 2007] It has been shown that a minimum axial force is essential to ensure generation of sufficient frictional heating. The axial force is monitored by force sensors, and maintained by either changes to the vertical position of the tool, rotation speed or welding speed.

In this paper, it is demonstrated that force values can be used to monitor and control alignment. Although the relationship between weld force and tool alignment is not straight-forward, it is possible to develop estimators which can predict offset

position from the force data. This paper outlines an approach of data fusion and feature extraction to enable the monitoring and control of alignment.

For force collection, a Kistler dynamometer is used. This apparatus can read axial (z) force, planar forces (x and y) as well as the moment about the z-axis. Optical interrupters were employed in order to determine the rotational angle of the tool and dynamometer relative to the welding sample at a given reading. Using this setup, one “force sample” is composed of 40 force readings: each of the 4 force readings taken at 10 different angular positions through one rotation. This is illustrated in figure 69.

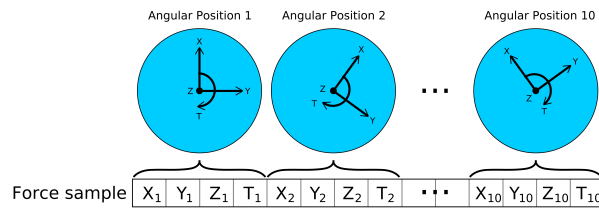


Figure 69: The fundamentals of a force sample using a Kistler dynamometer during FSW

Experimental setup

Experiment

In order to develop an offset estimator for T-joints, 30 T-joint welds were run with offsets ranging from 4mm to either side in incremental steps of 0.25mm.

The setup of the T-joints is illustrated in figure 70. Both the horizontal and vertical members are 6061 aluminum, with the horizontal member measuring 3.175mm in thickness and the vertical member being 9.525mm across. The clamps were steel, with a 3mm x 3mm notch milled in the top to simulate “open-air”. Though not shown, the horizontal member was also clamped down. Finally, the FSW tool consisted of a 5mm diameter 3.81mm long threaded probe and 19mm diameter shoulder. The rotation speed was fixed at 1000 RPM, and the weld speed at 100mm min⁻¹.

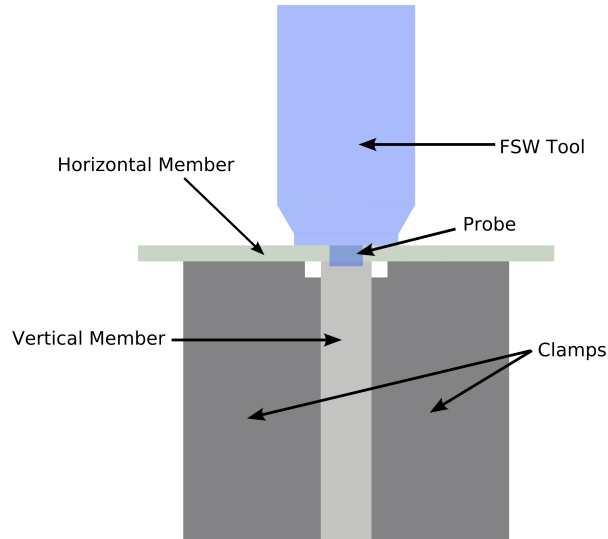


Figure 70: Schematic diagram of T-joint welding configuration used in this paper

Forces were recorded according to the method described earlier. These forces were then inspected to determine if any exhibited a correlating relationship with the changing offset. It was discovered that indeed some forces did demonstrate this relationship. In some cases, this relationship was simple. For example, the axial force generally increased as the offset magnitude approached 0. This relationship existed regardless of the angular position of the dynamometer relative to the material.

In figure 71 the recorded axial forces for each run are plotted against the offset of the tool for the weld in which they were recorded. The forces are organized into a box and whisker plot. A box and whisker plot is a tool for illustrating the distribution of a population. In general, the border edges of each box represent the upper and lower quartile of the data, the middle line constitutes the median, the whiskers typically extend 1.5 times the interquartile range, while any outliers are illustrated with a '+'. [Devore and Farnum, 1999] This plot style is used to indicate the distribution of axial forces throughout each weld, with approximately 1000 force readings used from each weld. Also shown are cross-sections of some of the welds corresponding to the same offset values. These are included to demonstrate representative cross-sections

of the welds at given offsets. The cross-sections differ largely through the presence or absence of voids and material expulsion.

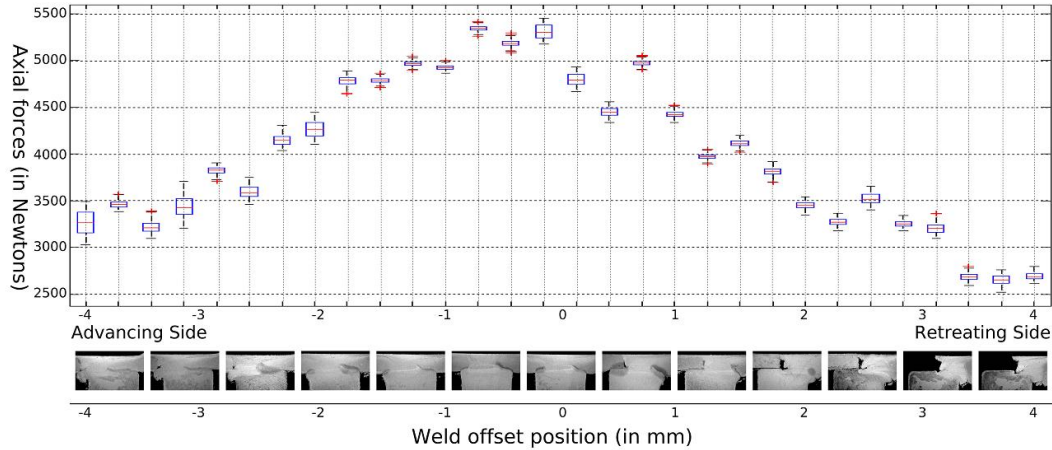


Figure 71: Comparing axial forces and offset

A similar, but less pronounced, relationship is observed for torque (see figure 72). However, when looking at the recorded x and y (planar) forces, there is a more complicated relationship. The relationship is dependent on the angular position of the dynamometer at the force recording. Some angles produce very useful relationships while other show little correlation. Figure 73 demonstrates the relationship of x-force values recorded at the first rotational position vs. offset as was done in figure 71

As illustrated in figure 73, the planar forces allow for differentiation of the tool offset with respect to the advancing side versus the retreating side. Combining the information from the axial force with that of the planar force allows for the determination of absolute position of offset (versus merely detecting magnitude of offset without direction). Because of this, it is possible to develop a complete representation of tool position which predicts both offset direction and magnitude accurately.

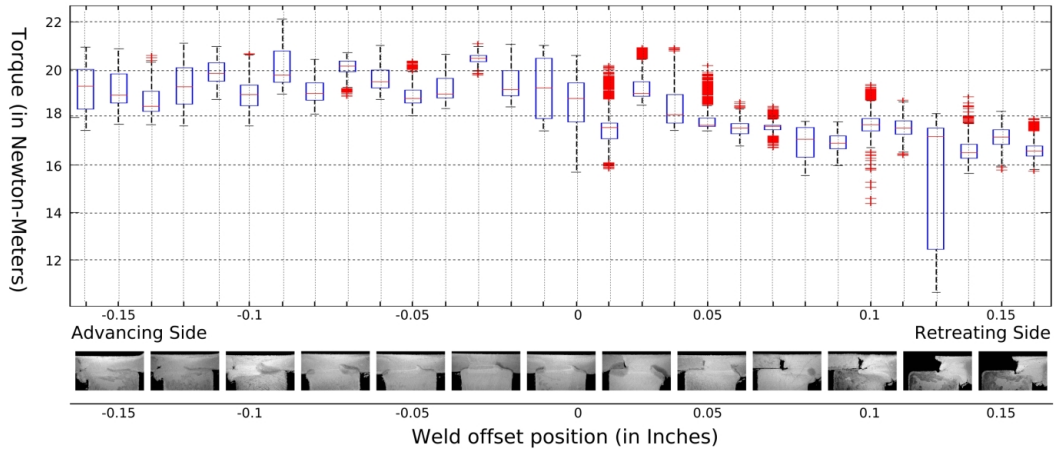


Figure 72: Comparing torque and offset

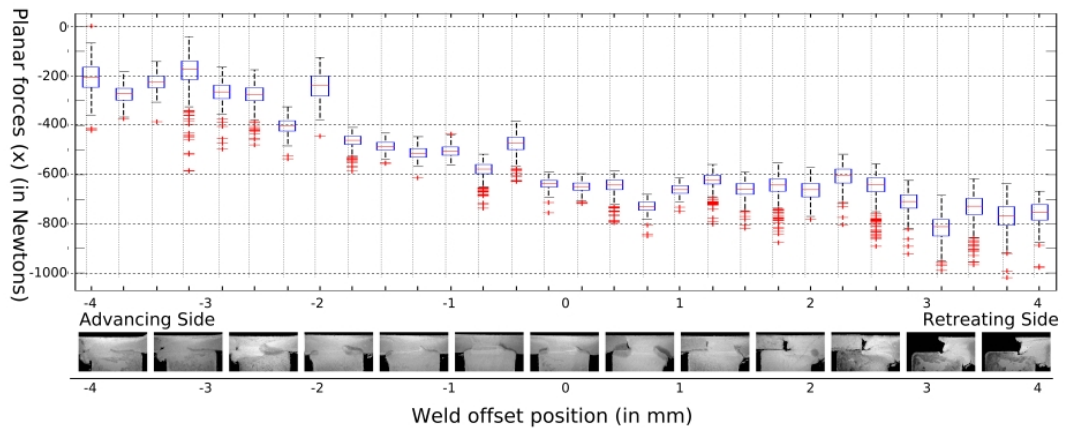


Figure 73: Comparing planar forces and offset

Development of offset position estimator for T-joints

Based on these signals, an estimator was developed to predict offset given these force samples. A general regression neural network (GRNN) was selected to accomplish this. A GRNN is an artificial neural network which estimates continuous variables using non-parametric estimators of probability density functions.[Specht, 1991] A principle advantage of using a GRNN is that it converges to the conditional mean regression surface and can form “very reasonable” regression surfaces with only a few samples.[Specht, 1991]

In this experiment, thirty welds were performed, each with a different offset. Each weld run generated approximately 1000 force samples (40 dimensional vectors of collected forces). Using “backward wrapping”, the dimensionality of the samples was reduced from 40 to 15. In backward wrapping, features are removed one at a time, and their effect on the performance of the classifier is observed. Features are removed until the classifier performance ceases to improve.

Next the network was repeatedly trained and tested using “leave-one-out cross-validation”. Cross-validation estimates how well the network will perform on unseen data.[Russell and Norvig, 2003] In this method, one run was removed from the data, the network was then trained using the remainder of runs. The trained network was then used to predict the offset of the held-out run for each force sample. The results were recorded, and then the process repeated for each weld run. The results of this experiment are shown in figure 74.

Shown in figure 74 is the prediction of the samples of each run organized into a box and whisker plot. Each box is composed of approximately 1000 position predictions. The estimator averaged an absolute error of 0.42mm and the standard deviation for all samples relative to true offset was 0.508mm.

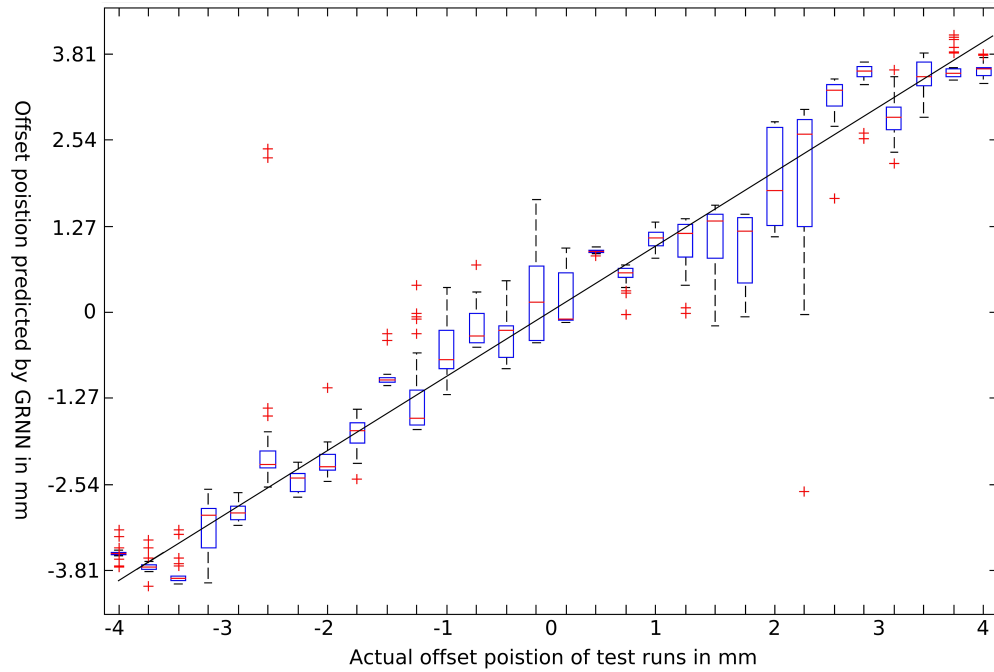


Figure 74: Offset predictions of GRNN

Results

To demonstrate the capabilities of using this technique for tracking a weld seam, a number of welds were run where the offset position varied during welding. The actual values of the offset position were recorded. Next the collected force data were applied to the estimator network and its predicted offset for each force sample were compared with the true position. Some of these results are shown in figure 75 and figure 76. The figures show the actual offset position of the FSW tool with respect to the weld-seam, along with the predicted. Also illustrated for comparison is a shaded region which marks the region of offset values which did not contain a void.

In figure 75, the probe begins with an offset to the advancing side of the weld, it then shifts into the void-free region of offset positions, and finally shifts into the retreating side. The offset position estimates are close to the true positions. However, the lateral motion causes force disturbances which affect the prediction causing the

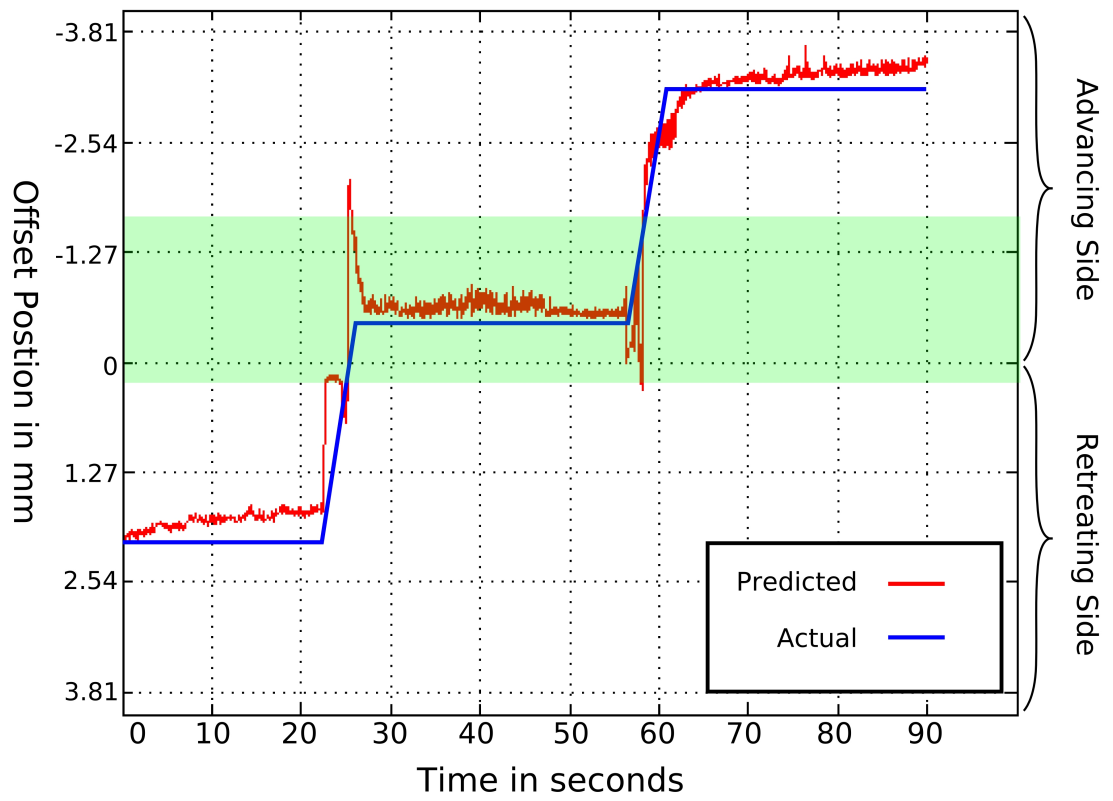


Figure 75: Predicted and actual offsets over time

overshoot around 25 seconds as well as the drop around 60 seconds. This effect will need to be considered in any real-time control algorithm based on this method of offset prediction.

In figure 76, the tool moves from the advancing side of the weld free region, to the retreating side in order to demonstrate the ability of the estimator to track within one region type. Figure 76's first section is noisier than anything in figure 75 which likely indicates the need for improvement of the estimator in the area of 0 offset. This could be accomplished by adding more examples of 0 offset for the system to learn from. In the later part of the figure, the tool shifts quickly out of the weld free region to the advancing side. Although the estimator does predict the weld is too far off to the advancing side, there is a degree of error. This also indicates that thirty welds is probably too few to completely capture the relationship between offset and forces and likely more examples are needed to further refine the estimator.

Discussion

The techniques employed in this paper for determining offset position in T-joint FSW can be applied to the other joint types. The method functions by discovering the way in which offsets affect weld forces and then using a technique based on regression, pattern recognition or machine learning to develop a function or algorithm which maps from forces to estimated offset position. In the case of T-joints, changing offset position affects a number of physical characteristics which in turn affects forces. For one example, with increasing offset from the center, the composition of the material directly below the shoulder changes from only aluminum to also including the steel clamps and air gaps, which likely affect the axial force. Additionally, the proximity of the probe to the edge of the vertical member increases the likeliness of material expulsion which duly affects force.

Although anecdotal, these physical manifestations exist in the other FSW joint

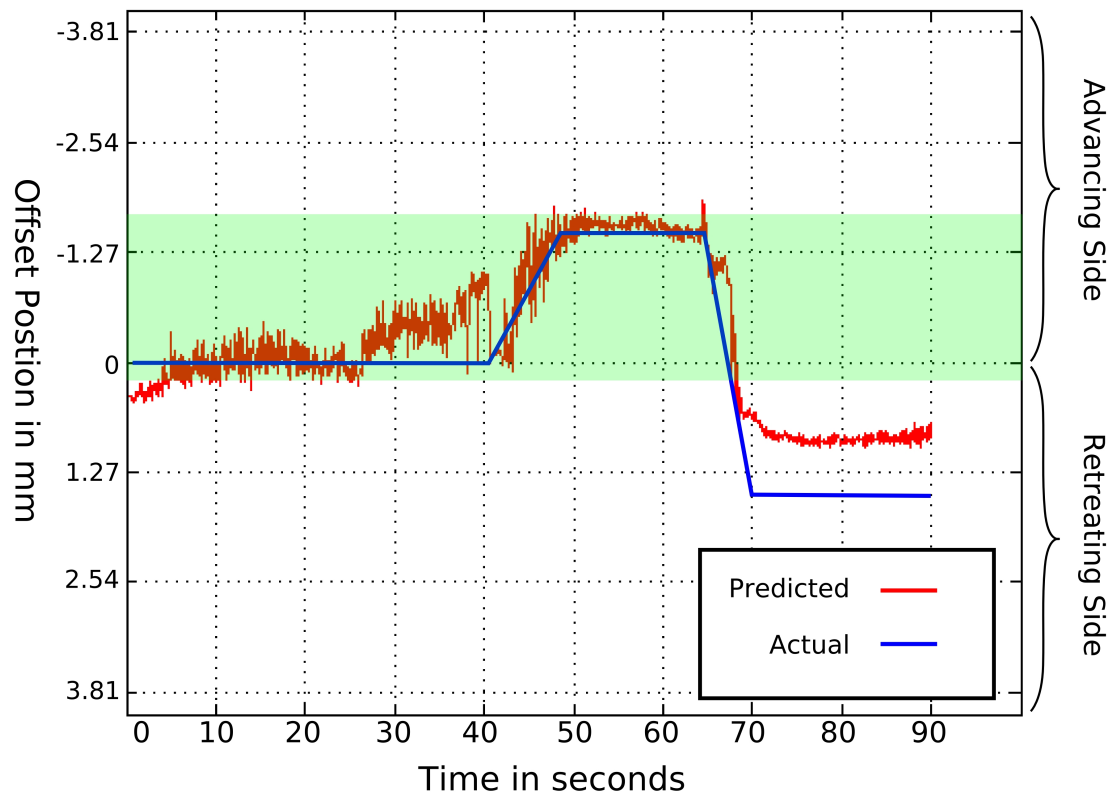


Figure 76: Predicted and actual offsets over time

types. In the event that changing offset positions produces only mild changes in forces, there is always the possibility of adding features such as grooves or elevations to the material or backing plate to augment the signals. Finally, in the event that offset produces equivalent changes when offset in either direction, then a weaving method could be used to gain the center position.

Conclusions and future work

1. The forces present in T-joint FSW have been shown to be able to be used as a signal for the monitoring of position of the FSW tool relative to the weld seam. Current research indicates this is true for lap joints as well.
2. An estimator can be developed which predicts the position of the FSW tool by learning a function which maps weld forces to position.
3. Current research focuses on the refinement of prediction techniques, application to other joint types and the implementation of a feedback control loop to maintain a desired position relative to the joint line.[Fleming et al., 2008a]
4. This technology could be beneficial for the implementation of automated and robotic friction stir welding applications.

CHAPTER VIII

PAPER 3: AUTOMATIC SEAM-TRACKING OF FRICTION STIR WELDED T-JOINTS USING WEAVING

Paul A. Fleming, Christopher E. Hendricks, D. M. Wilkes, George E. Cook and Alvin M. Strauss

International Journal of Advanced Manufacturing Technology, Under Review.

Abstract

In this research, a method for implementing automatic seam-tracking for friction stir welding is presented, based on weaving. In this extremum-seeking control technique, the tool weaves back and forth during welding to maintain the location where axial force is greatest, which is shown to be the center of the weld. Results demonstrate the effectiveness of this technique in tracking both known and unknown weld-seams. Comparisons of tensile test results of weaved and non-weaved welds, and findings in related literature, indicate that weaving's impact on weld quality could be positive. Finally, methods for incorporating seam-tracking into existing friction stir welding control systems (such as load control) are discussed.

Introduction

Friction stir welding (FSW) is a type of welding where material is joined through mechanical stirring via a rotating tool which traverses the joint line. It was first patented in 1991 by the Welding Institute and is currently employed in an increasing number of industries, including aerospace, rail and maritime.[Thomas et al., 1991b]

FSW has been shown to be applicable to a number of joint configurations, such as butt joints, lap joints and T-joints.[Mishra and Ma, 2005]

Seam-tracking allows a robotic welder to automatically follow the joint line. It has been implemented for a variety welding technologies, including arc-welding, laser-welding etc. Seam-tracking has a number of benefits including it eliminates the need for path planning, or at least reduces the precision required as the robot is able to track the weld-joint automatically. This simplifies the setup of robotic welding by reducing the need for precise trajectory planning and fixturing as the robotic welder becomes robust to small changes or inexactness in initial setup, either of parts or programming. This ability to quickly implement welds without rigorous setup reduces the cost of implementing 1-off welds, making the robot more versatile and useful.

A common method of implementing seam-tracking in other welding methods, is to include in the system external sensors for the detection of position. One example would be to include cameras and use computer vision to determine the location of the welding tool relative to the joint-line. However, other approaches, such as Through the Arc sensing, measure process variables in order to determine position. In the case of Through the Arc sensing, arc voltage and current are used as feedback signals which are used to determine position. These methods often have a number of advantages in simplicity, effectiveness and cost.[Cook, 1983]

In this research, a method for implementing seam-tracking in FSW is presented. This method, based on weaving, uses axial force as a feedback signal in order to maintain a desired position during welding. In many FSW systems currently in operation, axial forces are already measured due to their correlation with weld quality. T-joint welds are used in this paper, but results demonstrate that the method is applicable to lap joints as well. Seam-tracking is especially helpful in T-joints because the joint line is not observable from above.

This technology is one implementation of “Through the Tool Tracking”, which is

a collection of methods for implementing either position monitoring or seam-tracking in FSW using forces recorded through the FSW tool.[Fleming et al., 2008a] Through the tool tracking is useful as a method of ensuring proper alignment of the FSW tool to the joint, or as a method of automatically tracking the joint-line. This technology will be helpful in robotic FSW, and will enable tracking of non-linear joint-lines. Additionally, it provides robustness to noise in the position sensors of robotic welders and to errors in fixturing and positioning.

Forces and position

In this research, force is employed as the feedback signal. Using force as a feedback signal is typical in the literature of monitoring and control of friction stir welding. Boldsaikhan et al. used the frequency content of the dynamic force signal to discover metallurgical defects and evaluate tensile strength during the welding process.[Boldsaikhan et al., 2006a] Hattingh et al. demonstrated a relationship between forces experienced by the tool and process parameters such as welding and rotation speeds, as well as tool geometry.[Hattingh et al., 2004] Fleming et al. investigated the use of force monitoring for in-process detection of gaps between the material to be joined.[Fleming et al., 2008c]

In a later paper, Fleming et al. demonstrated that an estimator could be developed to predict the position of the tool relative to the joint-line using forces as a feedback signal.[Fleming et al., 2008b] This is possible because forces vary as a function of position. In that paper, it was shown that, for instance, the x-force (the force which is parallel to the joint-line) increased in magnitude as the tool position changed from advancing to retreating sides in T-joints. Additionally, the axial force was shown to exhibit an inverse-parabola shape, where the magnitude of the axial force is maximized near the center of the joint.

Based on this result, it can be seen that a control algorithm which adjusts position

so as to maximize the axial force would provide seam-tracking, because by moving to maximize axial force, the tool is continuously forced toward the center of the weld. We present weave-based seam-tracking for FSW, an extremum-seeking control algorithm, as a means to this end. In this paper, we demonstrate that this seam-tracking system is effective, robust to changes in tooling and weld parameters, and is likely to improve weld quality. Finally, we will show how it can be incorporated into existing control strategies such as load control.

Weaving

Extremum control is a type of control system where the goal is not to maintain a known set-point, but instead to track a varying maximum or minimum value.[Astrom and Wittenmark, 1989] In one variation of extremum control, a known time-varying perturbation signal is added to the input and its effects are measured on the output in order to determine in which direction is the extremum.

The seam-tracking technology presented in this research is an extremum-seeking control system for FSW. In it, the tool weaves back and forth perpendicular to the joint-line during welding in order to discover the position of maximal axial force. This weaving motion allows comparison between axial forces at two close positions. The controller adjusts the center of this weaving motion according to the comparison, moving the center closer to the side which exhibits the higher axial force.

In figure 77, the tracking technique is illustrated. The perturbation signal is trapezoidal. As can be seen, the controller maintains an estimate of the center of the weld, which it updates after each weave cycle by adjusting it towards the direction which exhibited the higher axial force. This adjustment occurs every cycle. In this algorithm, there are a number of parameters including the weave radius, or width of the weave; the rate at which the tool moves between extremes; the time paused before

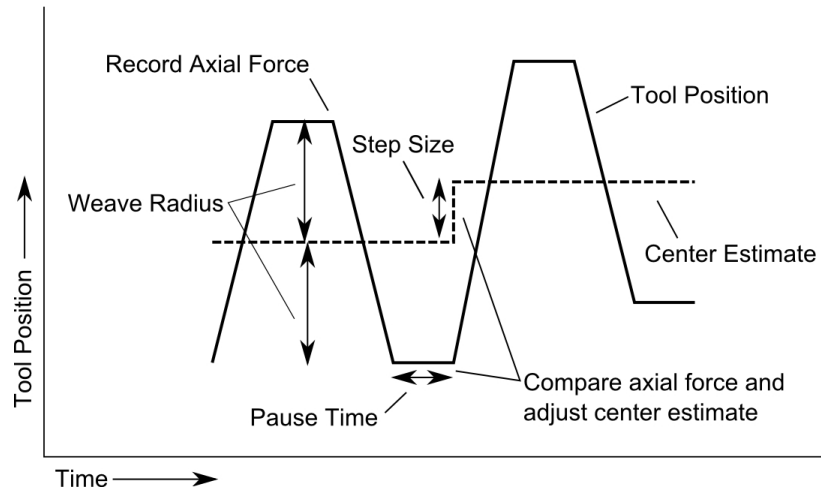


Figure 77: Illustration of weaving

taking a force reading; and finally the step size of the estimated center position made after comparisons.

Varying these parameters affects the performance of the controller, and future work is needed to find optimal settings. Additionally, improvements in the algorithm such as allowing the step size to vary proportionally to differences in axial forces or integrating forces over time rather than taking single samples would doubtless further improve performance. However, the research presented in this paper demonstrates that this technique currently implements a robust seam-tracking method for friction stir welding.

Experimental Results

In order to demonstrate the ability of the tracking system to automatically track the joint-seam, a number of example welds are presented. Figure 78 illustrates the setup and fixturing for the T-joints used in this research.

The material used is 6061 aluminum, with the horizontal member of the T-joint having a thickness of 3.175mm and the vertical member a thickness of 9.525mm. The tool used was a Flared TriFlute with a 15.875mm shoulder and a 3.81mm long probe

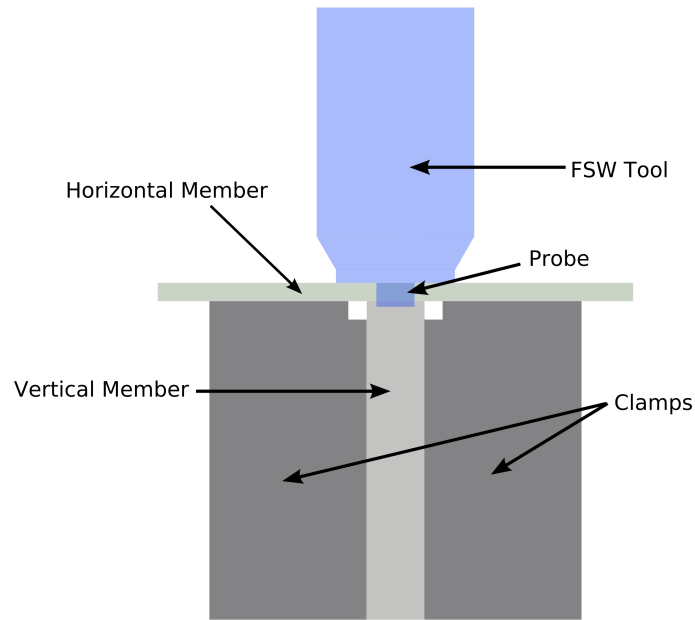


Figure 78: Diagram of T-joint fixturing used in research

with a diameter of 5mm. The rotation speed with 1000RPM and the welding speed was 5cm min^{-1} .

The first demonstration is a straight weld, where the weld is fixtured parallel to the direction of stage travel. However, at the start of the weld, the tool position is offset from the center of the weld seam. For this experiment, the weave radius is .25mm (total weave width is .5mm), the center step change is .25mm, the rate of change is 2.545 mm s^{-1} (15.25cm min^{-1}). These values were chosen experimentally.

Observing figure 79, the tool is initially offset 2mm from the center of the weld. When seam-tracking is started at 40s, the control system drives the tool to the center of the weld. The tracking system then maintains this centered position for the duration of the weld.

In the experiment display in figure 80, the weld joint is fixtured at an angle relative to the stage travel of the welding machine. Because of this, the position of the center changes continuously throughout the weld. The control parameters are the same as were used in the previous experiment. Initially, the tool is again offset from the center.

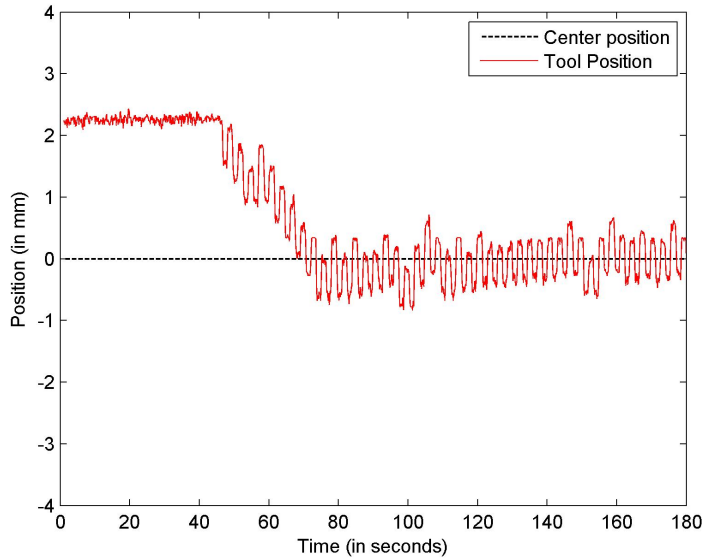


Figure 79: Tracking a straight weld-seam with weaving

When seam-tracking is started at around 50s, it first forces the tool to converge on the center position. It then tracks the center throughout the weld until seam-tracking is turned off at around 250s.

These tests demonstrate the ability of the seam-tracking control system both to maintain a known position, and also to track a moving position.

Quality and weaving

A question which needs to be addressed is how does this weaving affect the quality of the weld joint. Based on the performance of FSW technologies with similar descriptions, as well as initial testing conducted in this research, weaving at least should do no harm, but also very likely improves weld quality.

While this weave-based seam-tracking method was developed to assist in control, it has similarities to other new variations of friction stir welding developed by TWI. Recently, TWI has discovered a variety of methods for widening the weld region through the use of new technologies including A-skewTM welding and Com-StirTM

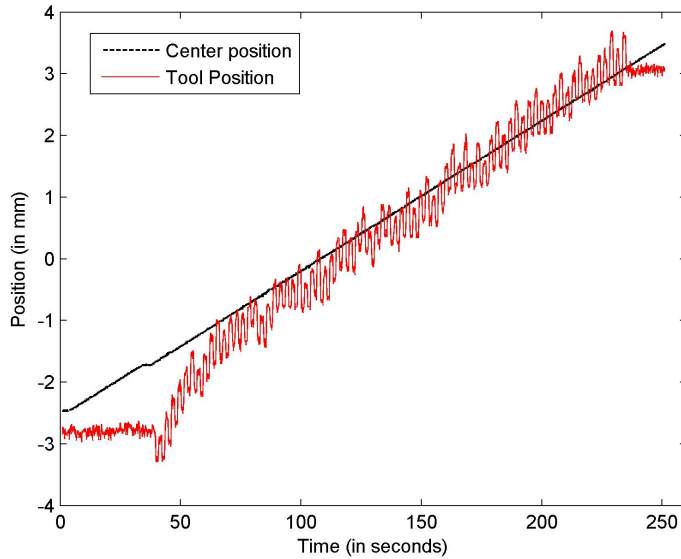


Figure 80: Tracking a linearly changing weld-seam with weaving

welding. The tool used for A-skewTM welding has its axis at a slight inclination to that of the machine spindle. This results in an orbital motion of the pin which allows more material to be processed.[Thomas et al., 2003a, Cantin et al., 2005] Com-StirTM welding involves a compound motion of the tool which allows varying types of motion from complete orbital motion of the tool to complete rotary motion depending on the selection of a relative rotational speed.[Thomas et al., 2003b] It is believed that these techniques enhance the weld quality by improving flow path around and underneath the pin, widening the welding region, and allowing further fragmentation and mixing of the oxide layer.[Mishra and Ma, 2005]

The weaving used in this research appears at present to be a lower frequency version of the techniques discussed in the above. For this reason, it seems probable that the weaving which is performed for extremum-seeking could improve weld quality for the reasons described in the literature, if to a lesser extent because of the lower frequency.

Looking at cross-sections comparing weaved and non-weaved welds, the weaving

was able to widen the weld region. As seen in the cross-sectional images in figure 81, the width of the weld increases by about 0.5 mm when a weave width of 0.5 mm was used. In lap welds, as well as T joint welds, this widened weld region is seen as beneficial and necessary for increased peak stress values because of the possibility of a higher volume of material processed.[Mishra and Ma, 2005] Again however, due to the lower frequency of material processing, our results will not necessarily coincide with those in the literature.

Tensile tests were performed on samples of weaved and non-weaved welds as illustrated in figure 82. The results from the lateral tensile test were mixed and no clear pattern emerged. On average, the weave samples had a higher peak stress than the non-weave welds; however, the difference was not significant. The same can be said about the shear tests on both the retreating and advancing sides. The most important result was the increase in the peak stress of vertical tensile tests. Every weave weld was stronger when compared to non-weave, normal welds. In addition, the average of the weave welds was 11.5% stronger than the normal welds for the vertical tensile test. While this result is promising, more research needs to be carried out to optimize the weave width and other weaving parameters for maximal tensile strength improvement. At this point, it can be shown that the weaving does not appear to hurt the strength of the weld, and future work will be able to ascertain whether weaving can significantly improve the peak stress values in all dimensions.

Discussion

Weave-based tracking has been demonstrated as a technique for automatic seam-tracking in the friction stir welding of T-joints. Additionally, research has demonstrated that the axial forces varies in the same way in lap-joints and that this method could be applied to this joint-type as well.

Weave-based seam-tracking has a number of useful properties. As discussed in

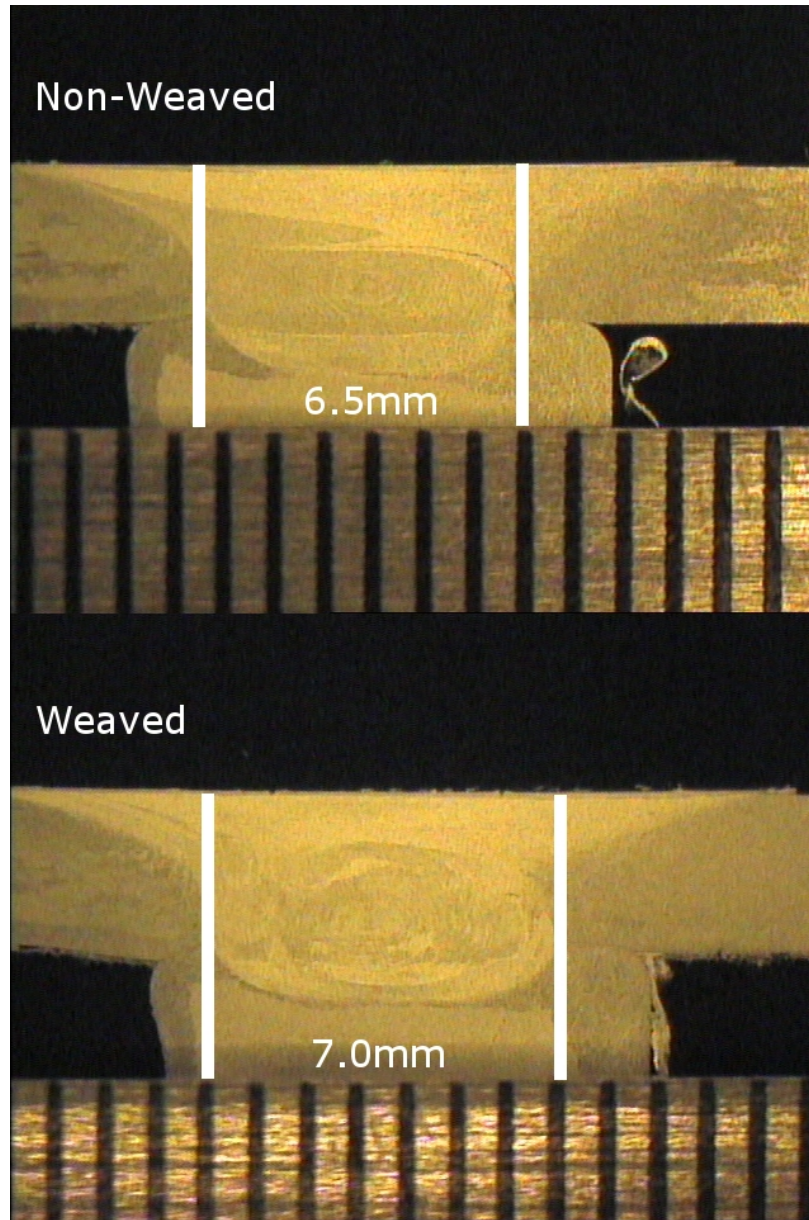


Figure 81: Comparing cross-sections of weaved and non-weaved welds

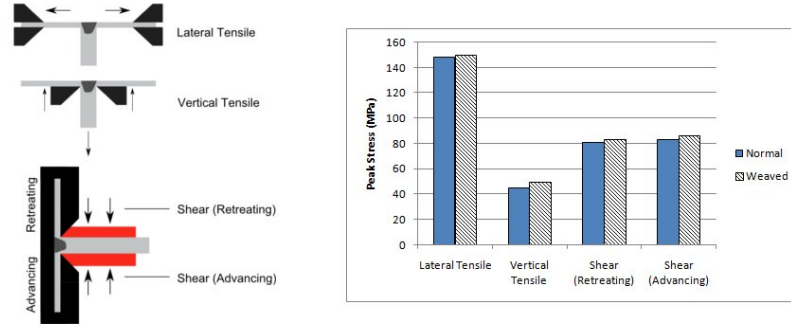


Figure 82: Left: Tensile test fixturing Right: Tensile test results

section VIII, weaving likely increases the tensile properties of T and lap-joints. Additionally, because of its setup as an extremum-seeking control algorithm, it is robust with respect to FSW parameters and design choices. The absolute value of axial force changes with varying tool designs and welding parameters (rotation speed, welding speed, rake angle), but the relative values of axial forces at varying distances from the center will remain throughout these changes. This robustness to changes in the system makes the system widely applicable to industrial FSW applications.

An additional benefit of this robustness, is that existing load control methods can be incorporated into the control cycle. In a typical load control method, the vertical height of the tool or traverse speed are continuously adjusted to maintain a reference axial force.[Kinton and Tlusty, 2000] [Stotler and Trapp, 2007] An example algorithm would alternate a weaving cycle to move the tool closer toward the center and a vertical adjustment to move the axial force toward the desired value. So long as the vertical adjustment is performed outside of a weave cycle, it does not effect the tracking algorithm which only considers the comparison of forces on the extremes of weaving.

This technology is expected to be of good use to a number of industrial applications. Currently, seam-tracking is employed in a number of other welding technologies,

and provides numerous benefits. By enabling seam-tracking for FSW, this system allows the tracking of non-linear joint lines by robotic welders. Additionally, it reduces the necessity of precision fixturing and trajectory planning and allows robustness to unexpected changes in either fixturing or position of the welding apparatus.

Future research will focus on improving this technology and expanding its applications. One area will be in the application of seam-tracking to lap joints. Additional research will focus on optimizing the system for tracking and quality improvement. In this regard, there are a wide number of control improvements which could be attempted including allowing the center estimate step to vary proportionally to the difference in axial force, dynamically changing the weave radius and rate of change. Additionally, incorporating information about the effect of the lateral motion during weaving into a model-based control approach could also potentially yield gains in performance.

Conclusion

- A robust control system for automatic seam-tracking for T-joint FSW was presented based on weaving
- Weaving does not seem to negatively impact weld quality and very likely improves weld quality
- Weave-based seam-tracking is ambivalent to FSW parameters and design considerations and could therefore be implemented directly in a wide variety of FSW applications without training or specific configuration
- Because the axial force exhibits the same pattern in lap joints as it does in T-joints, this system is expected to work in the same way in lap joints
- Seam-tracking can be combined with load control in an alternating control scheme

CHAPTER IX

PAPER 4: SEAM-TRACKING FOR FRICTION STIR WELDED LAP JOINTS

Paul A. Fleming, Christopher E. Hendricks, George E. Cook, D. M. Wilkes, Alvin M. Strauss, and David H. Lammlein

In preparation for: *Materialwissenschaft und Werkstofftechnik*.

Introduction

Friction stir lap welding

Friction Stir Welding (FSW) is a relatively new solid-state welding process. It was patented in 1991 by TWI, and is finding an increasing range of industrial applications. [Thomas et al., 1991a] In FSW, a rotating tool is plunged into the material to be joined and then traverses the joint line. The FSW tool typically consists of a shoulder which rides along the surface of the weld applying heat and pressure, and a probe which is plunged into the material and accomplishes stirring. FSW is performed either by a large machine, often a converted milling machine, where the tool is effectively stationary, aside from rotation, and the stage moves to allow traversal of the joint, or by a robot which both rotates the tool and traverses along the joint line. The larger machine allows for greater rigidity, while the robot provides flexibility in positioning.

FSW has shown to be applicable to a number of joint types, including butt-, lap- and T-joints. Lap (or overlap) joints are joint types where the material is laid one on top of the other creating an overlap region. The FSW probe plunges completely through the upper material, and slightly into the lower sample. An illustration of friction stir lap welding (FSLW) is shown in Fig. 83.

The above figure points out some important nomenclature used in this paper and

the literature. The advancing side of the weld is the side in which the direction of tool rotation and tool motion are the same, and the retreating is the opposite. Additionally, a right-handed lap weld is one in which the top member is on the right when viewed from the start of the weld.

Friction stir lap welding is currently used in a number of applications and has potential for wider application. [Ericsson et al., 2007] point out for example that “high-strength aluminium structures in airplanes (often of lap- or t-joint type), traditionally viewed upon as unweldable and fastened by rivets, can be friction stir welded.” An advantage to using FSLW is that the shear tensile strength of FSLW was found to be “2.4 times that of single row riveted joints.”

Seam-tracking and robotic welding

Robotic FSW represents an opportunity for a more flexible welding process, and the increased applicability of FSW. [Smith et al., 2003] demonstrate that by robotizing the FSW process, time and money can be saved due to a robot’s ability to perform numerous weld passes on a single fixturing. In the conclusion of [Smith et al., 2003], they point out that FSW is “following in the footsteps of several other welding processes with regard to the need for flexibility”, for instance Gas Metal Arc Welding (GMAW).

A common feature of arc welding robotics today is the seam-tracking ability of the robot. This enables the robot to follow the joint-seam automatically, and reduces the need for precision fixturing. A typical instantiation of seam-tracking for arc welding robots is called through-the-arc sensing. As discussed in [Cook, 1983], through-the-arc sensing follows the joint-seam during welding by adjusting position according to signals which are intrinsic to the welding process: arc current and voltage. Seam-tracking enables robotic arc-welding to cope with variations in joint positioning and therefore reduces the need for precise fixturing and path-planning.

Through-the-tool tracking, implements automatic seam-tracking for friction stir welding. Like through-the-arc sensing in arc welding, it uses signals intrinsic to the welding process, in this case the forces and torques transmitted "through-the-tool".[Fleming et al., 2008a] An important benefit of through-the-tool tracking is its use of a feedback signal which is likely already monitored in most existing robotic FSW systems. [Smith et al., 2003] in their discussion of robotic FSW state the need for force feedback in robotic FSW in order to monitor and control the axial load and penetration depth. Therefore a system which uses force signals to maintain joint position requires no additional sensing equipment. This reduces the time and cost of adding a seam-tracking system. Additionally, it will be shown that tracking can be accomplished simultaneously with load-control during welding.

Because through-the-tool tracking accomplishes seam-tracking using sensed forces as a feedback system, it is therefore required that the relationship between the location and velocity of the tool relative to the joint-seam and the resultant forces be known. [Fleming et al., 2008b] trained a neural network to predict lateral position of the tool with respect to the joint line for T-joint FSW. This system would provide an error signal which could be fed into a position controller to enable seam-tracking and demonstrates the possibility of correlating lateral position with force and torque signals.

WeaveTrack is an instantiation of through-the-tool tracking in which the tool weaves back and forth across the weld in order to discern the center of the joint-line. This method is similar to the process used in through-the-arc sensing. In (Fleming et al, 2008 manufacturing), WeaveTrack was used to successfully track blind T-joints.

In this paper, the WeaveTrack technology for FSW lap welds is presented. Experiments demonstrate the ability of WeaveTrack to track both steady and changing lap-seam positions. Additionally, the effect of weaving on the mechanical properties

of lap welds is inspected. Finally, recommendations for the continued development and implementation of WeaveTrack and its use to industry are presented.

WeaveTrack System

In the WeaveTrack technology, the FSW tool traverses back-and-forth perpendicular to weld travel, monitoring force or torque signals at the limits of travel and comparing them to determine the direction of the center of the weld with respect to the current position. This mirrors mechanically what is done electrically in through-the-arc sensing (with force and torque replacing voltage and current). Figure 84 illustrates the WeaveTrack process algorithmically.

In the above algorithm, $\Sigma_{current}$ is the current force or torque signal value while Σ_{Adv} represents the force or torque signal recorded on the advancing side of the weave. There are three free parameters in the above algorithm, they are:

1. *WeaveRate*: The speed of the weaving motion in cm min^{-1}
2. *WeaveWidth*: The width of the weave in mm
3. *StepSize*: The length, in mm, of the adjustment made to the center of the weave when moving based on indicating signals

$Weave_{Adv}$ and $Weave_{Ret}$ then are the distances to move toward the advancing side or retreating side in the current weave motion. Essentially, the direction which is determined to be closer to the center will have a longer weave ($WeaveWidth + StepSize$).

As can be seen from the WeaveTrack algorithm, the process assumes that some signal (a force, torque or functions of force and torque) indicates position in that when the weave is centered about a position on one side of the center of the seam, said signal is larger on the side closer to the center, and on the other side, the reverse is true.

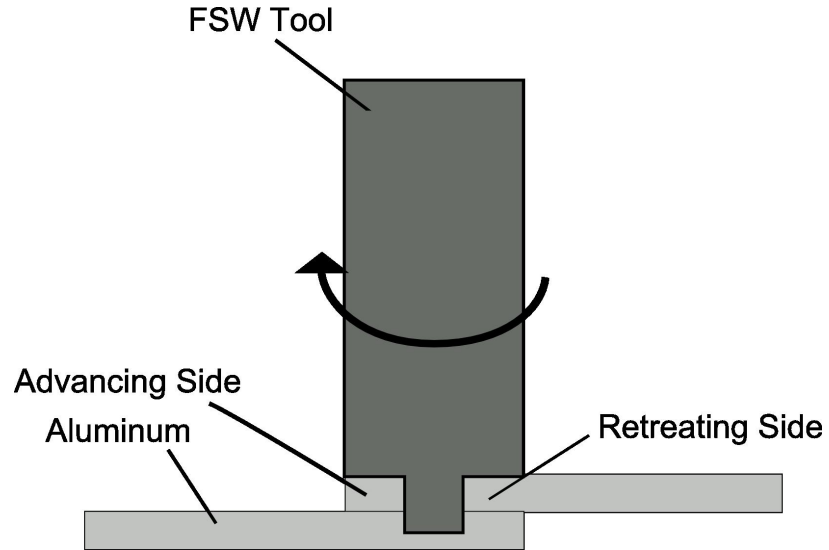


Figure 83: Lap Welding Diagram

```

while Weaving do
  Move  $Weave_{Adv}$  mm at  $WeaveRate$   $cm\ min^{-1}$  toward advancing side
  Store  $\Sigma_{current} \rightarrow \Sigma_{Adv}$ 
  Move  $Weave_{Ret}$  mm at  $WeaveRate$   $cm\ min^{-1}$  toward retreating side
  if  $\Sigma_{current} > \Sigma_{Adv}$  then
     $WeaveWidth \rightarrow Weave_{Adv}$ 
     $WeaveWidth + StepSize \rightarrow Weave_{Ret}$ 
  else
     $WeaveWidth + StepSize \rightarrow Weave_{Adv}$ 
     $WeaveWidth \rightarrow Step_{Ret}$ 
  end
end

```

Figure 84: WeaveTrack Algorithm

(Fleming et al, 2008 manufacturing) showed that in the case of “open-air” T-joints, the axial force fulfilled this role with the greatest signal to noise ratio. However, in lap-joints, the torque has this desired property. When the weave is about a position offset to the advancing side of the weld, the torque collected on the retreating side will be higher, with the converse true as well. This was determined experimentally.

Experimental Setup

A series of experiments were performed, both to test the ability of WeaveTrack to automatically follow a lap-joint, and also to examine the effects of WeaveTrack on the mechanical properties of an FSW lap weld.

The material used in these tests was 3.175mm thick 6061 aluminum, and the lap welds were arranged in a right-handed configuration. The width of the overlapped area of the weld was 15.875mm. The FSW tool used in the experiments was a Flared TriFlute with a 15.875mm shoulder, and a probe which was 6.35mm wide by 5mm long. The rotation speed of the tool was 1000 RPM and the welding speed was 5cm min-1.

Results

Tracking a non-changing lap-joint position

In the first experiment, the lap joint is fixtured normally; however the tool starts the weld run with some offset with respect to the center of the overlap. The results for two of these welds are shown in figure 85.

In the upper result plot, the tool is started offset to the advancing side of the center. When WeaveTrack is engaged at 50s, the system moves directly to the center and then holds this position. In the lower figure, the tool is started offset to the advancing side, and WeaveTrack again moves the tool to the center and holds the

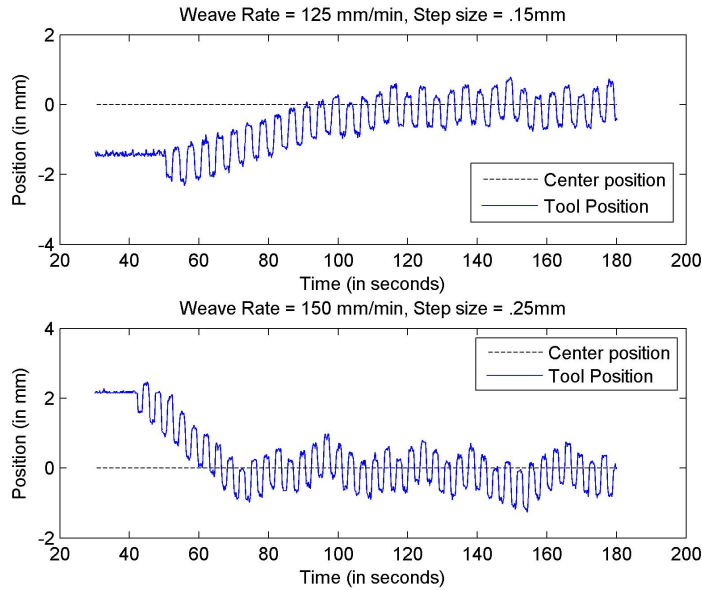


Figure 85: Step response

position. In the lower experiment, both the Weave Rate and Step Size have been increased with respect to the upper experiment and this results in a quicker convergence to the center. The optimization of these parameters, and also the inclusion of more advanced control techniques is the subject of future work.

Tracking a changing center position

In a second experiment, the aluminum was machined at an angle, so that when clamped, the overlapped region would remain constant in width, but shift with respect to the direction of stage travel. In figure 86 the effects of welding this changing lap joint with and without WeaveTrack are shown.

In the above figure, the top view of the lap welds are shown on the left, with black lines drawn in on the outline of the weld surface to assist clarity. Notice that because the normal weld does not adjust to the changing position, it gradually becomes offset to the point where large surface defects appear. The WeaveTrack weld however,

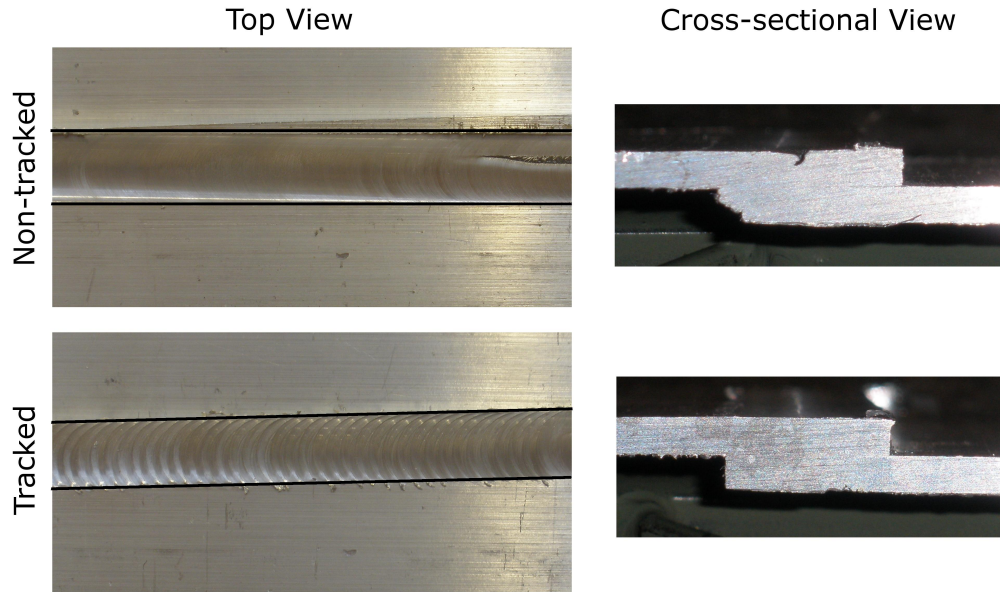


Figure 86: Comparing Tracked and Non-Tracked Welds Given Changing Center Position

follows the seam, and therefore does not exhibit this flaw. Looking at the cross-sections of the two welds on the right, one can see that the non-tracked weld was also extruding material. Figure 87 shows the position of the tool and the position of the center of the overlap region over time for the tracked weld.

Mechanistic results

WeaveTrack is a method for tracking the weld seam, however it is important to consider the impact of weaving on the quality of lap welds. In weaving, the tool is moved back-and-forth perpendicularly to the weld seam during traversal. This action is similar to some methods described for the improvement of lap welds in the literature. [Cantin et al., 2005] describe skew-stir, in which the probe is at an angle to the axis of rotation, thereby sweeping a larger area than the volume of the probe. The Com-Stir system, described in [Thomas et al., 2003b], combines orbital

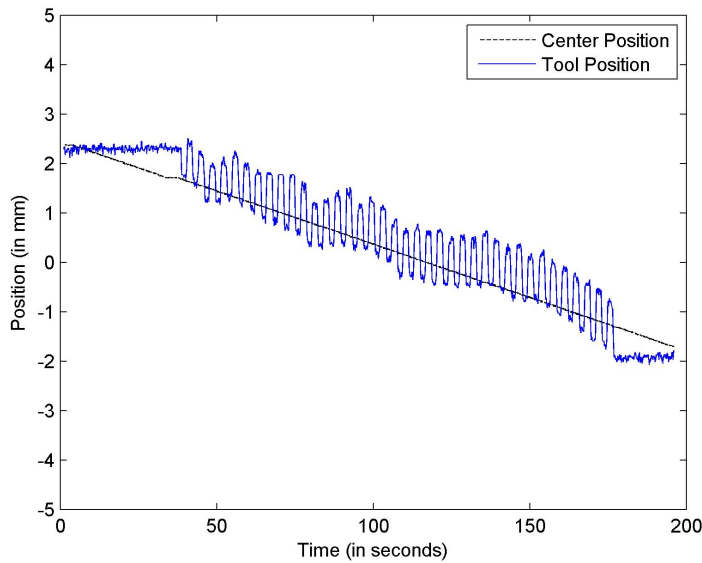


Figure 87: Tracking A Changing Center Position

and rotary motion of the tool. This produces both a wider weld and should give more “efficient surface fragmentation” than conventional FSW, both of these results implicating a higher quality lap weld.

Weaving is similar in nature to these two processes; it also causes the probe to sweep through a larger volume than the probe itself and thereby producing a wider weld. However it is not identical, and to date is performed at a lower frequency (weaves min^{-1} compared with orbits min^{-1} in Com-Stir or the rotation speed of skew-stir). Nevertheless, experiments indicate that weaving currently does produce similar, if less pronounced results as these related methods.

Tensile tests were performed to compare the peak stress of weaved and non-weaved welds and the results can be seen in Fig 88. Two weave rates were considered, and five weave widths. In all cases considered, the weaved lap welds achieved a higher peak stress. The 50 mm min^{-1} weaved welds performed slightly better than the 125 mm min^{-1} welds. Overall, there was a 7% increase in tensile strength between the average of the 50 and 125 mm min^{-1} weave results and non-weave results.

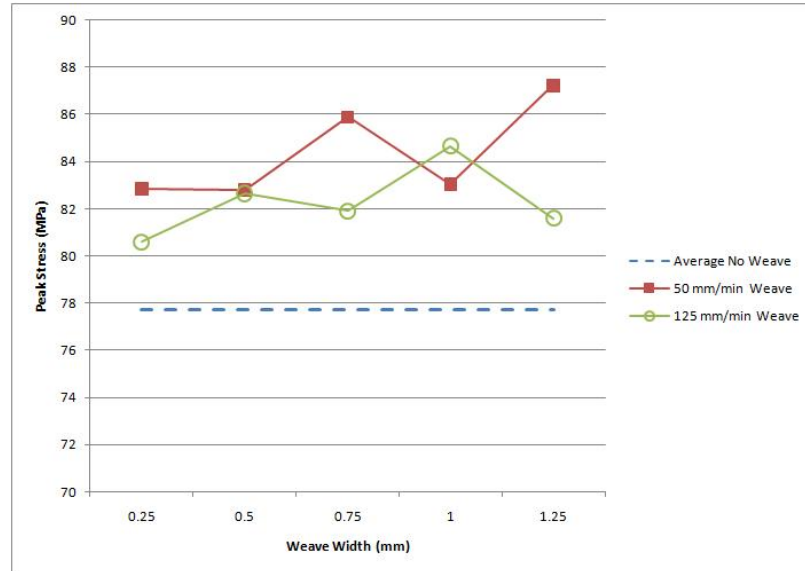


Figure 88: Tensile Results

In addition to tensile testing, the welds were also bend-tested according to the Hammer S-Bend procedure described in (Colegrove, 2004) as “a rudimentary experiment where the weld is bent into an S-shape which places the joint area in tension and opens any cracks that may have been produced by the welding process.” Further, [Thomas et al., 2002] state that bend test results give good correlation with fatigue test results for FSW lap welds. The results of bend testing a non-weaved and weaved weld are shown in figure 89.

In figure 89, the weaved weld has a weave width of .75mm and a weave rate of 125 mm min⁻¹. One result of bend testing was the demonstration that all weaved and non-weaved welds “passed” the bend test, in that no cracks were opened up at the ends of the unwelded notches. This further indicates that weaving at minimum does no harm to weld quality. However an additional result is the confirmation that weaving is widening the weld region, as shown in the above figure, which is an explanation for the increase in tensile strength.

WeaveTrack is intended as a technology for the implementation of automatic seam-tracking. The results of tensile testing and bend testing indicate that the process of

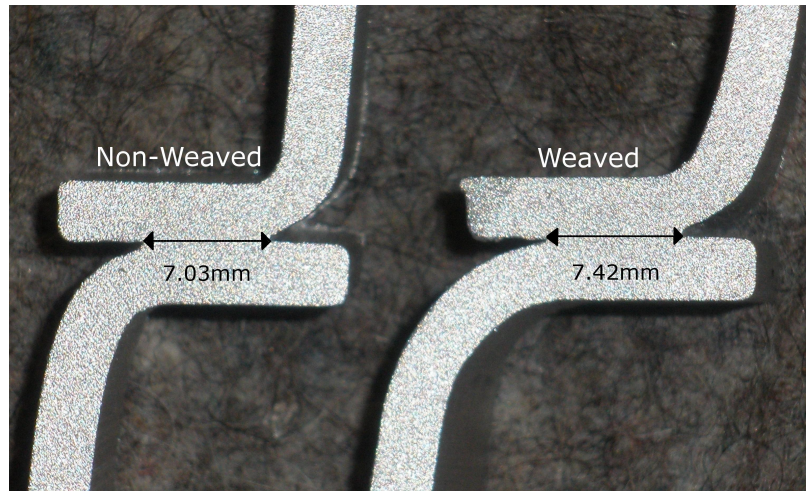


Figure 89: S-Bend Results

weaving either has a potentially positive effect on weave quality, or at least not a negative impact.

Discussion

The above tests demonstrate the ability of WeaveTrack to effectively track a lap joint. Additionally, mechanical testing and comparisons with related literature indicate that the implementation of WeaveTrack may represent an improvement of the physical properties of the weld.

As can be seen from the history of welding robots, seam-tracking technologies often serve to improve the robustness and flexibility of automated welders and therefore can decrease the amount of time and money which needs to be invested for a given weld run. Using WeaveTrack when performing lap welds implies that the robot can be relied upon to find and track the center of the overlap and can therefore handle variations in fixturing, thereby reducing the burden of precision positioning.

WeaveTrack has a number of useful features which should facilitate its adoption in industry. The first is that it uses the forces intrinsic to the welding process as its feedback. Forces are very typically sensed in FSW, and especially so in robotic

FSW where load control is considered essential. Therefore, for most robotic welding systems, WeaveTrack would not require additional sensors. Further, it can be shown that WeaveTrack can incorporate load control. Because WeaveTrack compares only the relative difference between the forces or torque observed at the limits of weaving, correcting the vertical height or spindle speed or traverse rate between weave cycles would not be a problem, doing so should effect the absolute levels of both readings, while their relative difference remains. It is also probable, that other force-based sensing techniques, such as the ones described in [Boldsai Khan et al., 2006a], which uses a neural network to identify metallurgical defects, could also be incorporated.

Future Work

Future progress on WeaveTrack should focus on the refinement of the system, both in terms of sophistication of the control algorithm, and with respect to its mechanical effects.

In terms of control, currently the algorithm has three fixed parameters: the weave width, the step size and the weave rate. One improvement could be to allow one or more of these values to vary dynamically in response to the relation of signals obtained on the sides of the weave. From here, it is conceivable to imagine this proportional style control leading to PID type control settings and from there to more advanced control laws. This initial system should serve as a proof of concept, with a later system achieving improved bandwidth and stability through refined control techniques.

Mechanically, the system should be improved to maximize the gain in weld quality through experimental and modeling means.

Conclusion

- WeaveTrack enables seam-tracking of lap-joints for Friction Stir Welding. Seam-tracking greatly improved the flexibility and applicability of other robotic welding technologies and could do the same for FSW.
- WeaveTrack uses the forces and torque intrinsic to the welding process, which likely is already sensed in many existing robotic FSW technologies
- WeaveTrack could incorporate existing force-based sensing techniques such as load-control, and quality monitoring.
- WeaveTrack currently causes a small but distinct quality improvement in lap welds and could likely be developed to the point of producing larger quality gains.

Part III

Unpublished Related Research

CHAPTER X

SYSTEM MODELING WITH MATLAB AND SIMULINK

Introduction

To further research the ability of the VUWAL FSW system to track, both in general and specifically with WeaveTrack, a model of the welding machine was developed in SIMULINK. Additionally, a mathematical model for predicting forces given lateral positions was developed as well. The purpose of these models was to explore the ability of the system at VUWAL to track a weld-seam.

Simulink model

The simulink model of the system related the reference motor speed sent to the lateral motor, to the actual stage velocity and position. This relationship was found to be non-linear, in that there is significant backlash in the stage motion. This backlash was measured, and included via the SIMULINK backlash block.

Additionally, step tests were run to discover the system dynamics (rise time, overshoot) experimentally. The results of one step test is shown in figure 90

Step tests were run both with the backlash wound out before hand, and without, and also in both directions. The system was found to be roughly 1st order.

The final component of the model is a block which predicts forces given the models lateral position and velocity. For this block, MATLAB's curve-fitting toolbox was used to discover polynomial approximations of this relationship based on experimental data. Position only was found to be sufficient for prediction.

The final SIMULINK model is shown in figure 91

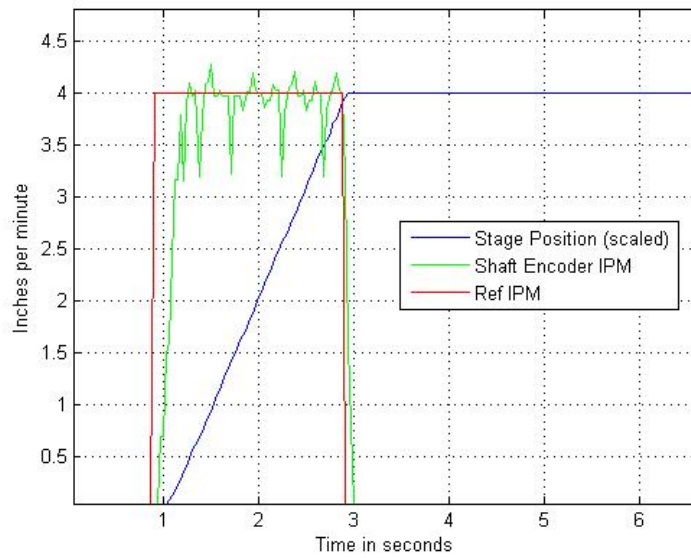


Figure 90: Step Test

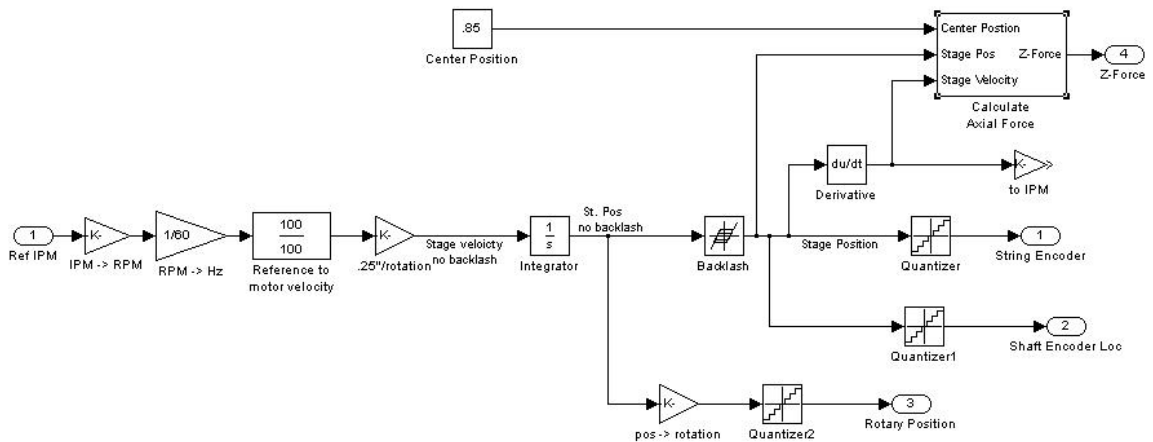


Figure 91: Simulink model of VUWAL FSW welder

Verification of model

The polynomial force models were verified by comparing the predictions of these models, with those recorded during actual runs, when given the lateral location of the welds. Some results are shown in Figs. 92 and 93

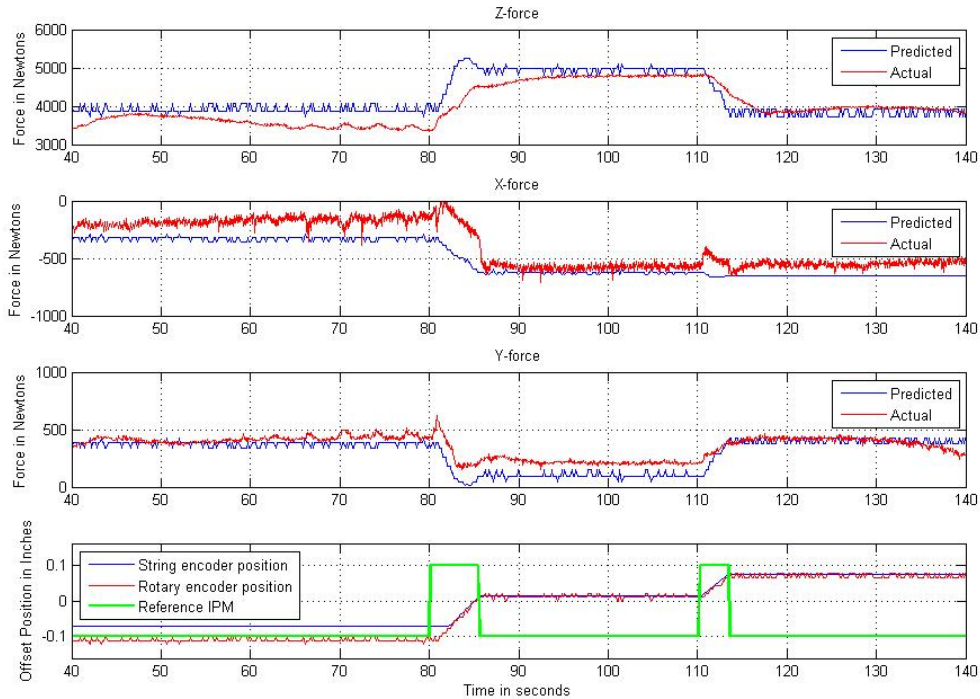


Figure 92: Comparing predicted and actual forces

Analysis with model

This model could be useful for future work developing tracking algorithms because it can provide simulated results to quickly tests new algorithms.

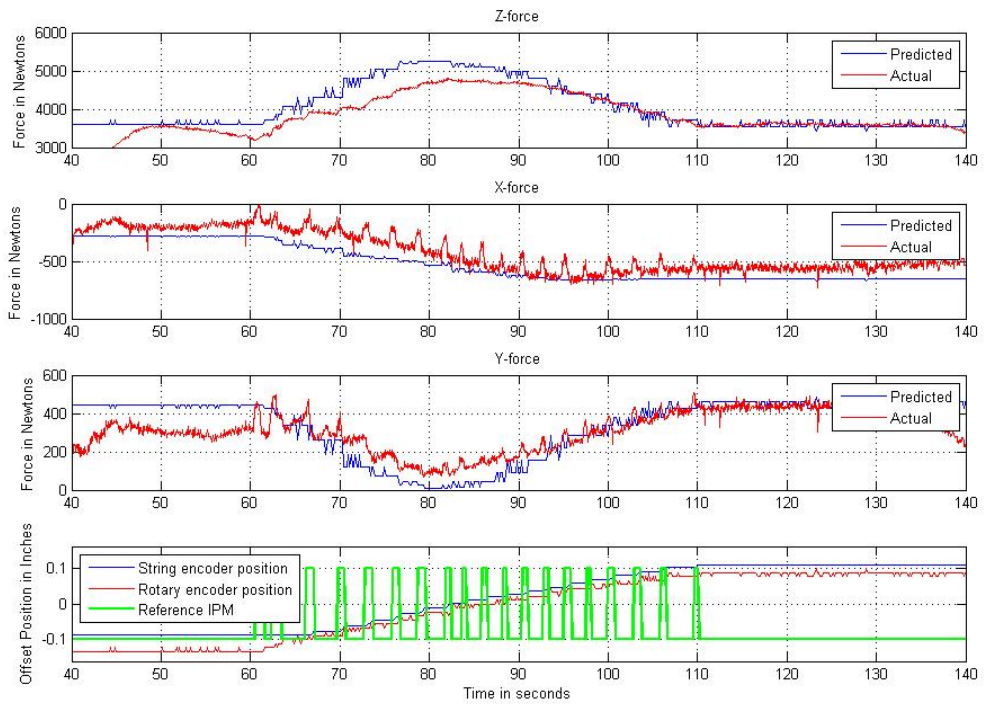


Figure 93: Comparing predicted and actual forces

Example usage

One case where the model has already been employed was in simulated experimentation with the weave rate in WeaveTrack. It was desired to determine the bandwidth of the VUWAL FSW welding machine in implementing WeaveTrack. A simulated experiment was devised where rather than the square waves currently used in WeaveTrack, sinusoids were input to the lateral motor reference of the simulation. The model then produces output stage velocities, which were then compared, with the inputs. This produced results like those shown in figure 94.

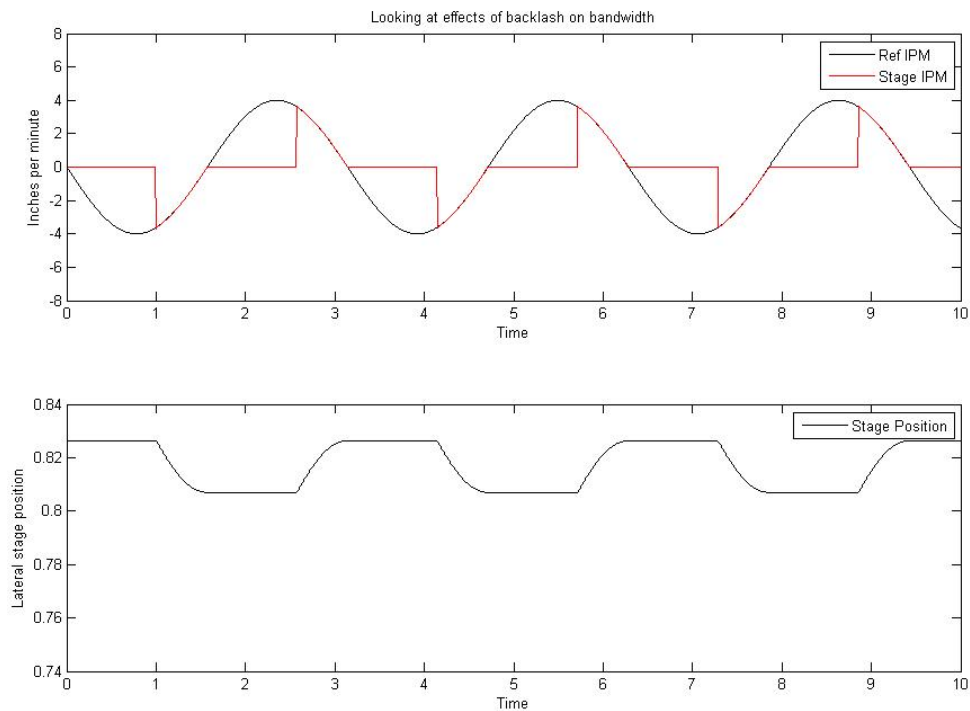


Figure 94: Simulated input motor reference velocity and resulting stage velocity

Because of the backlash, and to a lesser degree the system inertia, the output stage velocity is shown to attenuate. Experimentation found that for this system, this attenuation was found to be dependent on both the amplitude and frequency of the input sinusoid.

Because MATLAB allows SIMULINK models to be called from a script, a program was written which applied sinusoids with varying amplitudes and frequencies to the input of the model and measured the attenuation of the stage velocity signal. The results are shown in the “bode-like” plot of figure 95.

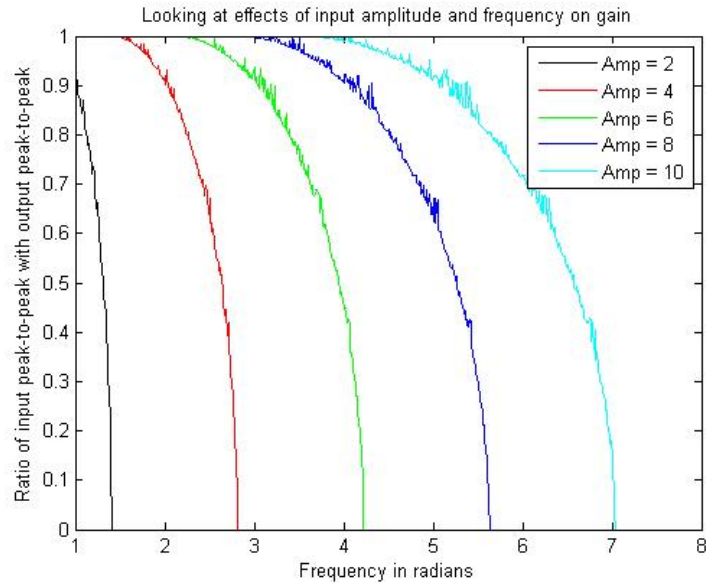


Figure 95: Attenuation vs. frequency for several amplitude inputs

This result indicates the range of amplitudes and frequencies of sinusoids the system can accommodate with little attenuation, and which are either too small or too fast.

Conclusion

The above example illustrates one use of the model in the development of tracking systems. It is believed that the model could be of use to further research at VUWAL in tracking systems using the VUWAL FSW welder.

CHAPTER XI

AUTOMATIC TOOL WEAR DETECTION

Paul Fleming, Thomas Bloodworth, David Lammlein, Tracie Prater, George E. Cook
Alvin Strauss, D. M. Wilkes, David DeLapp, Thomas Lienert and Matt Bement

Presented at Aeromat 2007

Introduction

This research was presented at Aeromat 2007, but not published. The research project was to determine if the FSW process forces, used throughout this research, would be affected by tool wear. Additionally, the research attempted to demonstrate the nature of this relationship and how it could be used for future tool wear detection systems in FSW.

Experimental setup

An FSW tool (threaded cylinder type) was constructed out of mild steel. Mild steel was chosen to increase the wear rate. Next the tool was run repeatedly through bead-on-plate type welds. A picture of a bead on plate weld is shown in figure 96

During welding, process forces were recorded, including the planar force, the axial force and the torque. Twenty welds were completed, and tool wear was visually noticeable. The shadow-graph shown in figure 97 illustrates this.

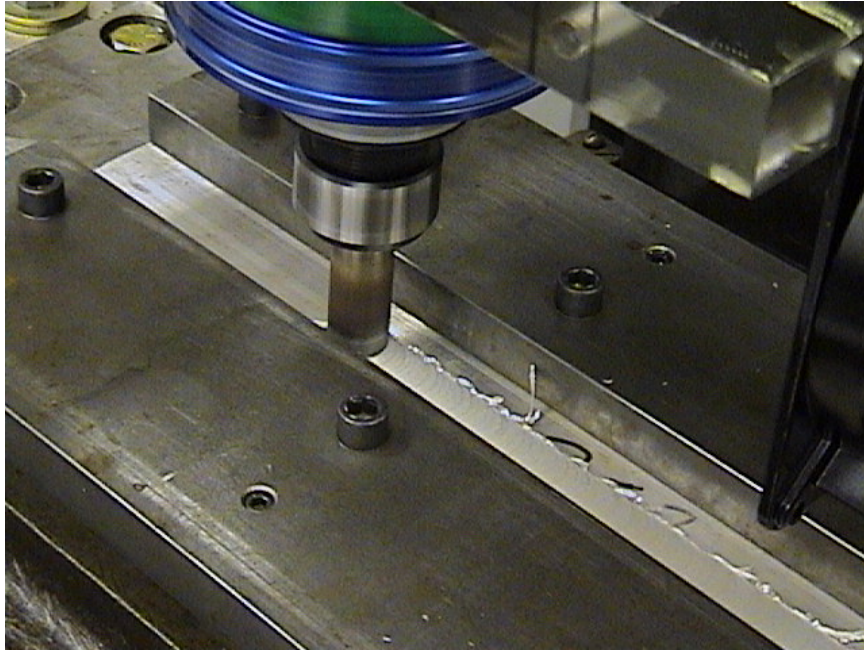


Figure 96: Bead on plate welding with mild steel tool

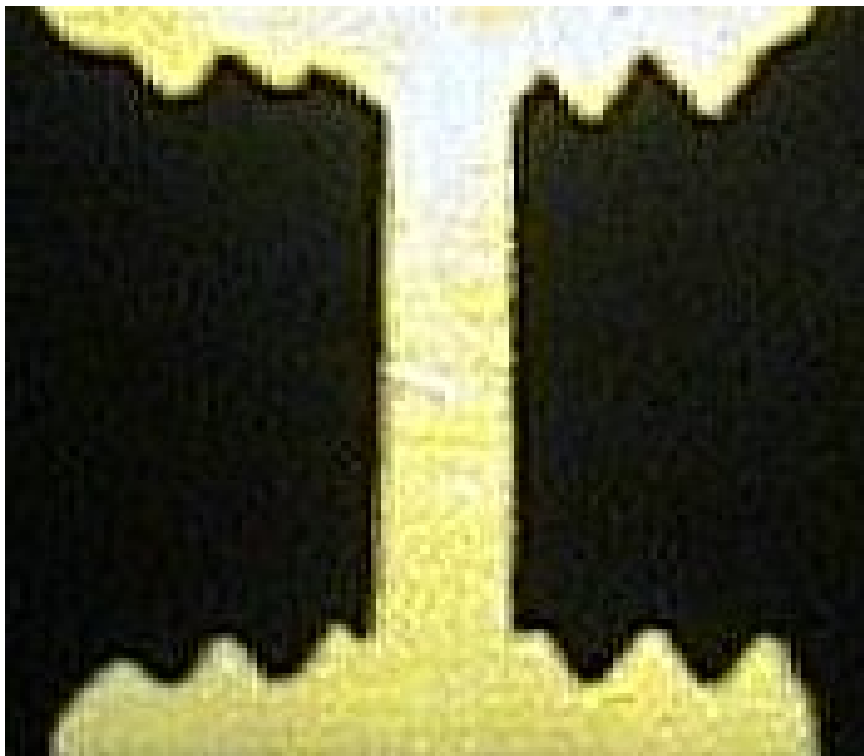


Figure 97: Shadowgraph of worn tool (left) and un-used tool (right)

Analysis

The forces were collected during welds at a rate of 1000 HZ, and the mean force for planar, axial and torque was computed for each run. The following figures indicate a relationship between forces and wear.

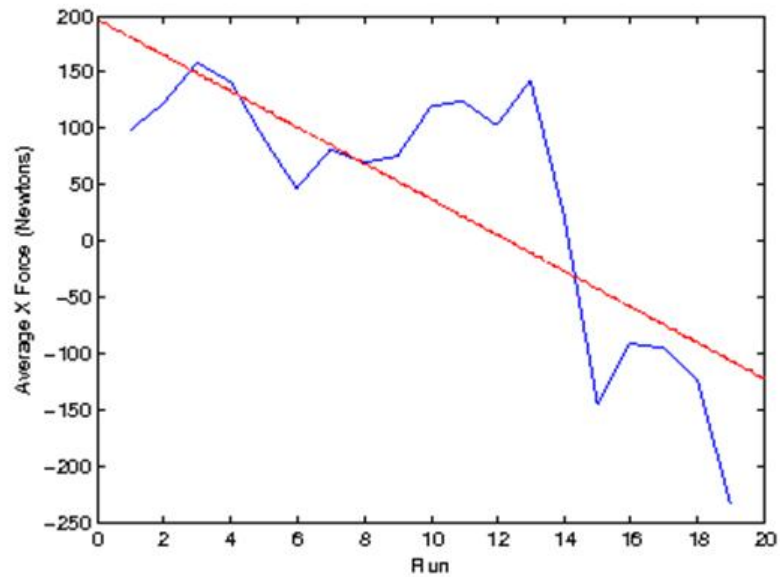


Figure 98: Average planar forces

Frequency analysis

Additionally, the frequency bands of each weld was computed using the fast fourier transform. The frequency bands of the welds are seen to change with wear.

Discussion and conclusion

This experiment indicates that the methods and techniques used for the monitoring and detection of gaps, and of misalignment, presented in this dissertation, could likely be extended to the monitoring and detection of tool wear in FSW. Like the previous

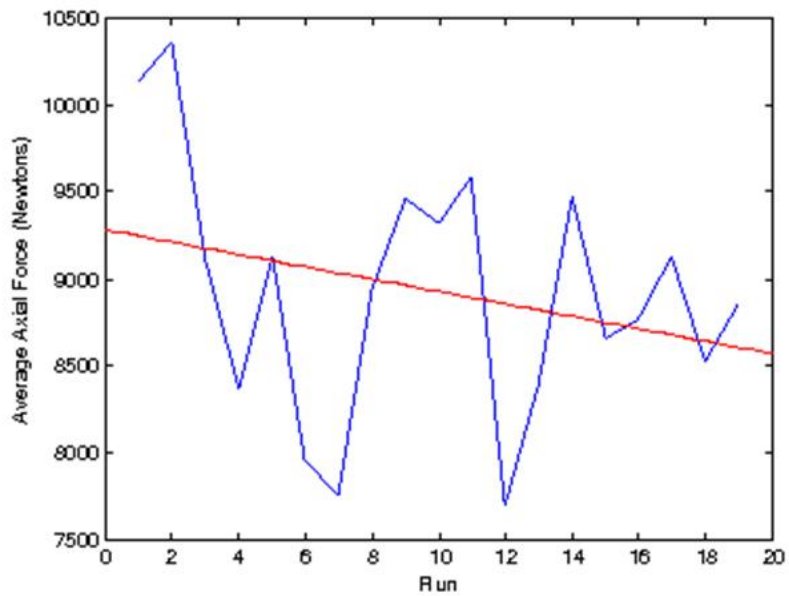


Figure 99: Average axial forces

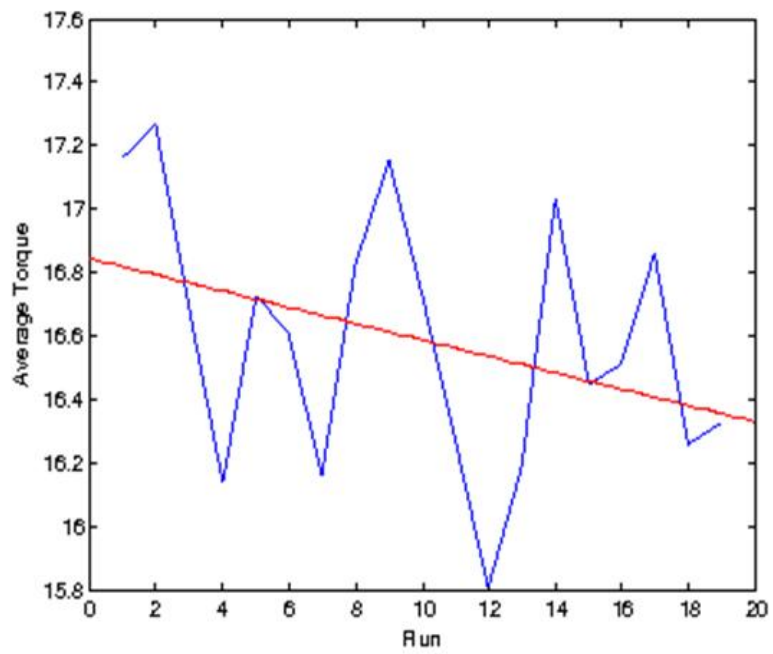


Figure 100: Average torque

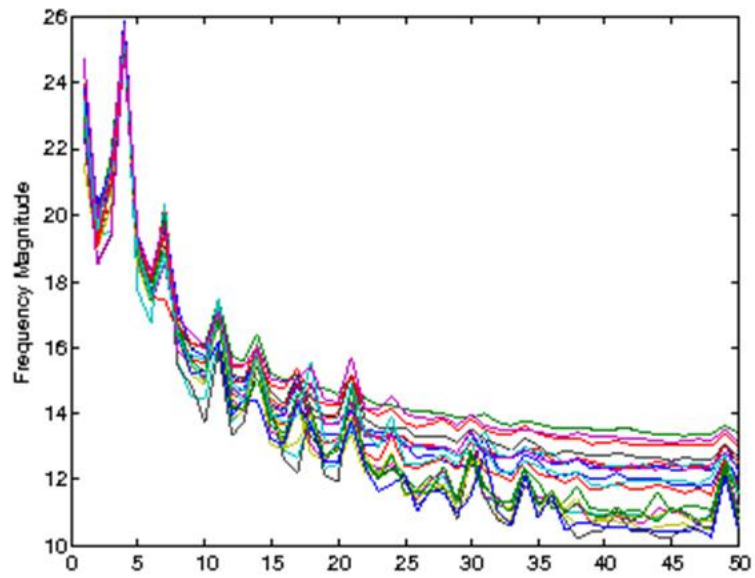


Figure 101: Frequency based analysis

methods, this system could be based on forces, because forces appear to correlate well with tool wear.

CHAPTER XII

HYDROGEN GENERATION IN SUBMERGED FRICTION STIR WELDING OF ALUMINUM

Paul Fleming, Thomas Bloodworth, George E. Cook, Alvin M. Strauss, D. M. Wilkes,
David R. DeLapp, Chase D. Cox

Science and Technology of Welding and Joining, Under Review.

and

Presented at Fuel Cell 07, Brooklyn, NY, 2007.

Abstract

Friction Stir Welding (FSW) is a recently developed welding method where samples are joined through mechanical stirring. FSW is used in an increasing number of industries. Submerged FSW (SFSW) is a type of FSW in which the welding is accomplished under-water. SFSW has been shown to produce beneficial results in some cases compared with traditional FSW. In this paper, hydrogen gas is shown to be released during SFSW. An experiment is presented which demonstrates this release of hydrogen, and the uses of this release are discussed.

Introduction

Friction Stir Welding

Friction Stir Welding (FSW) is a recently developed welding technique (1991) in which materials are joined by a rotating tool applied along the weld line that causes the material to be stirred together and form a joint while in the solid-state.[Khaled, 2005]

A basic schematic demonstrating this process is shown in figure 102.

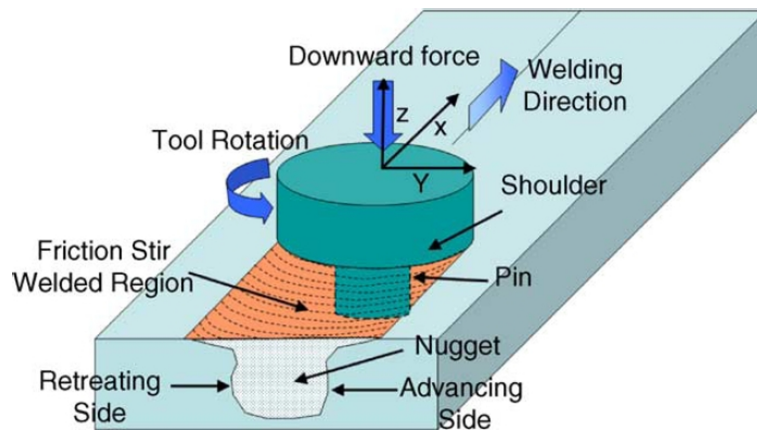


Figure 102: The essential schematic diagram of FSW[Mishra and Ma, 2005]

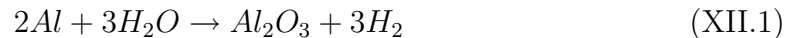
As demonstrated in figure 102, the tool rotates and applies an axial force to the material while traversing the weld line. Frictional heat is generated by the shoulder of the tool and the plasticized material is stirred together by the pin which extends out from the shoulder. One of the major advantages of FSW is that because welding occurs at the solid state, welds do not contain melt-related defects and exhibit high joint strength, even in materials such as aluminum which are considered “non-weldable by conventional techniques”. [Khaled, 2005] For this reason, processes that require aluminum to be joined are increasingly using FSW for this purpose.

Submerged Friction Stir Welding

A sub-field of FSW is Submerged Friction Stir Welding (SFSW), in which FSW is performed underwater. There are a number of reasons to research SFSW. One would be to discover FSW's potential as an underwater welding technology for use on aquatic construction and repair. SFSW could also be used to improve the quality of non-aquatic welds. The report "An analysis of microstructure and corrosion resistance of underwater friction stir processed 204L stainless steel," discusses an example motivation for using SFSW, in that the tool temperature is kept lower, which could yield less sigma phase.[Clark, 2007] Another motivation, discussed in the paper "Submerged friction stir processing (SFSP): An improved method for creating ultra-fine-grained bulk materials", is that submerged FSP (FSP is a process where the approach used in FSW is employed for creating fine-grained microstructures rather than joining) leads to a reduction in grain size compared to FSP run in air.[Hofmann and Vecchio, 2005] Because of these advantages, it is possible that submerged FSW will find applications in a number of industries.

Aluminum and hydrogen generation

In the paper "Hydrogen gas generation in the wet cutting of aluminum and its alloys", hydrogen is shown to be released when aluminum is cut underwater.[Uehara et al., 2002] The paper attributes this to the reaction of the freshly revealed aluminum with water. The chemical formula for the reaction is stated to most likely be:



The explanation for the release of hydrogen is the oxidation of freshly exposed aluminum. The surface of aluminum has an oxide layer which prevents the inner material

from oxidizing. When this inner material is exposed by cutting or machining it oxidizes. When this is done underwater, the oxygen is taken from water molecules and hydrogen gas is released.

In the paper, bubbles are shown to develop along the freshly cut surface of aluminum. A flame test and hydrogen detector were used to demonstrate that these bubbles were indeed hydrogen.

Experiment

An experiment was performed to demonstrate the release of hydrogen gas during SFSW. The experimental setup included a tank system for clamping aluminum samples underwater, as well as components to collect released hydrogen. This setup is shown in figure 103.

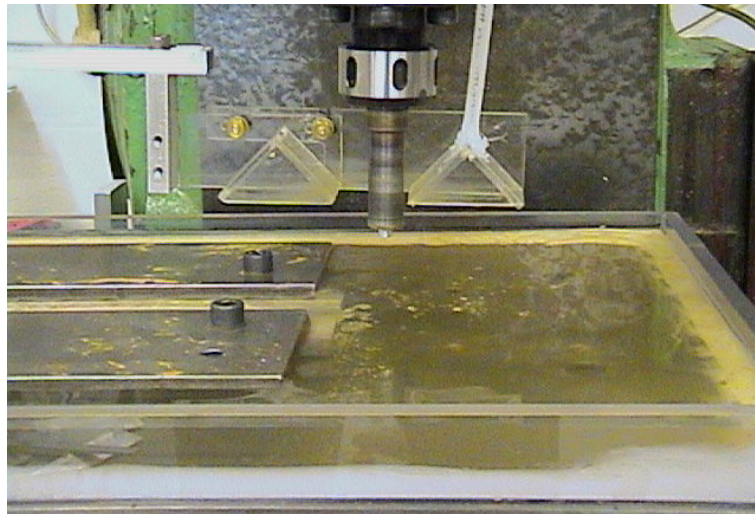


Figure 103: Submerged FSW setup

In the experiments, the aluminum to be welded is clamped underwater. The sample is a 25cm x 7.5mm section of .635mm thick 6061 aluminum. The FSW tool is made of steel and uses a square probe. Triangular funnels were used to collect hydrogen gas generated during the weld. The funnels were connected by tubing to a hydrogen fuel cell. The voltage of the fuel cell was monitored and used to indicate

the presence of hydrogen. A block diagram of the experimental setup is shown in figure 104.

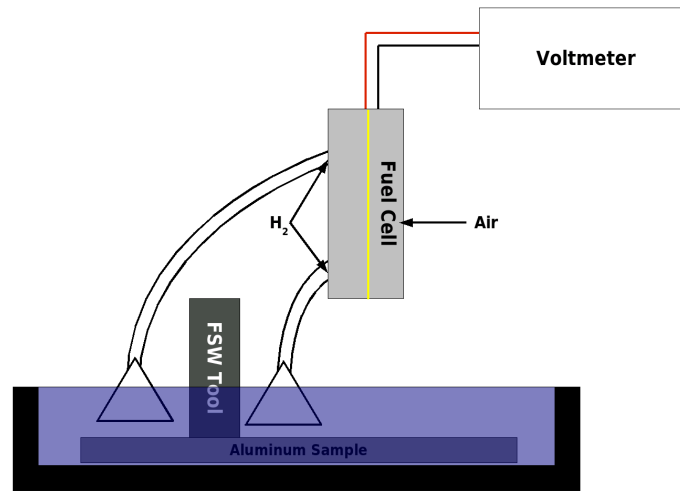


Figure 104: Block diagram of experimental setup

In the first experiment, the aluminum was processed three times. Essentially, the FSW tool traversed through the same weld line three times. During this time, the voltage measured across the fuel cell was periodically recorded. After all three passes were made, a short circuit was created across the fuel cell and the resulting voltages were recorded; this was repeated a second time. The tubes connecting the fuel cell to the hydrogen collecting funnels were then disconnected and the fuel cell short circuited a third time. The recorded voltages for this experiment are shown in figure 105.

It is evident that hydrogen is being released during submerged friction stir welding of aluminum. As a means of further investigation, a second experiment was performed where a resistor of 985 Ohms was added to the circuit. The resistor connected the terminals of the fuel cell to provide a load path for the accumulated charges. A second experiment was run, however, this time only one pass was made and the process monitored until the voltage across the resistor returned to zero. The voltage across this resistor is shown in figure 106

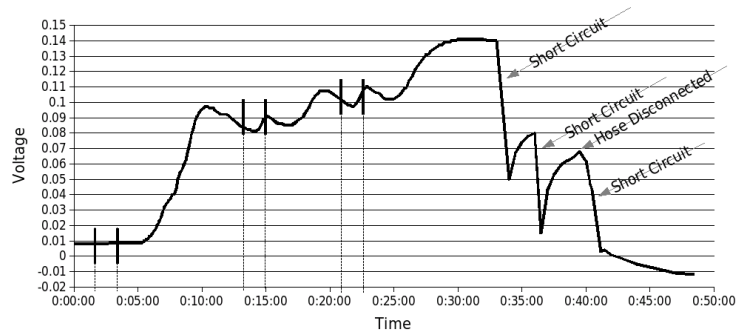


Figure 105: Fuel cell voltage in experiment 1: dashed lines indicate start and stop of welds.

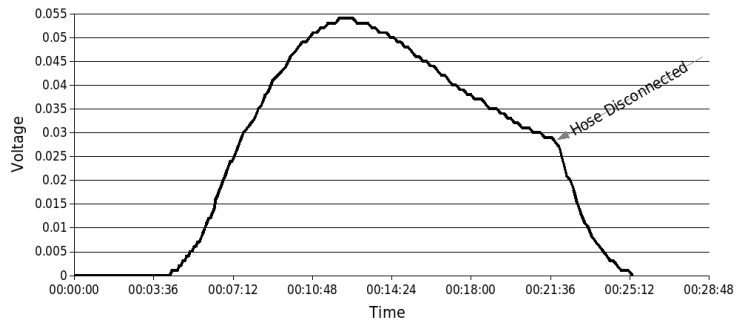


Figure 106: Resistor voltage in experiment 2

This experiment gives an indication of the total number of charges generated by the process and therefore an indication of the total amount of hydrogen released. However, it is not likely that all released hydrogen gas was collected by our system so this represents an incomplete count. This problem will be further discussed in the future work section.

Discussion

This research documents the presence of released hydrogen gas during SFSW. This release during SFSW could be useful as a feedback signal during welding. Future research may determine a correlation between the amount of hydrogen released during SFSW and the quality of the weld. This would represent a method for in-process non-destructive evaluation of welds. Additionally, the produced hydrogen may be collected by the manufacturer as a useful byproduct.

Conclusions and future work

The release of hydrogen gas in submerged FSW was demonstrated. An apparatus for collecting and measuring the hydrogen was exhibited.

Future work should focus on capturing 100% of released hydrogen and quantifying that amount. This could then be related to equation (1) to more fully understand and verify the chemical process underlying the generation. Additionally, determining if a useful relationship exists between hydrogen generation and weld quality is a subject for future research.

Acknowledgments

This research was funded by the American Welding Society and the NASA Tennessee Space Grant Consortium

Part IV

Discussion and Conclusion

CHAPTER XIII

DISCUSSION OF RESULTS

Overview

The research discussed in this dissertation is believed to be of potential value to industry. Considering the prevalent use of seam-tracking and monitoring in other welding technologies, the potential to apply these techniques to FSW could improve the robustness and applicability of the FSW process.

In this chapter, the research presented will be discussed along with its implications.

Gap Detection

In the research performed in gap fault detection, a relationship was demonstrated between weld forces, and the presence and size of gaps in fixturing. Statistical analytical techniques were applied to determine the degree to which these process forces separated into separate classes of gap, no-gap. Finally, classifiers were developed to predict the presence of gaps, and the accuracy of these classifiers was examined.

The research presented and published in gap detection represents a method for in-process detection of gap in the fit-up of FSW welds. As has been discussed in the literature, depending on the welding parameters, a gap in fit-up could potentially yield faulty FSW welds. In-process gap-detection will improve the robustness and reliability of an FSW process through the automatic discovery of this fault-causing condition.

There are now a number of techniques for in-process and non-destructive quality monitoring techniques published in the literature. The presentation of the relationship between process forces and gaps, as well as the demonstration of monitoring

algorithms capable of detecting gaps of small sizes, hopefully introduces into the literature another useful technique. Automated FSW equipment (heavy machine or robotic) will likely benefit from monitoring systems which include these quality monitoring techniques.

Misalignment detection

The research in misalignment detection was conducted similarly to gap detection, and also yielded valuable results. It was demonstrated that, at least in T- and lap-joints, a useful relationship exists between weld forces and alignment. Because of this relationship, it was possible to develop position estimators to detect and estimate misalignment. The quality of this estimator was examined, and its ability to continuously track alignment was demonstrated.

Misalignment detection, like gap detection, would likely yield important quality control benefits, even when not included in a closed-loop alignment control system for seam-tracking. The purpose of the technology then would be to validate the alignment of the tool to the joint line in question (be it butt-, lap- or T-). There are some joint types and applications, (such as blind T-joints), where fixturing may not be precise enough to guarantee this otherwise, and so misalignment detection is an important tool for verification.

However, the most utility is obtained from misalignment detection when employed as a closed-loop seam-tracking system.

Seam-tracking

Seam-tracking was demonstrated in this research for T- and lap-joints with good results. Both step and ramp type inputs were successfully tracked for both joint types. Two types of tracking were discussed, one based on the alignment estimator

discussed in chapter VII, and the other, WeaveTrack, demonstrated in chapters VIII and IX. WeaveTrack was shown to have very desirable features: robustness to FSW parameter changes, ability to incorporate load control, and usage of intrinsic signals for feedback.

WeaveTrack, and seam-tracking for FSW in general, are the subject of a current patent application. As has been discussed in the papers, seam-tracking has been shown to be an important technology for more established welding techniques such as arc welding. It is likely that seam-tracking could be of equal importance to FSW, enabling applications which are infeasible without seam-tracking (as in the welding of sinusoidal stiffeners).

CHAPTER XIV

RECOMMENDATIONS FOR FUTURE WORK

Gap Fault and Misalignment Detection

The monitoring technologies discussed in this dissertation, (gap-fault detection, misalignment detection, and briefly wear detection), were all shown to be successful in performing required detection tasks. However, improvement of these techniques is certainly possible.

Future progress for gap and misalignment detection should focus on two areas. The first is in the continued refinement of the methods for detection. The second area is broadening the application of the applied techniques to other joint types, for instance butt-joints.

Continued refinement of techniques

Both monitoring techniques employed methods which developed predicting algorithms based on experimental results. These algorithms would attempt to develop a predicting function based on training over a set of known examples. These examples would include the input (the forces collected during welding) and the desired output (either the presence and size of gap, or the degree of misalignment). This type of problem, where one attempts to “learn” a functional relationship given examples, is common in the field of machine learning, and therefore many techniques are available for comparison with those employed here.

Pre-processing

In this research, some preprocessing was attempted. These included transforms of the input data, such as the Fourier transform, as well as statistical methods such as principal components. However, there are other possibilities outside of these, and some of these might yield better overall results.

For conversion to frequency, the wavelet transform might be employed in lieu of the Fourier transform. In terms of statistical techniques, non-linear dimensional reductions, could be employed and may yield promising results. Additionally, signal filtering could be applied to the data, either to reduce high-frequency noise, or to focus in on a particular frequency band. Finally, combinations of these techniques and similar ones could be attempted to further optimize final results.

A study which compares the results of using these different pre-processing techniques in a detection algorithm could improve the overall quality of such systems.

Machine Learning

There is now a wide variety of machine learning techniques, as well as software tools to facilitate quick applications of these methods. In this research, modern techniques such as support vector machines and neural networks were applied to the data. However, both of these methods come in a number of varieties, and additionally, there are still other methods which could have been applied to greater success. Future research could focus on a comparison of methods for discovering the machine learning technique (paired with the most successful pre-processing technique) which yields the best overall predictivity and accuracy.

Application to other joint types

The application of the techniques employed for detection and estimation to other joint types should be accomplished by repeating experiments similar to those described in this dissertation in T-joints to lap and butt-type joints. This methodology should very likely yield equally successful results. By repetition and comparison, the technologies for detection and estimation of gaps in fixturing and misalignment should mature to industry-ready reliable technologies.

Development of online real-time monitoring

The misalignment estimation system in chapter VII was demonstrated tracking a changing alignment position. This could also be attempted for samples with varying gap-sizes. For instance, monitoring the output of the trained SVM for predicting gap presence when the force data from a weld with gaps inserted could yield interesting results.

Additionally, future consideration should focus on the real-time applicability of various systems. Support vector machines, neural networks and related methods have different computational demands, and the optimal offline system may not be the best choice for in-process real-time detection. Future research could focus on the real-time capabilities of the different approaches.

Seam Tracking

As discussed earlier, seam-tracking for FSW could likely be of large benefit to industrial FSW. Seam-tracking was demonstrated with WeaveTrack for both T- and lap-joints. Future research could begin with the application of WeaveTrack to butt-joints, following the same experimental techniques used in this dissertation. Additionally,

future research should also investigate non-WeaveTrack type seam-tracking, which likely could pose some advantages of its own.

WeaveTrack seam-tracking

WeaveTrack has proven effective at tracking both T- and lap-joints in FSW. In this section, several ideas for the continued refinement of WeaveTrack are presented.

PID-style control

PID style control (proportional + integral + derivative control) is a feedback control system, where control input is made to be a linear combination of the error signal, its time integral and derivative. Looking at the Weave-Track algorithm as it is, it can be seen that the WeaveTrack response to offset, the step, is static. One could imagine however, allowing this step size to vary with the size of the difference between the forces collected on either side of the weave, either simply proportionally (P-type) or including integral and differential terms. The algorithm in this case might be as below:

```

while Weaving do
  Move WeaveAdv mm at WeaveRate cm min-1 toward advancing side
  Store  $\Sigma_{current} \rightarrow \Sigma_{Adv}$ 
  Move WeaveRet mm at WeaveRate cm min-1 toward retreating side
  Store  $\Sigma_{current} - \Sigma_{Adv} \rightarrow Diff$ 
  Store  $(K * Diff) + (K_I * \int Diff) + (K_D * dDiff/dt) \rightarrow StepSize$ 
  if StepSize > 0 then
    WeaveWidth  $\rightarrow WeaveAdv$ 
    WeaveWidth + StepSize  $\rightarrow WeaveRet$ 
  else
    WeaveWidth + StepSize  $\rightarrow WeaveAdv$ 
    WeaveWidth  $\rightarrow StepRet$ 
  end
end

```

In the above algorithm, *Diff* is the difference between the force signal at either side of weave. It is shown then that the step size is now a function of this difference. K , K_I , K_D represent the proportional, integral, and differential gains.

Variable weave widths

Another variation on WeaveTrack would be allowing the weave-width to vary dynamically, in addition to the step size. This too could yield benefits such as quicker response times, or better mechanical properties.

One approach for this method is to integrate the difference between the force signal being tracked during weaving and some desired value, and then reverse when the integration reaches a certain point. Using this method, the weave-width is not fixed, and the variation might prove useful.

It is possible that this method could produce an “optimal” weave width. By allowing the weave width to vary with respect to sensed force signals, an algorithm

might be developed which produces the weave width which yields best mechanical results for a given joint.

Incorporation of load control

WeaveTrack is able to incorporate load control because its signal is the relative difference in force or torque at the extremes of weaving, and therefore the absolute changes made by a load control algorithm between weaves is acceptable.

A joint system (load-control and seam-tracking) should be built and tested in future research. There are a number of ways this could be accomplished (differing types of WeaveTrack, and various types of load control (rotation-speed-control, weld-speed-control)). Therefore, it would be useful to develop and test these types against each other to discover a robust and reliable seam-track plus axial-load control system.

Such system could represent an all-in-one control system for FSW and could be of great value to industry.

Mechanical strength

Because the literature informs that systems similar to WeaveTrack produce significant gains in the mechanical quality of welds, another goal of future research should be to tune WeaveTrack to produce similar results. This may be accomplished through higher weave-rates, larger weaves etc.

Combination of signals

Another line of exploration for the continued development of WeaveTrack is in the force and torque signals monitored. Currently, a single choice is selected, either axial force or torque. However, improvements could be made by allowing instead a function of several signals to fulfill this role. That way, if in a given weld type, none of the four

“primitive” signal types is maximized about the center, perhaps a function (ranging from simple combinations to neural networks) could be devised which does exhibit this property.

Non-WeaveTrack seam-tracking

The misalignment estimator discussed in chapter VII provides an estimate of alignment which could be employed in a non-weaved seam-tracking system. Future research should be invested in developing this type of system. Such a system is very likely a good alternative to WeaveTrack.

Inspecting seam-tracking ability

At some point in the further development of seam-tracking systems for FSW, a good experiment would be to examine the limits of seam-tracking in terms of the shape and angle of joints that can be tracked. Experiments should be conducted on tracking S-shaped joints and other non-linear paths. Additionally, the divergence angle between the joint line and direction of stage travel could be incrementally increased in another experiment to discover the maximum angle possible with a given seam-tracking system.

Other future recommendations

Signal enhancements

A final important topic for future research is that of signal enhancements. Signal enhancements are discussed in the patent application for seam-tracking [Fleming et al., 2008a], and could likely be of great use in applying the technologies described in this dissertation.

The concept of signal enhancements is to include in the weld, features, either in the workpiece itself, or into the fixturing and machinery, which “enhance” the signal employed in seam-tracking, while not negatively impacting quality. By enhancement, an increase in signal-to-noise is meant. In the patent [Fleming et al., 2008a], these enhancements are separated by type: enhancements made to the work-piece, and enhancements made to the machinery.

Work-piece enhancements

There are many possible ways to include signal enhancements into the work-piece. One example is to include machine small protrusions along side where the weld seam would be. Another example would be an indentation machine similarly near the weld seam. Figure 107, is a tree from [Fleming et al., 2008a] which categorizes the possible work-piece enhancements (all following figures are from [Fleming et al., 2008a]).

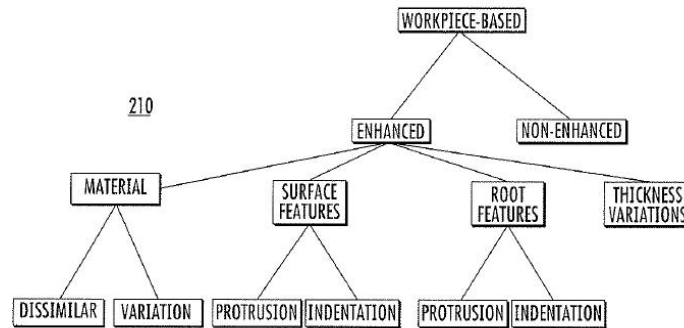


Figure 107: Categories of work-piece based enhancement

Figs. 108 and 109 demonstrate examples of feature enhancement for T-joints and butt-joints.

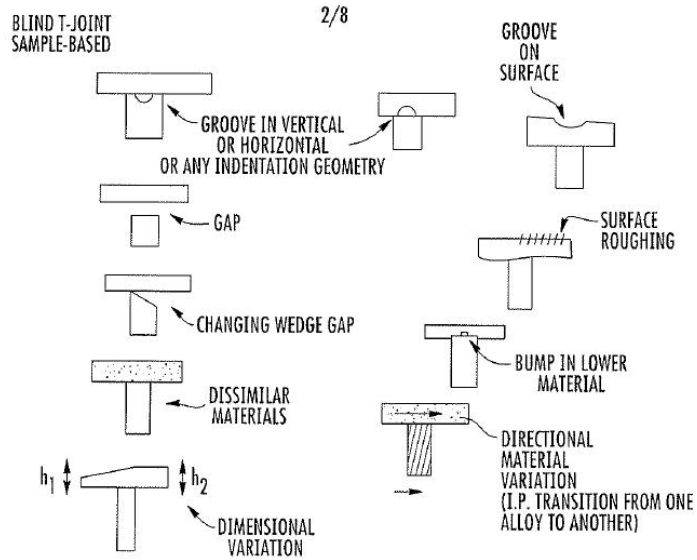


Figure 108: Examples of workpiece based enhancements in T-joints

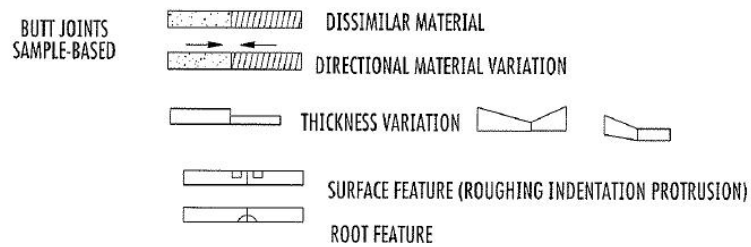


Figure 109: Examples of workpiece based enhancements in butt-joints

Machinery/fixturing based enhancements

Additionally, it may be possible to effect signal improvements through enhancements made to the fixturing or machine. A tree showing the categories of these enhancement types is shown in figure 110.

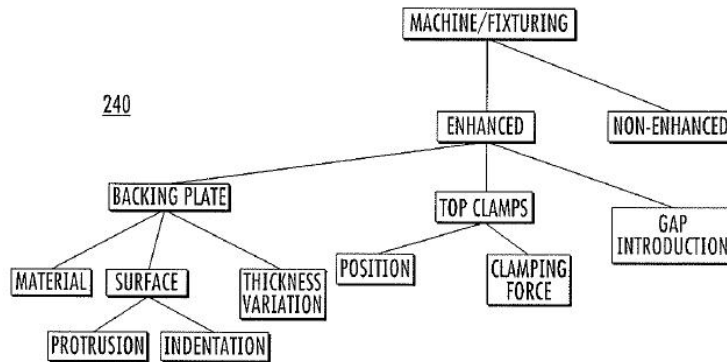


Figure 110: Categories of machine/fixturing based enhancement

Finally, examples of this type of enhancement are shown in figures 111, 112 and 113.

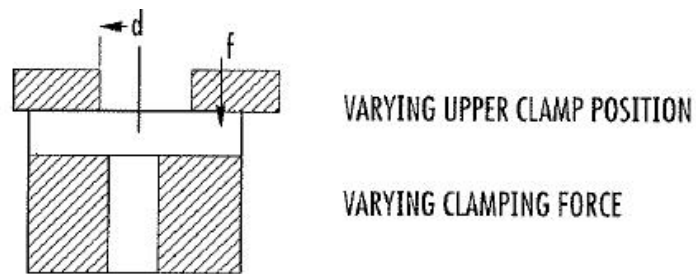


Figure 111: Examples of machine/fixturing based enhancements in T-joints

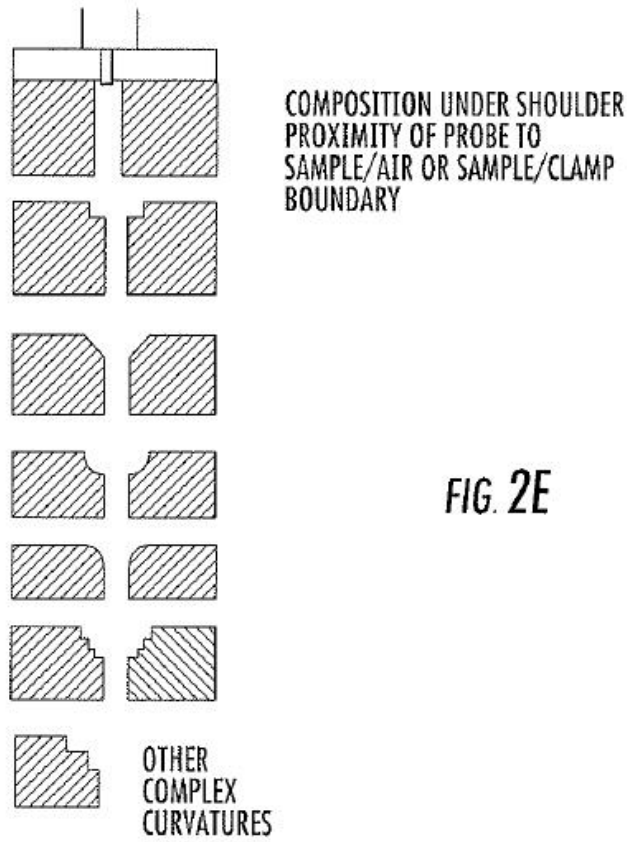


FIG. 2E

Figure 112: Examples of machine/fixturing based enhancements in T-joints

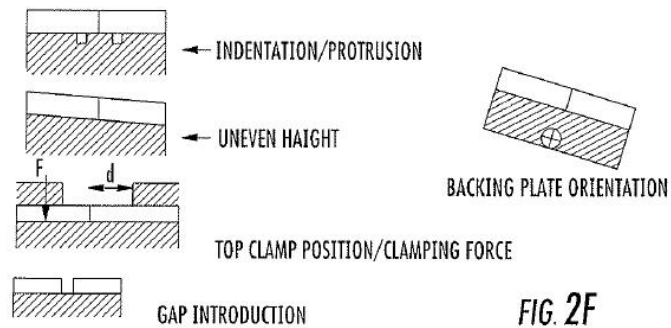


Figure 113: Examples of machine/fixturing based enhancements in butt-joints

CHAPTER XV

CONCLUSIONS

Friction stir welding is a technology which is continually expanding its applications in industry. Because of some of the desirable properties of the weld, it is often preferable to established methods of welding and joining, such as arc welding and riveting.

The research in this dissertation is expected to aid this expansion of friction stir welding. The monitoring techniques presented demonstrated methods for automated in-process non-destructive evaluation which will help ensure the quality and repeatability of the FSW process. These techniques will allow for the discovery of fault causing conditions, such as fit-up gaps, tool wear and misalignment immediately. This is important both for consistent quality, and also economically, as it prevents material waste by catching problems early.

Seam-tracking for FSW was also developed in this research. The prevalence of seam-tracking in other more-established welding technologies, such as through-the-arc sensing in arc-welding (pioneered at Vanderbilt as well), illustrate how useful this technology can be. It aids the application of a welding technology to scenarios which might otherwise be too difficult or too expensive to weld with a fixed, non-tracking process. The seam-tracking for FSW developed in this research, allows robotic FSW to perform welds which it could not otherwise be done, and enables welding without precision fixturing or tooling, as the robot can be relied upon to maintain a desired welding position relative to the joint-line. This flexibility and adaptability could likely be a great boon for robotic FSW.

It is believed that the continued development and application of the technologies developed at the Vanderbilt University Welding Automation Laboratory will help make robotic friction stir welding a robust and prevalent welding technology in many industrial areas.

REFERENCES

- [Abe, 2005] Abe, S. (2005). *Support vector machines for pattern classification*.
- [Arbegast, 2005] Arbegast, W. J. (2005). Using process forces as a statistical process control for friction stir welds. In Jata, K. V., Mahoney, M. W., Mishra, R. S., and Lienert, T. J., editors, *Friction Stir Welding and Processing III*, San Francisco, CA.
- [Astrom and Wittenmark, 1989] Astrom, K. J. and Wittenmark, B. (1989). *Adaptive control*. Addison-Wesley, Reading, Massachusetts.
- [Barnes et al., 2006] Barnes, J. E., McMichael, J., and Reynolds, A. (2006). Effects of friction stir welding defects on 7075 joint strength and fatigue life. In *6th International Symposium on Friction Stir Welding*, Saint-Sauver Nr Montreal, Canada.
- [Beamish et al., 2006] Beamish, K., Lewis, P., and Cheetham, P. (2006). Development of a low cost friction stir welding monitoring system. In *6th International Symposium on Friction Stir Welding*, Saint-Sauver Nr Montreal, Canada.
- [Bennett and Campbell, 2000] Bennett, K. P. and Campbell, C. (2000). Support vector machines: Hype or hallelujah? *SIGKDD Explor. Newsl.*, 2(2):1–13.
- [Bird, 2003] Bird, C. (2003). Ultrasonic phased array inspection technology for the evaluation of friction stir welds. In *4th International Friction Stir Welding Symposium*, Park City, USA.
- [Bird, 2004] Bird, C. R. (2004). The inspection of friction stir welded aluminum plant. In *5th International Friction Stir Welding Symposium*, Metz, France.
- [Boldsai Khan et al., 2006a] Boldsai Khan, E., Corwin, E., Logar, A., and Arbegast, W. (2006a). Neural network evaluation of weld quality using fsw feedback data. In *Friction Stir Welding, 6th International Symposium*, Saint-Sauver, Nr Montreal, Canada.
- [Boldsai Khan et al., 2006b] Boldsai Khan, E., Corwin, E., Logar, A., and Arbegast, W. (2006b). Neural network evaluation of weld quality using fsw feedback data. In *Friction Stir Welding, 6th International Symposium*.
- [Cantin et al., 2005] Cantin, G. M. D., David, S. A., Thomas, W. M., Lara-Curzio, E., and Babu, S. S. (2005). Friction skew-stir welding of lap joints in 5083-o aluminum. *Science & Technology of Welding & Joining*, 10(3).
- [Canu et al., 2005] Canu, S., Grandvalet, Y., Guigue, V., and Rakotomamonjy, A. (2005). Svm and kernal matlab toolbox. In *Perception Systemes et Information*.
- [Center,] Center, N. R. Basic principles of ultrasonic testing. [Online; accessed 10-October-2007].

- [Chen et al., 2003a] Chen, C., Kovacevic, R., and Jandgric, D. (2003a). Acoustic emission in monitoring quality of weld in friction stir welding. In *4th International Symposium on Friction Stir Welding*, Park City, Utah, USA.
- [Chen et al., 2003b] Chen, C., Kovacevic, R., and Jandgric, D. (2003b). Wavelet transform analysis of acoustic emission in monitoring friction stir welding of 6061 aluminum. *International Journal of Machine Tools and Manufacture*, 43(13):1383–1390.
- [Chen et al., 2003c] Chen, C., Kovacevic, R., and Jandgric, D. (2003c). Wavelet transform analysis of acoustic emission in monitoring friction stir welding of 6061 aluminum. *International Journal of Machine Tools and Manufacture*, 43:1383–1390.
- [Clark, 2007] Clark, T. (2007). An analysis of microstructure and corrosion resistance of underwater friction stir processed 304l stainless steel. Technical report, BYU.
- [Cook, 1983] Cook, G. E. (1983). Robotic arc welding: Research in sensory feedback control. *IEEE Transactions on industrial electronics*, IE-30(3).
- [Cook et al., 2004] Cook, G. E., Crawford, R., Clark, D. E., and Strauss, A. M. (2004). Robotic friction stir welding. *Industrial Robot*, 31(1):55–63.
- [Corinna and Vapnik, 1995] Corinna, C. and Vapnik, V. (1995). Support-vector networks. *Machine Learning*, 20:273–297.
- [Dawes and Thomas, 1995] Dawes, C. J. and Thomas, W. M. (1995). Friction stir joining of aluminium alloys. *TWI Bulletin*, pages 120–128.
- [Devore and Farnum, 1999] Devore, J. and Farnum, N. (1999). *Applied Statistics for Engineers and Scientists*. Duxbury Press, Pacific Grove, CA, 2nd edition.
- [Dickerson and Przydatek, 2003] Dickerson, T. L. and Przydatek, J. (2003). Fatigue of friction stir welds in aluminium alloys that contain root flaws. *International Journal of Fatigue*, 25(12):1399–1409.
- [Erbsloh et al., 2003] Erbsloh, K., Donne, C. D., and Lohwasser, D. (2003). Friction stir welding of t-joints. *Materials Science Forum*, 426-432:2965–2970.
- [Ericsson et al., 2007] Ericsson, M., Jin, L.-Z., and Sandstrom, R. (2007). Fatigue properties of friction stir overlap welds. *International Journal of Fatigue*, 29(1):57–68. Lap.
- [Fisher, 1936] Fisher, R. (1936). The use of multiple measurements in taxonomic problems. *Annals of Eugenics*, 7(2):179–188.
- [Fleming et al., 2008a] Fleming, P. A., Lammlein, D. H., Cook, G. E., Wilkes, D. M., Strauss, A. M., DeLapp, D., and Hartman, D. A. (2008a). Through the tool tracking for friction stir welding. us patent filed may 30, 2008. serial no. 12/130,622.

- [Fleming et al., 2008b] Fleming, P. A., Lammlein, D. H., Wilkes, D. M., Cook, G. E., Strauss, A. M., DeLapp, D. R., and Hartman, D. A. (Accepted: To be published in 2008b). Misalignment detection and enabling of seam tracking for friction stir welding. *Science & Technology of Welding & Joining*.
- [Fleming et al., 2008c] Fleming, P. A., Lammlein, D. H., Wilkes, D. M., Fleming, K. A., Bloodworth, T. S., Cook, G. E., Strauss, A. M., DeLapp, D., Lienert, T. J., Bement, M., and Prater, T. (2008c). In-process gap detection in friction stir welding. *Sensor review*, 28(1).
- [Fratini et al., 2006] Fratini, L., Buffa, G., Filice, L., and Gagliardi, F. (2006). Friction stir welding of aa6082-t6 t-joints: process engineering and performance measurement. *Proceedings of the I MECH E Part B Journal of Engineering Manufacture*, 220(5):669–676.
- [Fukunaga, 1972] Fukunaga, K. (1972). *Introduction to Statistical Pattern Recognition*. Academic, New York.
- [Hartman et al., 2005] Hartman, D. A., Dave, V. R., Cola, M. J., and Carpenter, R. W. (2005). Method and apparatus for in-process sensing of manufacturing quality.
- [Hattingh et al., 2004] Hattingh, D. G., Niekerk, T. I. v., Blignault, C., Kruger, G., and James, M. N. (2004). Analysis of the fsf force footprint and its relationship with process parameters to optimise weld performance and tool design. *Welding in the world*, 48(1/2):50–58.
- [He et al., 2007] He, Y., Boyce, D. E., and Dawson, P. R. (2007). Three-dimensional modeling of void growth in friction stir welding of stainless steel. In *NUMIFORM '07*. American Institute of Physics.
- [Heideman et al., 2000] Heideman, R. J., Blachowiak, E. G., Smith, C. B., Carian, S. L., Tarr, B. S., Duffie, N. A., and Predith, M. H. (2000). Three dimensional tactile seam tracing device.
- [Hofmann and Vecchio, 2005] Hofmann, D. C. and Vecchio, K. S. (2005). Submerged friction stir processing (sfsp): An improved method for creating ultra-fine-grained bulk materials. *Materials Science and Engineering a-Structural Materials Properties Microstructure and Processing*, 402(1-2):234–241. underwater.
- [Huang et al., 1998] Huang, M., Jiang, L., Liaw, P., Brooks, C., Seeley, R., and Klarstrom, D. (1998). Using acoustic emission in fatigue and fracture materials research. *JOM*, 50(11):1–14.
- [Jackson, 2003] Jackson, J. (2003). *A User's Guide to Principal Components*. Wiley-IEEE.
- [Jain et al., 1996] Jain, A., Mao, J., and Mohiuddin, K. (1996). Artificial neural networks: a tutorial. *Computer*, 29(3):31–44.

- [Jain et al., 1999] Jain, A., Murty, M., and Flynn, P. (1999). Data clustering: a review. *ACM Computing Surveys (CSUR)*, 31(3):264–323.
- [Kawasaki et al., 2004] Kawasaki, T., Makino, T., Masai, K., Ohba, H., Ina, Y., and Ezumi, M. (2004). Application of friction stir welding to construction of railway vehicles. *JSME International Journal Series A*, 47(3):502–511. Trains.
- [Khaled, 2005] Khaled, T. (2005). An outsider looks at friction stir welding. Technical report, Federal Aviation Administration.
- [Kim et al., 2005] Kim, Y. G., Fujii, H., Tsumura, T., Komazaki, T., and Nakata, K. (2005). Three defect types in friction stir welding of aluminum die casting alloy. *Materials Science and Engineering: A*, 415(1-2):250–254.
- [Kinton and Thusty, 2000] Kinton, J. D. and Thusty, J. (2000). Method and apparatus for controlling downforce during friction stir welding.
- [Kruger et al., 2004] Kruger, G., van Niekerk, T., Blignault, C., and Hattingh, D. (2004). Software architecture for real-time sensor analysis and control of the friction stir welding process. In *AFRICON*, Africa.
- [Lathi, 1998] Lathi, B. P. (1998). *Signal Processing & Linear Systems*. Berkely Cambridge Press.
- [Leal and Loureiro, 2004] Leal, R. and Loureiro, A. (2004). Defects formation in friction stir welding of aluminum alloys. In *International Materials Symposium*, Caprica, Portugal.
- [Leonard and Lockyer, 2003] Leonard, A. J. and Lockyer, S. A. (2003). Flaws in friction stir welds. In *4th International Symposium on Friction Stir Welding*, Park City, Utah, USA. Defects and Faults.
- [Loftus et al., 1999] Loftus, Z., Venable, R., and Adams, G. P. (1999). Development and implementation of a load-controlled friction stir welder. In *1st International Symposium on Friction Stir Welding*, Thousand Oaks, California, USA.
- [Mallet et al.,] Mallet, U., Coomans, D., and de Vel, O. Recent developments in discriminant analysis on high dimensional spectral data. *Chemometrics and Intelligent Laboratory Systems*, 35.
- [Manly, 1986] Manly, B. (1986). *Multivariate statistical methods*. Chapman and Hall New York.
- [Mishina and Norlin, 2003] Mishina, O. K. and Norlin, A. (2003). Lap joints produced by fsw on flat aluminum en aw-6082 profiles. Lap.
- [Mishra and Ma, 2005] Mishra, R. S. and Ma, Z. Y. (2005). Friction stir welding and processing. *Materials Science & Engineering R-Reports*, 50(1-2):iii–78.

- [Montgomery et al., 2001] Montgomery, D., Runger, G., and Hubele, N. (2001). *Engineering statistics - 2nd ed.* Wiley New York.
- [Muthukumaran et al., 2006] Muthukumaran, S., Pallav, K., Pandey, V. K., and Mukherjee, S. K. (2006). A study on electromagnetic property during friction stir weld failure. *International Journal of Advanced Manufacturing Technology*.
- [Nelson et al., 2007] Nelson, T. W., Sorensen, C. D., Carter, P. W., Jr., T. L. K., and Kirkham, D. V. (2007). Apparatus and method for performing non-linear friction stir welds on either planar or non-planar surfaces.
- [Okuyucu et al., 2005] Okuyucu, H., Kurt, A., and Arcaklioglu, E. (2005). Artificial neural network application to the friction stir welding of aluminum plates. *Materials and Design*, 28:78–84.
- [Pearson, 1901] Pearson, K. (1901). On lines and planes of closest fit to systems of points in space. *Philosophical Magazine*, 2(6):559–572.
- [Pham, 2006] Pham, H., editor (2006). *Handbook of engineering statistics*, chapter Support vector machines for data modeling with software engineering applications.
- [Russell and Norvig, 2003] Russell, S. J. and Norvig, P. (2003). *Artificial Intelligence: A Modern Approach*. Prentice Hall, Upper Saddle River, NJ, 2nd edition.
- [Shlens, 2005] Shlens, J. (2005). A tutorial on principal component analysis. Technical report, Systems Neurobiology Laboratory, University of California, San Diego, La Jolla, CA.
- [Sinha et al., 2006] Sinha, P., Muthukumaran, S., Sivakumar, R., and Mukherjee, S. K. (2006). Condition monitoring of first mode of metal transfer in friction stir welding by image processing techniques. *International Journal of Advanced Manufacturing Technology*.
- [Smith et al., 2003] Smith, C. B., Hinrichs, J. F., and Crusan, W. A. (2003). Robotic friction stir welding: The state-of-the-art. In *4th International Symposium on Friction Stir Welding*.
- [Specht, 1991] Specht, D. F. (1991). A general regression neural network. *IEEE transactions on neural networks*, 2(6):568–576.
- [Stotler and Trapp, 2007] Stotler, T. V. and Trapp, T. J. (2007). Friction stir welding travel axis load control method and apparatus, us patent 7,216,793 b2.
- [Thomas et al., 2003a] Thomas, W. M., Johnson, K. I., and Wiesner, C. S. (2003a). Friction stir welding - recent developments in tool and process technologies. *Advanced Engineering Materials*, 5(7).
- [Thomas et al., 1991a] Thomas, W. M., Nicholas, E. D., Needham, J. C., Murch, M. G., Temple-Smith, P., and Dawes, C. J. (1991a). Friction welding.

- [Thomas et al., 1991b] Thomas, W. M., Nicholas, E. D., Needham, J. C., Murch, M. G., Temple-Smith, P., and Dawes, C. J. (1991b). G.B. Patent Application No. 9125978.8.
- [Thomas et al., 1995] Thomas, W. M., Nicholas, E. D., Needham, J. C., Murch, M. G., Temple-Smith, P., and Dawes, C. J. (1995). Friction welding. Patent.
- [Thomas et al., 2003b] Thomas, W. M., Staines, D. G., Johnson, K. I., and Evans, P. (2003b). Com-stir - compount motion for friction stir welding and machining. *Published on the internet*.
- [Thomas et al., 2002] Thomas, W. M., Staines, D. G., Norris, I. M., and de Frias, R. (2002). Friction stir welding tools and developments.
- [Threadgill, 2007] Threadgill, P. L. (2007). Terminology in friction stir welding. *Science and Technology of Welding & Joining*, 12(4):357–360.
- [Uehara et al., 2002] Uehara, K., Takeshita, H., and Kotaka, H. (2002). Hydrogen gas generation in the wet cutting of aluminum and its alloys. *Journal of Materials Processing Technology*, 127:174–177. Hydrogen Generation.
- [Vugrin et al., 2004] Vugrin, T., Staniek, G., Hillger, W., and Donne, C. D. (2004). Non-destructive detection of flaws in fsw and their metallographic charecterization. In *5th International Friction Stir Welding Symposium*, Metz, France.
- [Wikipedia, 2007] Wikipedia (2007). K-means algorithm — Wikipedia, the free encyclopedia. [Online; accessed 16-October-2007].